

Reactivity of Chromium with Aluminates: The Quest for Monovalent Chromium Complexes

Saba HajiAli Afzali

June 27, 2013

Thesis submitted to the
Faculty of Graduate and Postdoctoral Studies
University of Ottawa
For MSc degree in chemistry
Faculty of Science
Ottawa-Carleton Chemistry Institute

© Saba HajiAli Afzali, Ottawa, Canada, 2013

Abstract

Progress in catalytic ethylene oligomerization and polymerization processes creates an enormously valuable and active field in both industry and academia.

From the naive point of view, gathering ethylene molecules to generate carbon-carbon bonds can be assumed as a no electron, no energy, facile chemical process which results from interaction of several π -electrons, but this process never can afford macromolecules without applying catalysts. It is no wonder that major efforts have been committed to designing novel catalysts to perform oligo- and polymerization processes, both recently and in the past, which provide the extensive library of catalysts today. Among all the metals applied in preparation of homogeneous catalysts for ethylene oligo- and polymerization, chromium has been ideal in providing versatile systems in terms of selectivity and activity for oligomer and polymer production.

In the first part of the current work we chose two different ligand systems (iminopyridine and bisiminophosphine) to investigate the activity of their chromium complexes for ethylene oligo- and polymerization at different conditions. In addition, we took on the substantial challenge of explaining the activities through isolation of intermediates during the catalytic runs. The major focus in this part was rationalizing catalytic behaviour of the catalysts through elucidation of metal oxidation states. To fulfill this goal, syntheses of chromium-aluminate complexes in different valence states as well as description of ligand-metal interactions were presented.

In the second part of this thesis, our main focus of study was on the development of novel species in the well-established field of radical chemistry of alkyl aluminum. Preferential cation radical and diradical formation and exploration of their stabilities through

both experimental and computational methods will be discussed. Also, in parallel with this work we discovered unprecedented double alkylation of the ligand system.

*I would like to dedicate this thesis to my parents for their
inspiration and kind-heartedness.*

Acknowledgments

First and foremost, I would like to thank my supervisor, Dr. Sandro Gambarotta. I would like to thank him for his financial support and inspiration during this work. Doubtlessly without his encouragement this thesis could not be accomplished.

I would like to give appropriate acknowledgement to Dr. Rohollah Firouzi for his enormous help in doing computational work in this thesis. I am appreciative to our expert crystallographer Dr. Iliia Korobkov. I had an opportunity to work with Ahmed Alzamley and benefit from his knowledge and also his empathy in the difficult time of this experience. It was my pleasure to work in the lab with the decent and helpful Indira, Joanna and Camilo.

I would like to send my special and incomparable thanks to my best friend Nastaran and also my benevolent friends Masoud and Mohammad must be thanked for their support. Thanks to Nick Trefiak for useful suggestions and discussions during the process of writing my thesis.

In the end, I would like to be incredibly thankful to my wonderful mother Manijeh, my encouraging father Ali and my helpful brother Sadra for their love, advice, support and inspiration to enable me to tackle the challenges I have encountered during my life.

Table of Contents

Abstract	1
Acknowledgment	4
Table of Contents	5
List of Figures	8
List of Tables	9
List of Abbreviation	10
Chapter 1: Introduction	12
1.1 Polymerization	18
1.2 Oligomerization	23
1.3 Thesis Aim	31
1.3.1 Chapter 2	31
1.3.2 Chapter 3	32
1.3.3 Chapter 4	32
1.4 References	33
Chapter 2: Chromium Iminopyridine Complexes as Catalyst Precursors for Ethylene Polymerization and Oligomerization	40
2.1 Introduction	40
2.2 Experimental Part	42
2.2.1 Synthesis of the Ligand	43

2.2.2 Synthesis of Complexes	43
2.3 X-Ray Diffraction	45
2.4 General Oligomerization and polymerization procedure	48
2.5 Results and Discussion	48
2.6 Conclusion	59
2.7 References	60
Chapter 3: Chromium Complexes of a Pincer-type bis-Phosphinimide	
Ligand	65
3.1 Introduction	65
3.2 Experimental Part	68
3.3 X-Ray Diffraction	70
3.4 General Oligomerization and polymerization procedure	73
3.5 Results and Discussion	73
3.6 Conclusion	84
3.7 References	85
Chapter 4: Radical Chemistry of Alkyl Aluminum	88
4.1 Introduction	88
4.2 Experimental Part	89
4.2.1 Synthesis of Complexes	90
4.3 Computational Method	92
4.4 X-Ray Diffraction	94
4.5 Results and Discussion	96
4.6 Conclusion	114

4.7 References	115
Chapter 5: Conclusion	120
Appendix A: NMR Spectra of Synthesized Ligand	122

List of Figures

Figure 2.1. Partial thermal ellipsoid drawing of 2.1 at 50% probability	51
Figure 2.2. Partial thermal ellipsoid drawing of 2.2 at 50% probability	52
Figure 2.3. Partial thermal ellipsoid drawing of 2.3 at 50% probability	53
Figure 2.4. Partial thermal ellipsoid drawing of 2.4 at 50% probability	56
Figure 3.1. Partial thermal ellipsoid drawing of 3.2 at 50% probability	75
Figure 3.2. Partial thermal ellipsoid drawing of 3.3 at 50% probability	78
Figure 3.3. Partial thermal ellipsoid drawing of 3.4 at 50% probability	80
Figure 4.1. Partial thermal ellipsoid drawing of 4.1 at 50% probability	97
Figure 4.2. Partial thermal ellipsoid drawing of 4.2 at 50% probability	100
Figure 4.3. EPR spectrum of 4.2 recorded in toluene glass at 100 K.	101
Figure 4.4. The SOMO and spin density plots for 4.2	104
Figure 4.5. Partial thermal ellipsoid drawing of 4.3 at 50% probability	107
Figure 4.6. EPR spectrum of 4.3 recorded at room temperature.	108
Figure 4.7. Molecular orbital pictures and energy diagrams of HOMO and LUMO for 4.3 and 4.1 .	110
Figure 4.8. The shape of singly occupied molecular orbitals (SOMOs) of the triplet of 4.3 .	111
Figure 4.9. Partial thermal ellipsoid drawing of 4.4 at 50% probability	113
Figure 5.1. ^1H NMR of 2a	122
Figure 5.2. ^{13}C NMR of 2a	122

List of Tables

Table 1.1 α -olefin main applications and market share	13
Table 1.2: Industrial statistical processes for commercial ethylene oligomerization	25
Table 2.1. Crystal data and refinements for 2.1 – 2.4.	47
Table 2.2. Ethylene Oligomerization Results.	58
Table 2.3. Analysis of the α -olefin product distribution	59
Table 3.1. Crystal data and refinements for 3.1 - 3.4.	72
Table 3.2. Selected bond lengths (Å) and bond angles (°) for compounds 3.1 - 3.3	79
Table 3.3. Ethylene Oligomerization Results	83
Table 3.4. Analysis of the α -olefin product distribution	84
Table 4.1. Crystal data and refinements for 4.1 - 4.4.	95
Table 4.2. Selected bond distances and angles (calculated versus experimental)	102
Table 4.3. DFT calculated Spin densities value on each atom of the $\{[AlMe_2]_2(\mu-\kappa^2: \kappa^2-C_{18}H_{12}N_4)\}^+$.	103

List of Abbreviation

BP	British Petroleum
BuAO	butylaluminumoxane
CCD	charge coupled detector
CHN	carbon, nitrogen, hydrogen analyzer
DEAC	diethylaluminum chloride
DMAO	depleted methylaluminumoxane
DME	dimethoxyethane
EA	elemental analysis
EPR	electron paramagnetic resonance
ESI-MS	electrospray ionization mass spectrometry
ESR	electron spin resonance
GC-MS	gas chromatography mass spectrometry
HDPE	high density polyethylene
ICI	Imperial Chemical Industries
IR	infrared spectroscopy
LAO	linear alpha olefin
LDPE	low density polyethylene
LLDPE	linear low density polyethylene
MAO	methylaluminumoxane
MeCy	methylcyclohexane
MMAO	modified methylaluminumoxane

NHAO	<i>n</i> -hexylaluminumoxane
NMR	nuclear magnetic resonance
PDI	polydispersity distribution index
PE	polyethylene
PP	polypropylene
SHOP	Shell higher olefin process
SK-Energy	South Korean Energy
TEAL	triethylaluminum
THF	tetrahydrofuran
TMA	trimethylaluminum
Z-N	Ziegler-Natta

Introduction

Understanding the sequence of steps through which reagents may form products has always been the ultimate goal of chemists interested in rationalizing the chemical behaviour of catalysts. Besides the fascination for unveiling the secrets of nature, gathering detailed information about catalytically active species and the prerequisite of ligands to improve or affect catalytic behaviour is central to the rational design of new and more performing catalytic systems. Thus, convenience and commercial reasoning together add stimulus to this quest.

The factors determining the switch of behaviour of chromium catalysts between ethylene polymerization and oligomerization or even selective oligomerization are an illustrative example of this undimmed interest for gathering information from mechanistic work to assist catalyst design.

Forming polymeric chains starting from inexpensive molecules such as ethylene has created in the last sixty years the ever growing business of polyethylene (PE) and polyolefins (PO) industry. The amount of PE produced in the world is in the range of 80 Megatons/year¹ and the volume of this business is expected to continue to grow in the next decade. With the term olefin oligomerization, it is intended instead a process, conceptually very similar to polymerization, but where the chain growth is terminated at its very early stage, thus forming a statistical distribution of α -olefins. Ethylene oligomerization in particular provides a

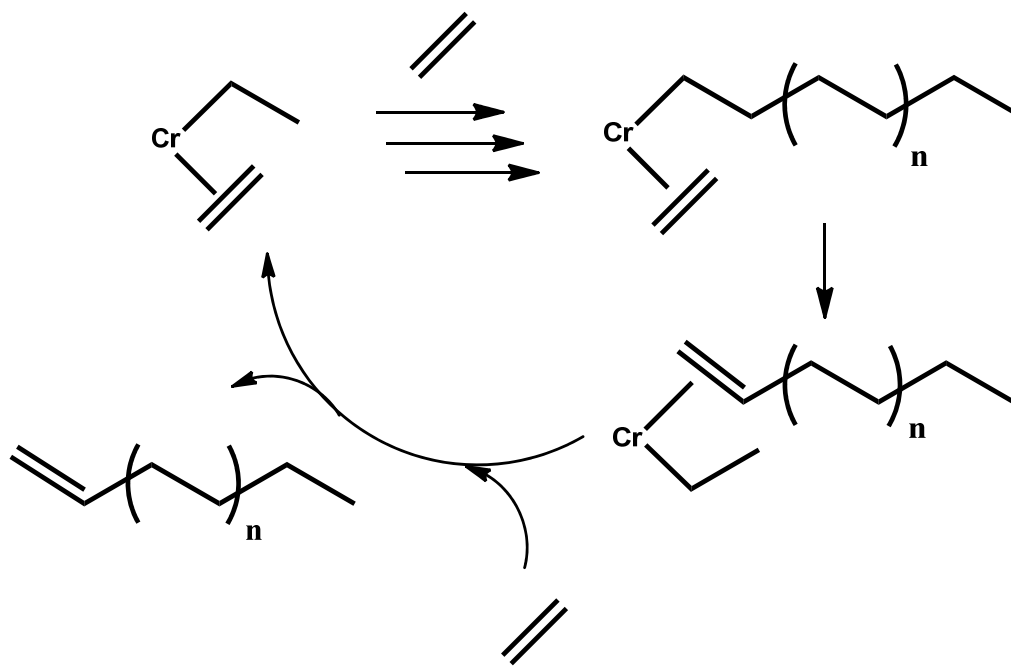
sizeable commercial business with a market share distribution among the several oligomers depending on their molecular weight and diversified fields of application (Table 1.1).²

Table 1.1 α -olefin main applications and market share

LAO	Important applications
C ₄	Polyolefin co-monomer (LLDPE, HDPE), poly-butene-1.
C ₆	Polyolefin co-monomer (LLDPE, HDPE), intermediate in the production of oxo alcohols, organo-aluminum compounds, hexyl mercaptans, synthetic fatty acids and plasticizer alcohol.
C ₈	Polyolefin co-monomer (LLDPE, HDPE), an intermediate in the production of oxo alcohols, organo-aluminum compounds, octyl mercaptans, amines, synthetic fatty acids and plasticizer alcohol
C ₁₀	An intermediate in the production of epoxides, oxo alcohols, amines, synthetic fatty acids, alkylated aromatics and synthetic lubricants, plasticizer alcohol.
C ₁₂	Production of linear alkylbenzene, synthetic lubricants, amines and amine oxides, epoxides and synthetic fatty acids, detergent alcohols, mercaptans.
C ₁₄	Production of linear alkylbenzene, amines and amine oxides, detergent alcohols (oxo alcohols), mercaptans, alkylated aromatics, lubricants, epoxides, oxo alcohols, fatty acids.
C ₁₆₊	Wax lubricants, alpha olefin sulfonate, oxo alcohols.

When only one specific α -olefin is sought (e.g. 1-hexene and 1-octene used as critical additives to control PE rheology) a selective catalyst is necessary for its formation. This is a certainly desirable alternative to embarking on energy intensive fractionation of statistical mixtures as obtained from non-selective oligomerization procedures. However, the design of

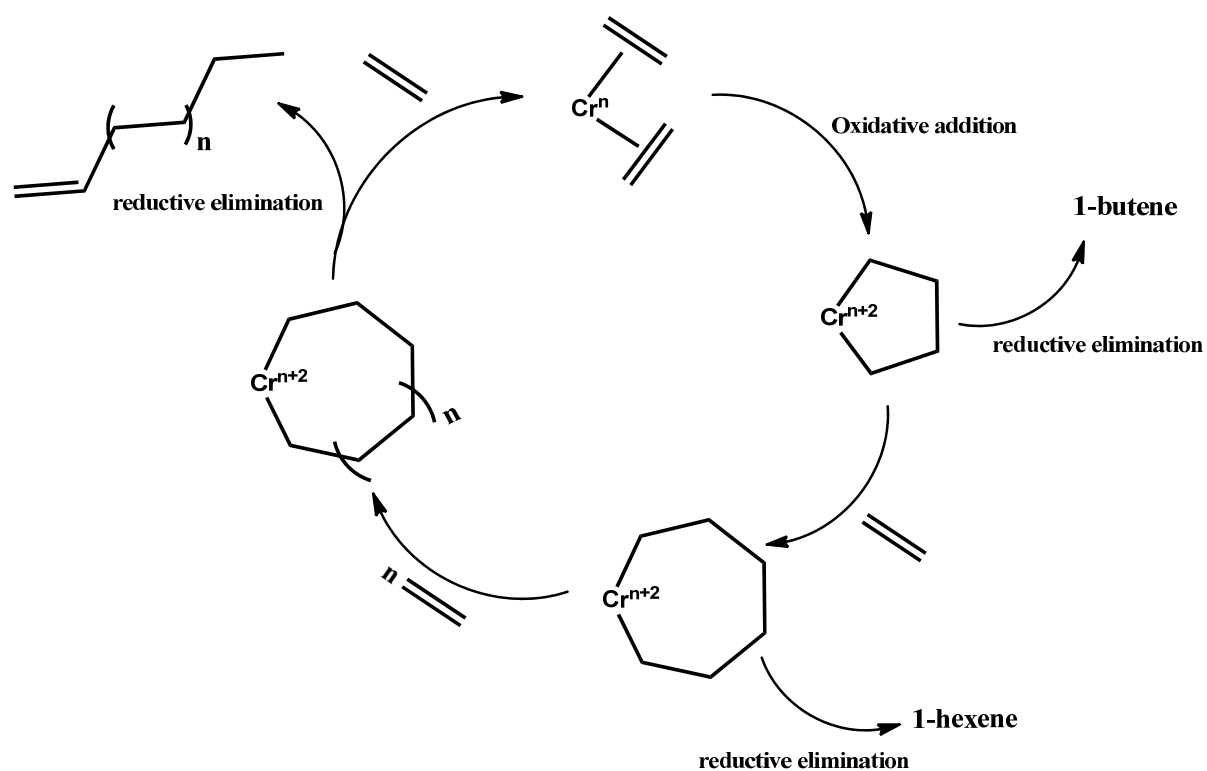
a selective catalytic system clearly poses an intellectual challenge requiring a good grasp on the mechanism of the targeted selective oligomerization. For example, there was a long debate in the literature about whether or not a selective tri- or tetramerization catalysts should follow the same path of a polymerization catalytic cycle (so called Cossee-Arlman mechanism Scheme 1.1).³



Scheme 1.1. Cossee-Arlman mechanism

An alternative mechanism was then proposed based on oxidative addition/reductive elimination elementary steps. Prerequisite of this mechanism is the formation of a metal in low oxidation state sufficiently reducing to perform the reductive coupling of two molecules of ethylene. As a result, the metal increases its oxidation state by a +2 unit. The so-formed metalla-cyclopentane expands via insertion of one or two additional molecules of ethylene

and then rapidly collapses reforming the original catalyst and releasing the desired α -olefin via reductive elimination (Scheme 1.2). The information that may be extracted from this mechanistic hypothesis guides the search for the factors stabilizing a certain low-oxidation state of the transition metal and of course the search for appropriate ligand systems.⁴



Scheme 1.2: Metallacycle mechanism.

In the specific case of ethylene tri- and tetramerization, the metal of preference is chromium.⁵ This in turn raises the question about which oxidation state may have the sufficient reducing power to trigger the coupling of two ethylene molecules. Interestingly

chromium also provides potent polymerization catalysts commercially used for the gas-phase production of PE. Therefore, chromium complexes are excellent substrates with which to study the factors affecting a specific catalytic behaviour.

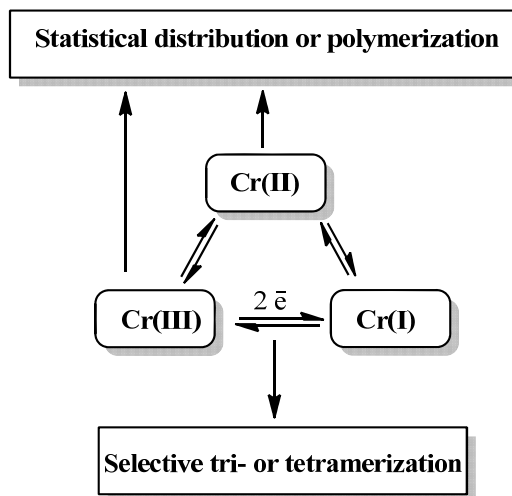
The identification of the chromium redox couple responsible for the selective oligomerization has been a point of vigorous literature debate. A major contribution to its identification has been the modeling study of Jolly who has prepared chromium complexes of well-defined structure, including, a rare example of an ethylene complex, and carried out the oligomerization step-by-step.⁶ The working hypothesis at the basis of this study has been the original metallacycle mechanism proposed by Mayniyk in 1964.⁷ Further mechanistic study have conclusively proved the existence of chromium intermediates in metallacycle pathway with chromacyclopentane and chromacycloheptane displaying different kinetic stability. For example, chromacyclopentane required temperatures in the range of 100 °C to reductively eliminate 1-butene while formation of 1-hexene from chromacycloheptane occurs at only 0 °C. Accordingly, it was demonstrated that the kinetic stability of intermediate species has a remarkable impact on the selectivity of the catalytic cycle.

More recent work from our group has analyzed three commercially used selective oligomerization systems and isolated and fully characterized the intermediate catalytically active species. In turn, this has enabled to identify the chromium oxidation states responsible for polymerization, oligomerization and trimerization.⁸ The merit of this work was to restrict the quest for new and more performing catalysts to the search of ligand systems capable of providing sufficient stability to the target oxidation state. In order to rationalize this critical and final point, it is therefore of primary importance to analyze the interaction of chromium complexes of a library of ligand systems and their interaction with alkyl aluminum

activators. Once these species are fully characterized, the catalytic behaviour, especially in the fortunate cases of self-activating catalysts,⁹ gives the crucial information about the nature of the catalytically active species and the factors responsible for a specific catalytic behaviour (e.g. polymerization versus oligomerization). In turn, this is central to guide the design of better and more performing catalysts.

As mentioned above, one of the main successes of this strategy of research has been the identification of the catalytically active metal oxidation state. While the monovalent state of chromium has been linked to selective oligomerization, the non-selective is linked to the divalent state. Polymerization is instead to be ascribed to the trivalent state and in turn to the formation of robust organometallic species.¹⁰ However, an unexpected complication discovered with this work was the possibility for the several oxidation states to interconvert through a series of dis- and comproportionation reactions triggered by the activator in what is now known as the “redox dynamism”. Namely, trivalent chromium can be readily reduced to the divalent state by the activator. If this oxidation state is not inclined to further reduction, a non-selective oligomerization results. In the opposite scenario, when the monovalent state is reached via further reduction, a selective tri- or tetramerization occurs. Instead if the original trivalent state is preserved throughout the catalytic cycle, for example because of a higher robustness of the trivalent organochromium species, a polymerization reaction will result.

However, if the oxidation states may rapidly interconvert because of the dynamism, the result will be a (very often observed) non-selective oligomerization, enriched in one oligomer and polluted by variable amount of polymer.



Scheme 1.3: Redox dynamisms.

To better highlight the aim of this thesis a brief review of the chromium catalyzed polymerization and oligomerization aspects will be herein reviewed.

1.1 Polymerization

Synthetic polymers and plastics are today ubiquitous, being an integral component of our modern lifestyle. The largest portion of the polymers produced worldwide is occupied by polyethylene. In turn, polyethylene can be categorized into two major groups: HDPE (high density polyethylene) and LDPE (low density polyethylene). Due to extensive branching, LDPE provides less mechanical strength than HDPE and can be employed for specific applications such as plastic bags. The highly linear chain of HDPE provide this polymer with

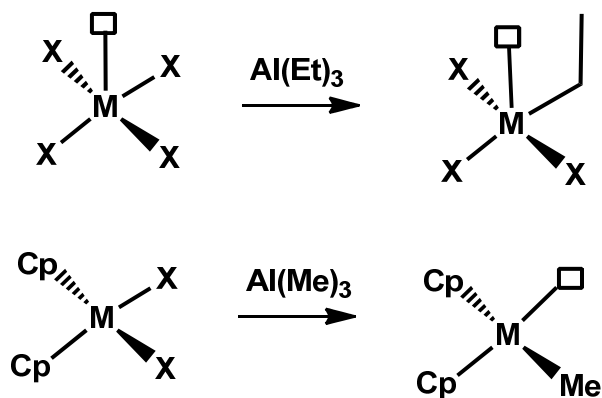
higher strength which is useful for different products like water pipe, fuel tanks, films, wrapping films, etc.

LDPE was first discovered at Imperial Chemical Industries in UK (ICI) in 1930 during an experiment where ethylene gas was subjected to conditions sufficiently harsh to trigger a free radical polymerization.¹¹ Since then, the business of PE and the related research continually expanded in an exponential fashion. Several breakthroughs have been obtained by scientist active in the field. The most famous has been the discovery of the Ziegler-Natta system (a combination of transition metal salts and alkyl aluminum activators).¹² Since then, several generations of Ziegler-Natta catalysts have been discovered and even commercialized for the homo- and heterogeneous phase production of this valuable polymer. The production of polyethylene by using chromium oxide on silica as discovered by Hogan and Banks, (Phillips Petroleum Company patent) is rather unusual and somewhat deviates from the standard Z-N paradigm.¹³ This system does not require the utilization of activators and it is simply considered to be a self-activating system. Obviously this fascinating system has been the target of many mechanistic studies attempting to unveil the secrets of its excellent catalytic performance. The Phillips technique currently accounts for 40% of the worldwide production of HD polyethylene. Another class of polyethylene, called LLDPE (linear low-density polyethylene), displays excellent physical properties in terms of resistance to stress cracking and which make it particularly suitable for sheet and film production. Producing this commercially valuable polymer requires the employment of additives such as 1-butene, 1-hexene and 1-octene. The availability of these co-monomers from petrochemicals cannot satisfy the demand of polymer industry and hence there is need

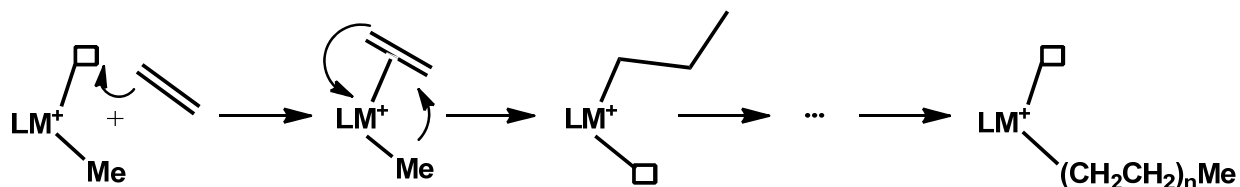
for developing catalytic systems able these species for readily available feedstock such as ethylene.¹⁴

No matter the particular catalytic system employed (homogeneous, heterogeneous, Ziegler-Natta or Phillips) there is agreement that there are some common steps in these catalytic cycles. A prerequisite is the presence of an alkylating function on the catalytically active metal and which in turn must possess a vacant site capable of providing enhanced Lewis acidity. The catalytic cycle proceeds then through the steps of initiation, propagation and eventually termination (Scheme 1.5). The competition between these last two steps determines the molecular weight distribution, while re-activation steps and chain migration may account for polymer branching.

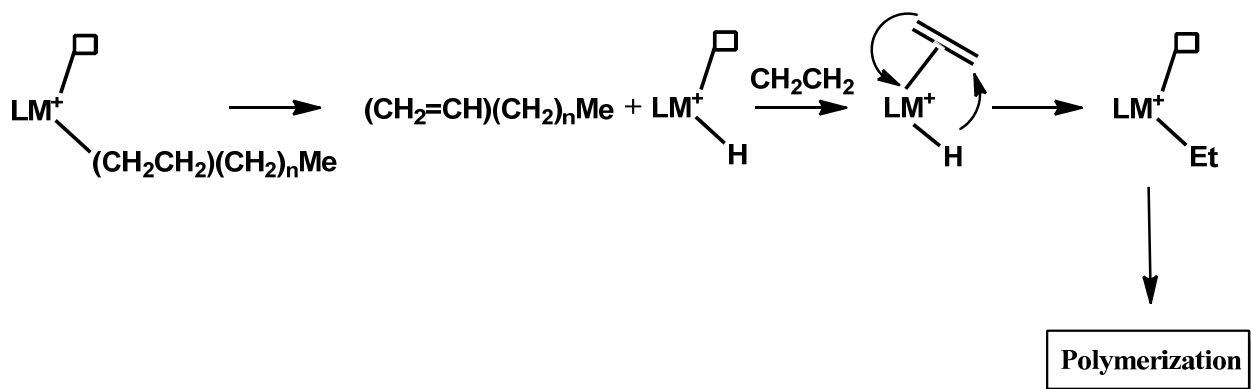
Scheme 1.5



a) Initiation step in olefin polymerization (two different pathways)



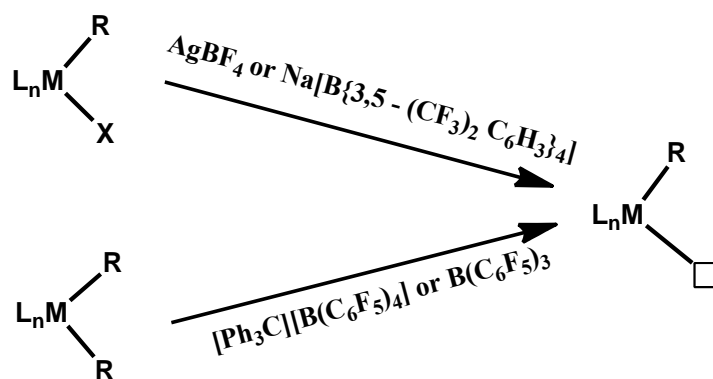
b) Propagation step in olefin polymerization



c) Termination step for polymer chain growth in olefin polymerization
(β -hydride elimination)

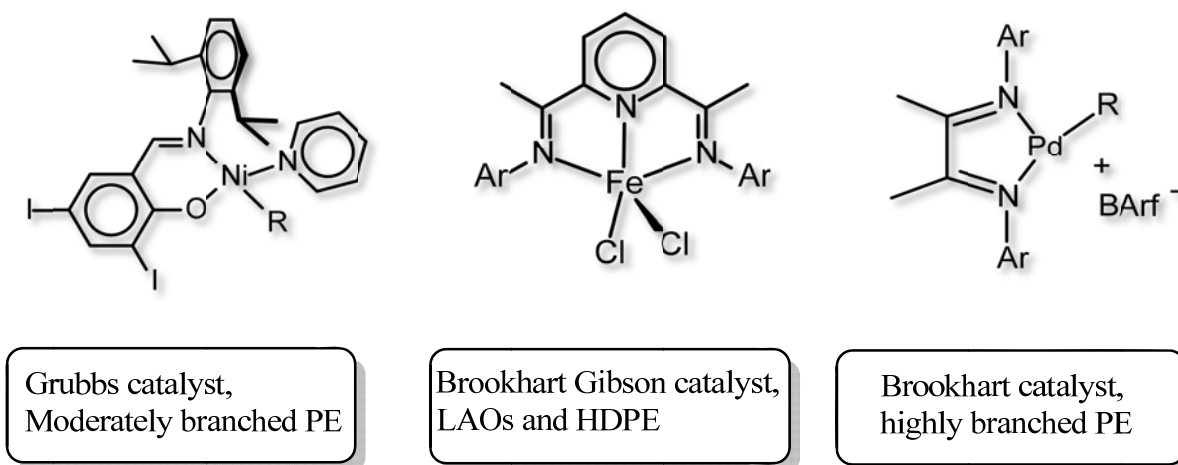
There are two possible initiation steps: the first is abstraction of an anionic or halide ligand (cationization), the second is abstraction of an alkyl group from the metal centre. Each of these two different activation techniques require a specific reagent (Scheme 1.6).¹⁵⁻¹⁶ The propagation step follows a modified, non-redox Cossee-Arlman mechanism (migratory insertion) and termination occurs via several processes the most common being β -hydride elimination. It should be reiterated for the present discussion that according to this mechanism, the catalytic center does not modify the oxidation state throughout the catalytic cycle.

Scheme 1.6



The search for suitable ligands has been an important component of the research in this field. Successful ligands must provide the metal center with a sufficient stability for the organometallic function to prevent reduction and deactivation. Sterics are also very important to control polymer rheology and tacticity.¹⁷ In addition, a successful ligand must display low-possibility of being involved into the organometallic chemistry of the catalytically active species. Finally, by controlling the extent of charge transfer the ligand may also enhance the catalytic behaviour of one system. This last point came recently on the spotlight of research with the finding of ligands capable of promoting polymerization activity with late metals, metals which by being poor Lewis acids, have been previously largely ignored.¹⁸ These ligands are basically based on conjugated Schiff bases and one of their primary characteristics is their ability to very substantially engage in electron transfer reactions (Scheme 1.7).¹⁹

Scheme 1.7



Some of these ligands are so efficient in this that they can promote radical cleavage of thermally robust Al-C bonds.²⁰

1.2 Oligomerization

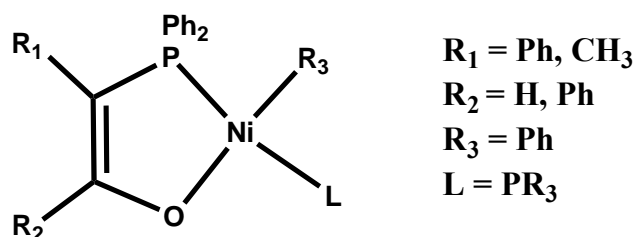
As mentioned above, linear α -olefins (LAO) are important commodity chemicals. The lightest members of this family (1-butene, 1-hexene and 1-octene) occupy the largest portions of the market share due to their employment as essential components in PE manufacturing. The extraction of these olefins from statistical mixtures, as obtained from non-selective oligomerization, is energy intensive and thus expensive. Therefore, the discovery of selective catalysts for their production from ethylene has been and currently is considered the most viable option. Hence, a large body of research is presently carried out in the world to solve this problem.

The first examples of a system producing LAO by using alkyl aluminum and organometallic compound dates back to 1950.²¹ The first example of selective trimerization catalyst instead, goes back to 1991 with the Phillips Petroleum catalyst system. A non-selective oligomerization process may generate two different types of oligomeric distributions. A Schultz-Flory distribution, as for example produced by the SHOP (Shell higher olefin process) process using Ni catalysts, is characterized by a ratio of chain expansion versus chain termination rates independent on the length of the chain. This resolves into a constantly decreasing concentration of the α -olefin as a function of its molecular weight.²² This process is economically viable and no co-catalyst is needed (at least for the SHOP process).²³ A Poisson distribution instead is a Gaussian type of distribution

centered on a certain α -olefin. In both cases, the Cossee-Arlman mechanism is followed. Typically in the chain growth mechanism the oxidation state of the metal centre remains unaltered.

Table 1.2 lists a few non-selective industrial processes. The Alphaselect, α -Sablin and Linear-1 processes display more selectivity in comparison to other processes.²⁴

The SHOP process is one of the best commercial systems, not only for the excellent productivity but also for the lack of need for activators (see Scheme 1.8). In contrast, all the other catalytic systems are Ziegler-Natta type catalysts and necessitate co-catalysts.²⁵



Scheme 1.8: SHOP catalytic system.

The Alphaselect process is typically carried out in an aromatic solvent where it affords a selective mixture of LAOs with even number of carbons (1-butene, 35–40%; 1-hexene, 29–30%; 1-octene, 19–21%; and 1-decene, 11–14%).¹¹ In 2009 the Linde Company in cooperation with Sabcic produced 150000 tons of ethylene oligomers in the range of $\text{C}_4\text{-C}_{18}$ using the proprietary α -Sablin process.²⁶

Table 1.2. Industrial statistical processes for commercial ethylene oligomerization to LAOs

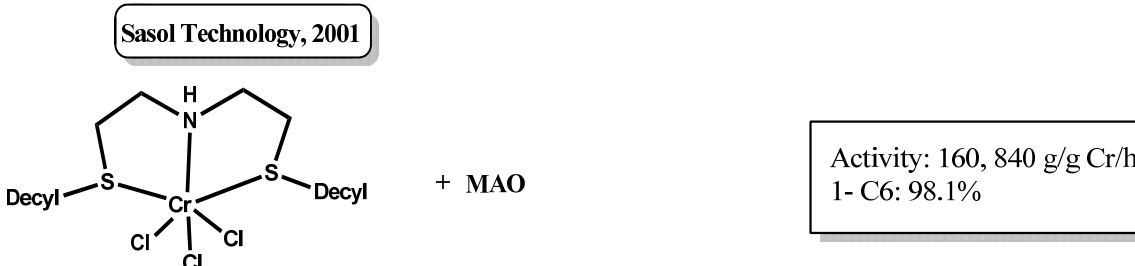
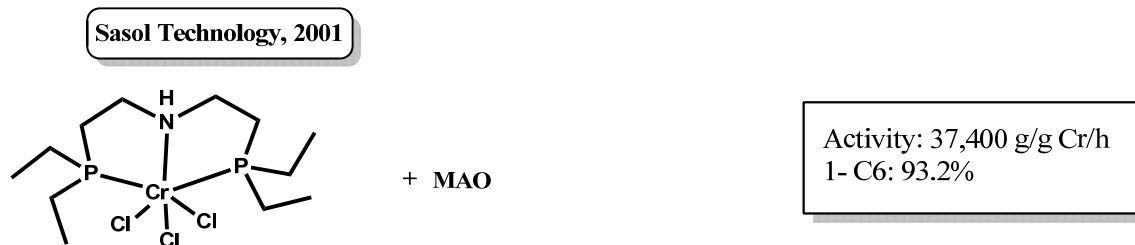
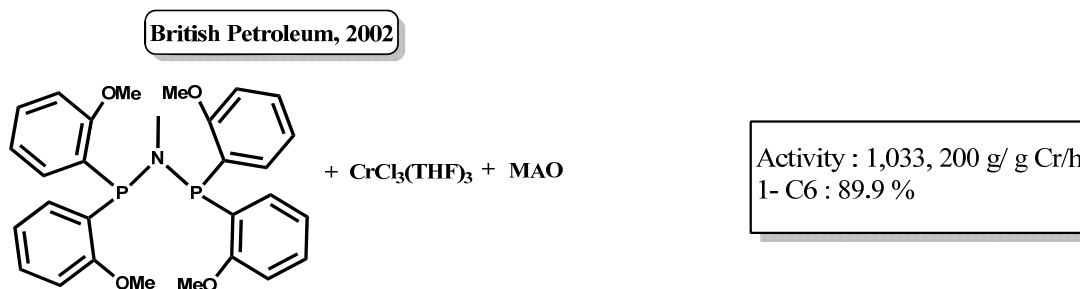
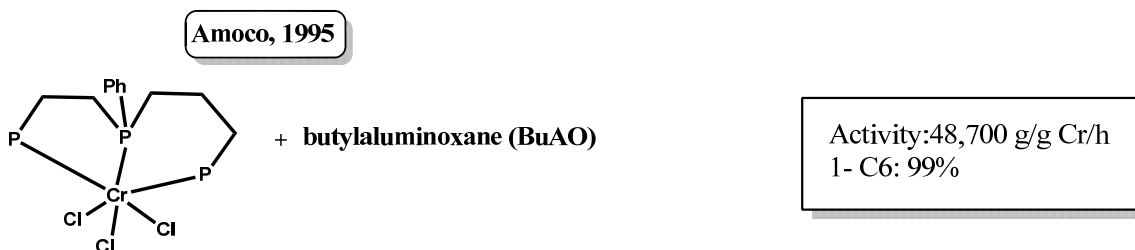
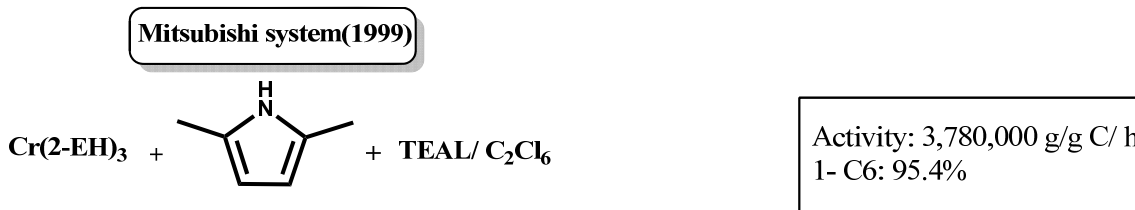
Company name	Process Title	Temperature (°C)	Pressure (MPa)	Product	catalyst
<i>Chevron Phillips</i>	Gulfene	40-100	3-6	C ₄ -C ₃₀₊	Ni complex + Al organic compound
<i>Ineos</i>	Ethyl	100-120	10-12	C ₄ -C ₃₀₊	AlR ₃ + modifier
<i>Shell</i>	SHOP	5-120	2-15	C ₆ -C ₃₀₊	Ni complex
<i>IFPA-Axens</i>	Alphaselect	40-120	0.5-15	C ₄ -C ₁₀	Zr + Al-organic compound + aluminum alkyl
<i>Sabir-Linde</i>	α -Sablin	60-100	2-3	C ₄ -C ₁₈	Zr + Al-organic compound + aluminum alkyl
<i>UOP</i>	Linear-1	30-80	6-14	C ₄ -C ₁₀	Ni complex

As mentioned above, all these processes are believed to follow the non-redox Cosse-Arlman mechanism. Although this mechanism cannot account for selective oligomerization. The redox metallacycle mechanism was therefore conceived to account for the selective formation of 1-hexene and 1-octene. This mechanism was based on the observation that several metals, while in low oxidation state, may couple olefins to generate metallacycles. Whitesides *et al.* found that a platinum metallacyclopentane is more stable than larger

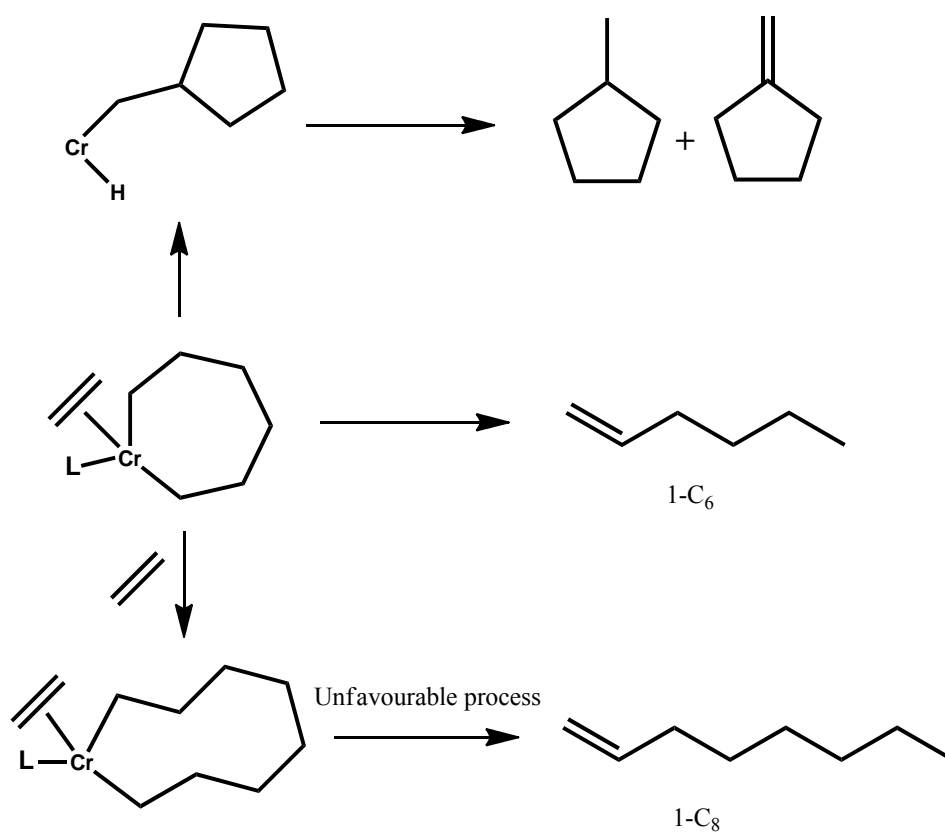
metallacycle rings.²⁷ In turn this account for the ability of this metal to produce 1-butene. Similar observations were made by Schrock for tantalum catalysts.²⁸ In the case of chromium catalysts which account for a large majority of oligomerization systems, a similar mechanism has been established as responsible for the selective trimerization but the metal oxidation state responsible for initiating the redox transformations remained debated.^{10,29}

Catalyst based on Ni triad may produce selective dimerization catalysts while chromium compounds may be selective for trimerization but only seldom dimerization. The explanation for this remarkable difference has to be found in how the nature of the metal affects the stability of the metallacycle versus further ring expansion.³⁰ The smaller atomic dimension of Ni for example while compared to chromium account for an early β -hydride elimination step at the level of the five membered ring. Instead the larger dimensions of chromium do not allow such an elimination and the more stable metallacyclopentane linger on to expand (also due to higher Lewis acidity of the metal) via migratory insertion. The metallacycloheptane ring which leads to the release of 1-hexene, has instead the appropriate instability to eliminate 1-hexene instead of further expanding. The stunning selectivity of some trimerization systems (up to 99%) (Scheme 1.9)³¹ indicates the presence in those systems of a very precise balance between the two crucial steps (expansion/versus elimination). However, this is all related to the ligand system bound to the metal. The situation is further complicated by the observations by Bercaw³² and Gibson³³ that the metallacycle pathway may also been followed for non-selective oligomerization (S-F distribution of LAO). Thus the ligand system plays in this chemistry a critical role in determining the stability of intermediate and driving the reaction either towards an early elimination or ring expansion.

Scheme 1.9: Outstanding catalytic systems for trimerization.



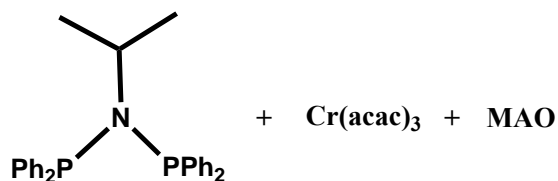
The search for tetramerization catalysts appears to be somewhat at the frontier between selective and non-selective ring expansion mechanism.³⁴ If one assume that a metallacycloheptane may expand into a metallacyclononane, it is truly hard to imagine how the ligand may longer affect the elimination in such a large ring (Scheme 1.10). Therefore, if the metallacycloheptane has the possibility of expanding a statistical distribution of LAOs has to be expected.³⁵ As a matter of fact the only two existing commercial tetramerization systems display selectivity well below the level of trimerization (~70% at the best)^{36a} (See scheme 1.11 for the best catalytic systems for tetramerization).^{36,29c}



Scheme 1.10

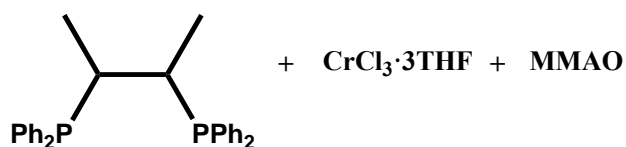
Scheme 1.11: Outstanding catalytic systems for tetramerization.

Sasol Technology, 2004



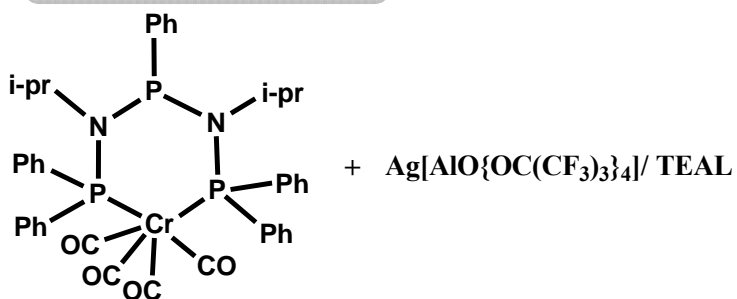
Activity : 285,000 g/g Cr/h
1- C8: 70% ; 1- C6:16%

SK Energy, 2010



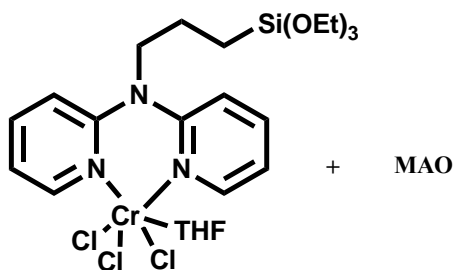
Activity : 1,929,000 g/g Cr/h
1- C8: 64%
1- C6: 22%

Wass *et al.*, 2011



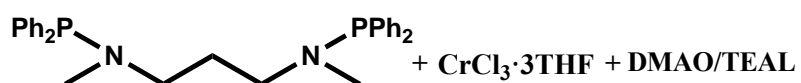
Activity : 37,850 g/g Cr/h
1- C8 : 57.1%
1- C6 : 28.6%

Gambarotta *et al.* 2010



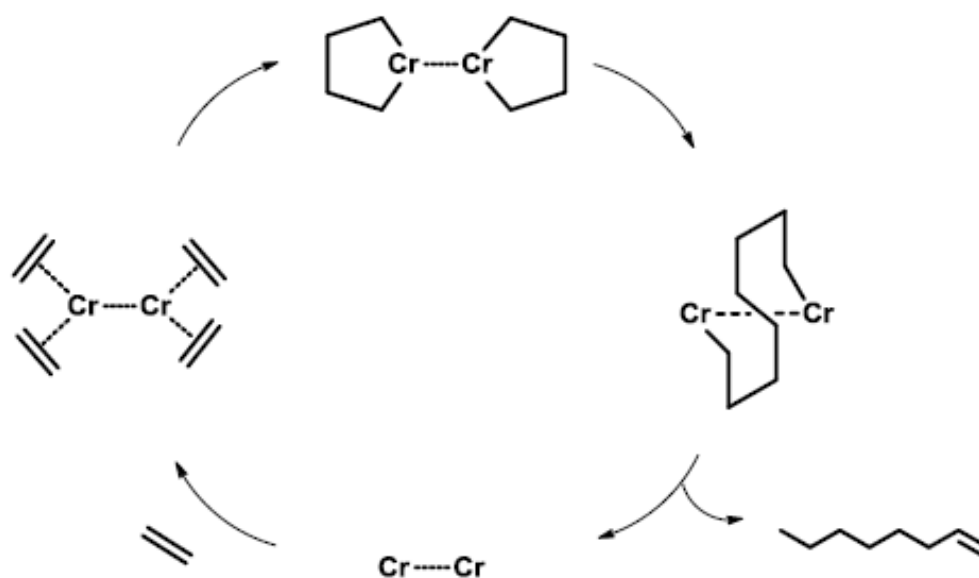
Activity : 66,442 g/g Cr/h
1- C8: 99%

Gambarotta *et al.* 2012



Activity : 25,424 g/g Cr/h
1- C8: 88%

This observation prompted Rosenthal to propose a hypothetical mechanism for a highly-selective tetramerization system. The salient features of the so-called bimetallic mechanism are highlighted in Scheme 1.12. The idea at the basis of this proposal is simple and yet ingenious. Assuming to be able to find an appropriate ligand system capable of hosting a dimeric chromium unit and yet preventing formation of Cr-Cr multiple bond, once the appropriate oxidation state is reached, two chromacyclopentadiene rings may be formed. The idea is that the close proximity of the two metallacycles may trigger an internal “bimetallic elimination forming a C-C bond between the two C4 residues and ultimately to 1-octene.³⁷



Scheme 1.12

Although this proposal has never been substantiated by supporting data, it is by using ligand systems of established binucleating ability that our lab has identified the only two tetramerization systems capable of producing 1-octene with record purity (>90%).^{36d,e}

1.3 Thesis Aim

This thesis was not aimed at the discovery of new and performing catalytic systems. It was more modestly focused on the isolation of complexes arising from the interaction of chromium catalyst precursors with alkyl aluminum activators. Thus, the main effort was for identifying ligand systems that could support chromium catalysts and hopefully provide low-oxidation states with sufficient stability to allow using these complexes as model systems for understanding the basic of selective and non-selective oligomerization. All the synthetic efforts have been directed towards the isolation of species containing both chromium and aluminum and a minor emphasis was given to their catalytic testing. Due to time constraint, we have focused on ligands which are known to embark on electron transfer reactions. It was hoped that those ligand could enable the isolation of complexes bearing chromium in monovalent state.

1.3.1 Chapter 2

Chapter 2 presents the synthesis and testing of chromium iminopyridine complexes and an account of the catalytic activity of these novel catalysts for oligo- and polymerization of ethylene. In particular we have focused on rationalizing the switch of catalytic behavior from polymerization to non-selective oligomerization.

1.3.2 Chapter 3

In this Chapter, a pincer-type bis-phosphinimide based ligand was selected because of the simultaneous presence of the PN functions in a conjugated framework. This ligand enabled the isolation of a mixed valence Cr(I)/Cr(II) species and to generate a series of dimeric chromium complexes. The oxidation-state of chromium has been related to the catalytic behaviour.

1.3.3 Chapter 4

In this chapter we have used a ligand with enhanced tendency to form stable radicals and to promote radical cleavage of organometallic species. The idea was again to analyze the impact on the metal oxidation states and on the organo-chromium intermediates. The results were quite unexpected showing that chromium indeed plays a role but only indirectly.

1.4 References

1. Piringer, O. G.; Baner, A. L. *Plastic packaging: interactions with food and pharmaceuticals*. Eds, Wiley-VCH: Weinheim, Germany, **2008**; p 32.
2. (a) Vogt, D. *Oligomerization of ethylene to higher linear α -olefins; in Applied Homogeneous Catalysis with Organometallic Compounds*; Cornils, B., Herrmann, W. A., Eds.; Wiley-VCH: Weinheim, Germany, **2000**; Chapter 2, p 245; (b) Lappin, G. R.; Sauer, J. D. In *Alpha Olefins Application Handbook*. Marcel Dekkers, INC: New York, **1989**; 37, 1.
3. (a) Cossee, P. *J. Catal.* **1964**, 3, 80; (b) Arlman, E. J. *J. Catal.* **1964**, 3, 89; (c) Arlman, E. J.; Cossee, P. *J. Catal.* **1964**, 3, 99.
4. (a) Carter, A.; Cohen, S. A.; Cooley, N. A.; Murphy, A.; Scutt, J.; Wass, D. F. *Chem. Commun.* **2002**, 858; (b) Mohamed, H.; Bollmann, A.; Dixon, J.; Gokul, V.; Griesel, L.; Grove, C.; Hess, F.; Maumela, H.; Pepler, L. *Appl. Catal., A.* **2003**, 255, 355; (c) Bhaduri, S.; Mukhopadhyay, S.; Kulkarni, S. A. *J. Organomet. Chem.* **2009**, 694, 1297; (d) McGuinness, D. S.; Wasserscheid, P.; Keim, W.; Morgan, D. H.; Dixon, J. T.; Bollmann, A.; Maumela, H.; Hess, F. M.; Englert, U. *J. Am. Chem. Soc.* **2003**, 125, 5272; (e) Zhang, J.; Li, A.; Hor, T. S. A. *Organometallics* **2008**, 27, 4277; (f) Aluri, B. R.; Peulecke, N.; Peitz, S.; Spannenberg, A.; Muller, B. H.; Schulz, S.; Drexler, H. J.; Heller, D.; Al-Hazmi, M. H.; Mosa, F. M.; Wohl, A.; Muller, W.; Rosenthal, U. *Dalton Trans.* **2010**, 39, 7911; (g) Yoshida, T.; Yamamoto, T.; Okada, H.; Murakita, H. (Tosoh Corporation) US 2002/0035029, **2002**; (h) McGuinness, D. S.; Wasserscheid, P.; Keim, W.; Hu, C.; Englert, U.; Dixon, J. T.; Grove, C. *Chem. Commun.* **2003**, 334; (i) Rensburg, W. J.; Grove, C.; Stark, K. B.; Huyser, J. J.; Steynberg, P. J. *Organometallics* **2004**, 23, 1207; (j) Zhang, J.; Braunstein, P.; Hor, T. S. A. *Organometallics* **2008**, 27, 4277; (k) Emrich, R.; Heinemann, O.; Jolly, P. W.; Kruger, C.;

Verhovnik, G. P. J. *Organometallics* **1997**, *16*, 1511; (l) Kohn, R. D. *Angew. Chem. Int. Ed.* **2007**, *46*, 2; (m) Beweries, T.; Fischer, C.; Peitz, S.; Burlakov, V. V.; Perdita, A.; Baumann, W.; Spannenberg, A.; Heller, D.; Rosenthal, U. *J. Am. Chem. Soc.* **2009**, *131*, 4463; (n) Peitz, S.; Peulecke, N.; Aluri, B. R.; Hansen, S.; Muller, B. H.; Spannenberg, A.; Rosenthal, U.; Al-Hazmi, M. H.; Mosa, F. M.; Wohl, A.; Muller, W. *Eur. J. Inorg. Chem.* **2010**, 1167; (o) Rensburg, W. J.; Berg, J.-A.; Stynberg, P. J. *Organometallics* **2007**, *26*, 1000;

5. (a) Dixon, J. T.; Green, M. J.; Hess, F. M.; Morgan, D. H. *J. Organomet. Chem.* **2004**, *689*, 3641; (b) Crewdson, P.; Gambarotta, S.; Djoman, M.C.; Korobkov, I.; Duchateau, R. *Organometallics* **2005**, *24*, 5214; (c) Agapie, T.; Day, M. W.; Henling, L. M.; Labinger, J. A.; Bercaw, J. E. *Organometallics* **2006**, *25*, 2733; (d) Bollmann, A.; Blann, K.; Dixon, J. T.; Hess, F. M.; Killian, E.; Maumela, H.; McGuinness, D. S.; Morgan, D. H.; Neveling, A.; Otto, S.; Overett, M.; Slawin, A. M. Z.; Wasserscheid, P.; Kuhlmann S. *J. Am. Chem. Soc.* **2004**, *126*, 14712.

6. Emrich, R.; Heinemann, O.; Jolly, P.; Kruger, C.; Verhovnik, G. *Organometallics* **1997**, *16*, 1511.

7. (a) Manyik, R.; Walker, W.; Wilson, T. US 3300458, **1967**; (b) Manyik, R.; Walker, W.; Wilson, T. *J. Catal.* **1977**, *47*, 197.

8. (a) Temple, C. N.; Jabri, A.; Crewdson, P.; Gambarotta, S.; Korobkov, I. *Angew. Chem. Int. Ed.* **2006**, *45*, 7050; (b) Temple, C. N.; Gambarotta, S.; Korobkov, I.; Duchateau, D. *Organometallics* **2007**, *26*, 4598; (c) Albahily, K.; Koç, E.; Al-Baldawi, D.; Savard, D.; Gambarotta, S.; Burchell, T. J.; Duchateau, R. *Angew. Chem. Int. Ed.* **2008**, *47*, 5816.

9. (a) Thapa, I.; Gambarotta, S.; Korobkov, I.; Murugesu, M.; Budzelaar, P. H. M. *Organometallics* **2012**, *31*, 486; (b) Albahily, K.; Shaikh, Y.; Ahmed, Z.; Korobkov, I.; Gambarotta, S.; Duchateau, R. *Organometallics* **2011**, *30*, 4159; (c) Albahily, K.; Fomitcheva, V.; Shaikh, Y.; Sebastiao, E.; Gorelsky, S. I.; Korobkov, I.; Gambarotta, S.; Duchateau, R. *Organometallics* **2011**, *30*, 4201; (d) Albahily, K.; Fomitcheva, V.; Korobkov, I.; Murugesu, M.; Gorelsky, S. I. *J. Am. Chem. Soc.* **2011**, *133*, 6380; (e) Vidyaratne, I.; Nikiforov, G. B.; Gorelsky, S. I.; Gambarotta, S.; Duchateau, R.; Korobkov, I. *Angew. Chem. Int. Ed.* **2009**, *48*, 6552.
10. Jabri, A.; Mason, C. B.; Sim, Y.; Gambarotta, S.; Burchell, T. J.; Duchateau, R. *Angew. Chem. Int. Ed.* **2008**, *47*, 9717.
11. Seymour, R.B. *History of polyolefins*. D. Riedel Pub. Co., Dordrecht, **1986**.
12. (a) Ziegler, K.; Holzkamp, E.; Breil, H.; Martin, H. *Angew. Chem., Int. Ed.* **1955**, *67*, 541; (b) Ziegler, K.; Breil, H.; Martin, H.; Holzkamp, E. *German Patent* 973, 626, **1960**; (c) Natta, G.; Pino, P.; Corradini, P.; Danusso, F.; Mantica, E.; Mazzanti, G.; Moraglio, G. *J. Am. Chem. Soc.* **1955**, *77*, 1708; (d) Chen, E.; Marks, T. *Chem. Rev.* **2000**, *100*, 1391.
13. (a) Hogan, J. P.; Banks, R. L. Phillips Petroleum Co. Belg. Pat. 530617, **1955**; (b) Hogan, J. P.; Banks, R. L. Phillips Petroleum Co. U. S. Pat. 2825721, **1958**.
14. Bercaw, E. J. KFUPM, *Lecture Series on Organotransition Metal Chemistry and Olefin Polymerization*, **2011**.
15. Britovsek, G. J. P.; Gibson, V.; Wass, D. F. *Angew. Chem. Int. Ed.* **1999**, *38*, 428.
16. Brookhart, M.; Grant, B.; Volpe, A. F. *Organometallics* **1992**, *11*, 3920.

17. Coates, G. W. *Chem. Rev.* **2000**, *100*, 1223.
18. (a) Killian, C. M.; Tempel, D. J.; Johnson, L. K.; Brookhart, M. S. *J. Am. Chem. Soc.* **1996**, *118*, 11664; (b) Johnson, L. K.; Killian, C. M.; Brookhart, M. S. *J. Am. Chem. Soc.* **1995**, *117*, 6414; (c) Britovsek, G. J. P.; Gibson, V. C.; Kimberley, B. S.; Maddox, P. J.; McTavish, S. J.; Solan, G. A.; White, A. J. P.; Williams, D. J. *Chem. Commun.* **1998**, 849; (d) Small, B. L.; Brookhart, M.; Bennett, A. M. A. *J. Am. Chem. Soc.* **1998**, *120*, 4049; (e) Wang, C.; Friedrich, S.; Younkin, T. D.; Li, R. T.; Grubbs, R. H.; Bansleben, D. A.; Day, M. W. *Organometallics* **1998**, *17*, 3149.
19. (a) Sugiyama, H.; Korobkov, I.; Gambarotta, S.; Moeller, A.; Budzelaar, P. H. M. *Inorg. Chem.* **2004**, *43*, 5771; (b) de Bruin, B.; Bill, E.; Bothe, E.; Weyhermueller, T.; Wieghardt, K. *Inorg. Chem.* **2000**, *39*, 2936; (c) Budzelaar, P. H. M.; de Bruin, B.; Gal, A. W.; Wieghardt, K.; van Lenthe, J. H. *Inorg. Chem.* **2001**, *40*, 4649; (d) Knijnenburg, Q.; Hetterscheid, D.; Kooistra, T. M.; Budzelaar, P. H. M. *Eur. J. Inorg. Chem.* **2004**, *6*, 1204; (e) Vidyaratne, I.; Gambarotta, S.; Korobkov, I.; Budzelaar, P. H. M. *Inorg. Chem.* **2005**, *44*, 1187; (f) Bart, S. C.; Lobkovsky, E.; Chirik, P. J. *J. Am. Chem. Soc.* **2004**, *126*, 13794; (g) Scott, J.; Gambarotta, S.; Korobkov, I.; Knijnenburg, Q.; de Bruin, B.; Budzelaar, P. H. M. *J. Am. Chem. Soc.* **2005**, *127*, 17204.
20. Shuster, V.; Gambarotta, S.; Nikiforov, G. B.; Korobkov, I.; Budzelaar, P. H. M. *Organometallics* **2012**, *31*, 7011.
21. Ziegler, K.; Gellert, H.; Kuhlhorn, H.; Martin, H.; Meyer, K.; Nagel, K.; Sauer, H.; Zoser, K. *Angew. Chem. Int. Ed.* **1952**, *64*, 323.

22. (a) Schulz, G. V. *Z. Phys.chem.Abt.B* **1935**, 379; (b) Flory, P. J. *J. Am. Chem. Soc.* **1936**, 58, 1677.
23. Vogt, D. In *Applied Homogeneous Catalysis with Organometallic Compounds*; Cornils, B., Herrmann, W. A., Ed.; VCH: Weinheim, Germany, **1996**; Chapter 2, p 245.
24. Lappin, G. R.; Sauer, J. D. In *Alpha Olefins Application Handbook*. Marcel Dekkers, INC: New York, **1989**, 37, 1.
25. Keim W. *Angew. Chem. Int. Ed.* **1990**, 29, 235.
26. Plaksunov, T. K.; Belov, G. P.; Potapov, S. S. In *Higher Linear α -Olefins and Ethylene Copolymers on Their Basis: Production and Application* IPKhF Ross. Akad. Nauk, Chernogolovka, **2008**, p 59.
27. McDermott, J. X.; White, J. F.; Whitesides, G. M. *J. Am. Chem.Soc.* **1973**, 95, 4451.
28. (a) McLain, S. J.; Schrock, R. R. *J. Am. Chem. Soc.* **1978**, 100, 1315; (b) Schrock, R. R.; McLain, S. J.; Sancho, J. *Pure Appl. Chem.* **1980**, 52, 729.
29. (a) Kohn, R. D.; Haufe, M.; Mihan, S.; Lilge, D. *Chem. Commun.* **2000**, 1927; (b) Bowen, L. E.; Haddow, M. F.; Orpen, A. G.; Wass, D. *Dalton Trans.* **2007**, 1160; (c) Licciulli, S.; Thapa, I.; Albahily, K.; Korobkov, I.; Gambarotta, S.; Duchateau, R.; Chevalier, R.; Schuhen, K. *Angew. Chem., Int. Ed.* **2010**, 49, 9225; (d) Vidyaratne, I.; Nikiforov, G. B.; Gorelsky, S. I.; Gambarotta, S.; Duchateau, R.; Korobkov, I. *Angew. Chem., Int. Ed.* **2009**, 48, 6552; (e) Dulai, A.; de Bod, H.; Hanton, M. J.; Smith, D. M.; Downing, S.; Mansell, S. M.; Wass, D. F. *Organometallics* **2009**, 28, 4613; (f) McGuinness, D. S. *Chem. Rev.* **2011**, 111, 2321; (g) van Rensburg, W. J.; Grove, C.; Steynberg, J. P.; Stark, K. B.; Huyser, J. J.;

Steynberg, P. J. *Organometallics* **2004**, *23*, 1207; (h) Ittel, S.; Johnson, L. K.; Brookhart, M. *Chem. Rev.* **2000**, *100*, 1169.

30. Speiser, F.; Braunstein, P.; Saussine, L. *Acc. Chem. Res.* **2005**, *38*, 784.

31. (a) Reagan, W. K. (Phillips Petroleum Company) EP 0417477; (b) Freeman, J. W.; Buster, J. L.; Kundsén, R. D. (Phillips Petroleum Company) US 5,856,257, **1999**; (c) Freeman, J. W.; Buster, J. L.; Kundsén, R. D. (Phillips Petroleum Company) US 5,856,257, **1999**; (d) Wu, F. J. (Amoco Corporation) US 5,811,618, **1995**; (f) Wass, D. F. (BP Chemicals Ltd) WO 02/04119, **2002**; (g) Carter, A.; Cohen, S. A.; Cooley, N. A.; Murphy, A.; Scutt, J.; Wass, D. F. *Chem. Commun.* **2002**, 858; (h) McGuinness, D. S.; Wasserscheid, P.; Keim, W.; Hu, C.; Englert, U.; Dixon, J. T.; Grove, C. *Chem. Commun.* **2003**, 334; (i) Dixon, J. T.; Grove, J. J. C.; Wasserscheid, P.; McGuinness, D. S.; Hess, F. M.; Maumela, H.; Morgan, D. H.; Bollmann, A. (Sasol Technology (Pty) Ltd) WO 03053891, **2001**; (j) Dixon, J. T.; Wasserscheid, P.; McGuinness, D. S.; Hess, F. M.; Maumela, H.; Morgan, D. H.; Bollmann, A. (Sasol Technology (Pty) Ltd) WO 03053890, **2001**; (k) McGuinness, D. S.; Wasserscheid, P.; Keim, W.; Morgan, D. H.; Dixon, J. T.; Bollmann, A.; Maumela, H.; Hess, F. M.; Englert, U. *J. Am. Chem. Soc.* **2003**, *125*, 5272;

32. (a) Agapie, T.; Labinger, J. A.; Bercaw, J. E. *J. Am. Chem. Soc.* **2007**, *129*, 14281; (b) Agapie, T.; Schofer, S. J.; Labinger, J. A.; Bercaw, J. E. *J. Am. Chem. Soc.* **2004**, *126*, 1304.

33. Tomov, A. K.; Chirinos, J. J.; Long, R. J.; Gibson, V. C.; Elsegood, M. R. J. *J. Am. Chem. Soc.* **2006**, *128*, 7704.

34. (a) Overett, M. J.; Blann, K.; Bollmann, A.; Dixon, J. T.; Haasbroek, D.; Killian, E.; Maumela, H.; McGuinness, D. S.; Morgan, D. H. *J. Am. Chem. Soc.* **2005**, *127*, 10723.

35. Tomov, A. K.; Chirinos, J. J.; Jones, D. J.; Long, R. J.; Gibson, V. C. *J. Am. Chem. Soc.* **2005**, *127*, 10166.
36. (a) Bollmann, A.; Blann, K.; Dixon, J. T.; Hess, F. M.; Killian, E.; Maumela, H.; McGuinness, D. S.; Morgan, D. H.; Neveling, A.; Otto, S.; Overett, M.; Slawin, A. M. Z.; Wasserscheid, P.; Kuhlmann S. *J. Am. Chem. Soc.* **2004**, *126*, 14712; (b) Han, T. K.; Ok, M. A.; Chae, S. S.; Kang, S. O.; Jung, J. H. WO Patent 2008/088178(SK Energy), **2008**; (c) Dulai, A.; McMullin, C. L.; Tenza, K.; Wass. D. F. *Organometallics* **2011**, *30*, 935; (d) Shaikh, Y.; Albahily, K.; Sutcliffe, M.; Fomitcheva, V.; Gambarotta, S.; Korobkov, I.; Duchateau, R. *Angew. Chem., Int. Ed.* **2012**, *51*, 1366.
37. Peitz, S.; Aluri, B. R.; Peulecke, N.; Müller, B. H.; Wöhl, A.; Müller, W.; Al-Hazmi, M. H.; Mosa, F. M.; Rosenthal, U. *Chem. Eur. J.* **2010**, *16*, 7670.

Chromium Iminopyridine Complexes as Catalyst Precursors for Ethylene Polymerization and Oligomerization

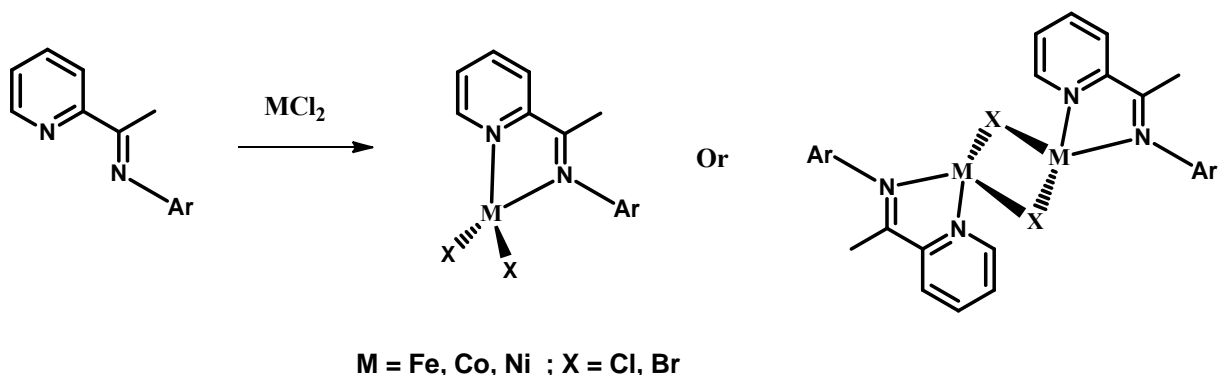
2.1 Introduction

Chromium catalyzed oligo- and polymerization of ethylene is a commercially valuable process¹⁻³ and which has increasingly attracted the attention of the academic sector for the mechanistic challenges associated with selectivity issues.⁴ In the vast library of supporting ligands enabling preparation of catalysts, 2,6-bis(imino)pyridine occupies a special place.^{5,6} Not only it has enabled Z-N catalysis with late metals, thus breaking a paradigm in the field,^{5,7} but it has also provided catalysts of very high activity as well as switchable catalysts.⁸ In combination with chromium, this particular ligand system has also provided potent polymerization catalysts while oligomerization remained strangely absent.⁹ This is particularly curious given the well-established versatility of chromium to provide oligomerization catalysts, including examples of very high selectivity.¹

Complexes of bis-iminopyridine and chromium have been studied first by Esteruelas obtaining potent ethylene polymerization catalysts.⁹ Independent work in our lab has highlighted the ability of the same ligand to support mono- and divalent Cr species. These complexes, in spite of the low oxidation state, also have shown high activity as polymerization catalysts.¹⁰

In the present study, we have modified the 2,6-bis(imino)pyridine ligand by simply removing one of the two imino functions. Previous work by Gibson and Erker on different metals (Fe, Co, Ni), and using the same iminopyridyl ligand, showed possibility of generating two different structures, both monomeric and dimeric (see Scheme 2.2).¹¹⁻¹³ The type of structure is determined by both metal halides and stereo/electronic features of the substituents carried by the pyridine ring. Erker *et al.* reported for both Fe and Co complexes that bulky groups afford complexes of monomeric nature while less sterically demanding generates dimers.¹²

Scheme 2.2



The competition between chain-transfer and chain-growth migratory insertion processes is the factor that can switch the catalytic behaviour from ethylene polymerization to oligomerization.¹⁴ The energy barrier for the chain-transfer reaction increases when a sterically demanding axial group is present around the metal centre and leads to higher molecular weight olefin or polymers. The ligand proposed for this study, provides only moderate steric hindrance and, therefore, it can be expected to promote formation of light oligomers.¹⁵

We have also used these precursors to investigate the aggregation with a variety of aluminate activators. This is in an attempt to shed light on the activation mechanism. We have also attempted the isolation of intermediates of the catalytic cycle by employing DEAC, TEAL and TMA and both di- and trivalent chromium precursors. By decreasing the ligand steric hindrance, we were hoping to preserve the same high activity of the bis-imino pyridine ligand and to introduce selectivity by controlling the aggregation of the aluminates activators. The ultimate goal was to shift the reaction towards oligomerization.

Last but not least, we were looking at isolating species which, by having alkyl aluminum residues directly bonded to the chromium center, might act as self-activating catalysts not requiring further activation. In turn, this was expected to provide important information for further catalyst design.

2.2 Experimental

All reactions were carried out under inert atmosphere by using drybox or Schlenk techniques. Solvents were dried using an aluminum oxide solvent purification system. $\text{CrCl}_2(\text{THF})_2$ and $\text{CrCl}_3(\text{THF})_3$ were prepared according to standard procedure. Methylolithium (3.0 M in diethoxymethane) and *n*-butyllithium (2.5 M in hexanes) reagent were purchased from Aldrich and used as received. Methylaluminoxane (MAO, 30% in toluene) was purchased from Albemarle Corporation, $\text{Al}(\text{Et})_3$ from Strem and used as received. Me_3Al depleted MAO (DMAO) was prepared by removing all volatile material at 40 °C for 6 hours *in vacuo* (2 mmHg). Elemental analysis was performed with a Perkin-Elmer 2400 CHN analyzer. Samples for magnetic susceptibility measurement were prepared and sealed in a dry box equipped with an analytical balance. Measurements were carried out

with a Johnson Matthey Magnetic Susceptibility balance at room temperature. NMR data were collected on a Bruker Avance 300 MHz spectrometer at 300 K. Data for X-ray crystal structure determination were obtained with a Bruker diffractometer equipped with a 1K Smart CCD area detector. Mass spectra were recorded on a Micromass Quattro-LC Electrospray-Triple Quadrupole Mass Spectrometer. A 300 mL Parr reactor equipped with a temperature control instrument and stirrer was used for oligomerization reactions.

2.2.1 Synthesis of the ligand

Preparation of 2-pyridyl-methyl-N-2,6-diisopropylphenylimine (**2a**)

A mixture of 2-acetylpyridine (6.7 mL, 60 mmol) and 2,6-diisopropylaniline (11.3 mL, 60 mmol) in ethanol (120 mL) in the presence of catalytic amount of trifluoroacetic acid (0.46 ml, 6 mmol) was refluxed overnight under nitrogen atmosphere. The volume of the resulting solution was reduced *in vacuo* and the solution was kept at -35 °C for 2 days, upon which, yellowish crystals of **2a** were obtained. (15.48 g, mmol, 92 %). ¹H NMR (300 MHz, CDCl₃) δ: 1.13 (d, J = 6.9 Hz, 12H), 2.19 (s, 3H), 2.73 (heptet, J = 6.9, 2H), 7.06-7.16 (m, 3H) 7.37-7.39 (m, 1H), 7.79 (m, 1H), 8.34 (d, J = 8, 1H), 8.86 (d, J = 4.8, 1H). ¹³C NMR (400 MHz, CDCl₃) δ: 166.9, 156.4, 148.5, 146.4, 136.5, 135.8, 124.8, 123.6, 122.9, 121.3, 28.2, 23.2, 22.9, 17.3. Elemental Analysis Calcd. (Found) for C₁₉H₂₄N₂: C 81.38 (81.40), H 8.63 (8.66), N 9.99 (9.95). ESI-MS *m/z* = 280.41 ([M+H]⁺).

2.2.2 Synthesis of Chromium Complexes

Preparation of $\{[(2,6\text{-Me}_2\text{C}_6\text{H}_3)\text{N-C}(\text{C}_5\text{H}_4\text{N})(=\text{CH}_2)]\text{Cr}(\mu^2\text{-Cl})\}_2 \{\text{AlCl}_3(\text{CH}_2\text{CH}_3)\}_2$ (**2.1**)

CrCl₃(THF)₃ (0.38 g, 1 mmol) and **2a** (0.28 g, 1 mmol) were mixed in toluene (5 mL) and stirred for 18 h. Neat DEAC (0.72 g, 6 mmol) was added dropwise to the resulting green suspension, affording a brown mixture. The small amount of insoluble material was eliminated by centrifugation. The resulting solution was allowed to stand overnight at -35 °C, upon which, brown crystals of **2.1** separated. The crystalline mass was isolated by filtration, washed with cold hexane and dried *in vacuo* (0.51 g, 0.49 mmol, 49 %), $\mu_{\text{eff}} = 4.95 \mu_{\text{B}}$. Elemental Analysis Calcd. (Found) for C₄₂H₅₈Al₂Cl₈Cr₂N₄: C 47.57 (47.60), H 5.51 (5.55), N 5.28 (5.30). ESI-MS $m/z = 1060.52$ ([M+H]⁺).

Preparation of $\{[(2,6\text{-Me}_2\text{C}_6\text{H}_3)\text{N-C}(\text{C}_5\text{H}_4\text{N})(=\text{CH}_2)]\text{Cr}(\mu^2\text{-Cl})\}_2\{\text{AlCl}(\text{CH}_2\text{CH}_3)_3\}_2$ (2.2**)**

CrCl₂(THF)₂ (0.27 g, 1 mmol) and **2a** (0.28 g, 1 mmol) were mixed in toluene (5 mL) and stirred for 18 h. Neat TEAL (0.11 g, 1 mmol) was added dropwise to the resulting brown suspension, affording a dark red solution. A small amount of insoluble material was eliminated by centrifugation. The resulting solution was allowed to stand overnight at -35 °C, upon which, brown crystals of **2.2** separated. The crystalline mass was isolated by filtration, washed with cold hexane and dried *in vacuo* (0.46 g, 0.45mmol, 45 %), $\mu_{\text{eff}} = 4.94 \mu_{\text{B}}$. Elemental Analysis Calcd. (Found) for C₅₀H₇₈Al₂Cl₄Cr₂N₄: C 58.03 (58.01), H 7.6 (7.58), N 5.41 (5.37). ESI-MS $m/z = 1034.95$ ([M+H]⁺).

Preparation of $\{[(2,6\text{-Me}_2\text{C}_6\text{H}_3)\text{N-C}(\text{C}_5\text{H}_4\text{N})(=\text{CH}_2)]\text{Cr}(\mu^2\text{-Cl})\}_2\{\text{AlCl}_2(\text{CH}_3)_2\}_2$ (2.3**)**

CrCl₃(THF)₃ (0.38 g, 1 mmol) and **2a** (0.28 g, 1 mmol) were mixed in toluene (5 mL) and stirred for 18 h. Neat TMA (0.29 g, 4 mmol) was added dropwise to the resulting green suspension, affording a brown solution. A small amount of insoluble material was

eliminated by centrifugation. The resulting solution was allowed to stand overnight at -35 °C, upon which, brown crystals of **2.3** separated. The crystalline mass was isolated by filtration, washed with cold hexane and dried *in vacuo* (0.35g, 0.35 mmol, 35 %), $\mu_{\text{eff}} = 4.88 \mu_{\text{B}}$. Elemental Analysis Calcd. (Found) for $\text{C}_{42}\text{H}_{60}\text{Al}_2\text{Cl}_6\text{Cr}_2\text{N}_4$: C 50.87 (50.84), H 6.10 (6.09), N 5.65 (5.61). ESI-MS $m/z = 990.14$ ($[\text{M}+\text{H}]^+$).

Preparation of $\{[(2,6\text{-Me}_2\text{C}_6\text{H}_3)\text{N}-\text{C}(\text{C}_5\text{H}_4\text{N})(=\text{CH}_2)]\text{Cr}(\text{CH}_3)\}$ (**2.4**)

A solution of **2a** (0.56 g, 2 mmol) in THF (8 mL) was treated with $\text{CrCl}_3(\text{THF})_3$ (0.38 g, 1 mmol) with stirring. The green suspension was cooled at -30 °C for 10 min. While stirring, a solution of methyllithium (1 mL, 3 mmol) was added dropwise. The colour of the solution turned from green to dark brown. After 30 min of further stirring the solvent was removed *in vacuo* and replaced with toluene. The solution was then centrifuged to remove LiCl. After filtration, the solvent was removed and replaced with ether. Cooling the solution at -35 °C for 5 days yielded green crystals of **2.4**, which were filtered, washed with cold hexane and dried *in vacuo* (0.188 g, 0.3 mmol, 30 %) $\mu_{\text{eff}} = 3.88 \mu_{\text{B}}$. Elemental Analysis Calcd. (Found) for $\text{C}_{39}\text{H}_{49}\text{CrN}_4$: C 74.81 (74.85), H 7.89 (7.88), N 8.95 (8.93). ESI-MS $m/z = 625.34$ ($[\text{M}+\text{H}]^+$).

2.3 X-Ray Diffraction

Suitable crystals were selected, mounted on thin, glass fibers with paraffin oil, and cooled to the data collection temperature. Data collections were performed with three batch runs at $\text{phi} = 0.00$ deg (600 frames), at $\text{phi} = 120.00$ deg (600 frames), and at $\text{phi} = 240.00$

deg (600 frames). Initial unit-cell parameters were determined from 60 data frames collected at different sections of the Ewald sphere. Semiempirical absorption corrections based on equivalent reflections were applied. The systematic absences and unit-cell parameters were consistent for the reported space groups. The structures were solved by direct methods, completed with difference Fourier syntheses, and refined with full-matrix least-squares procedures based on F2. All non-hydrogen atoms were refined with anisotropic displacement parameters with the exception of uncoordinated solvent lattice molecules. All scattering factors and anomalous dispersion factors are contained in the SHELXTL6.12 program library. Relevant data on crystal structure solution and refinement are given Table 2.1.

Table 2.1. Crystal data and refinements for **2.1 – 2.4**.

	Complex 2.1	Complex 2.2	Complex 2.3	Complex 2.4
Formula	C ₆₄ H _{84.50} Al ₂ Cl _{7.50} Cr ₂ N ₄	C _{35.50} H ₅₁ AlCl ₂ CrN ₂	C _{29.75} H ₄₀ AlCl ₃ CrN ₂	C ₃₉ H ₄₉ CrN ₄
MW	1333.69	655.66	610.97	625.82
Space group	Monoclinic, P2(1)/n	Monoclinic, P2(1)/n	Monoclinic, P2(1)/n	Triclinic, P-1
<i>a</i> (Å)	14.3224(4)	14.6642(3)	14.1638(4)	8.9297(4)
<i>b</i> (Å)	11.4131(3)	11.3265(2)	11.4616(3)	12.0575(5)
<i>c</i> (Å)	21.8096(6)	22.4806(4)	21.5766(5)	17.3081(7)
α, (deg)	90	90	90	73.092(2)
β, (deg)	95.710(2)	96.2910(10)	96.1410(10)	79.498(2)
γ, (deg)	90	90	90	80.000(2)
<i>V</i> (Å³)	3547.37(17)	3711.41(12)	3482.64(16)	1738.66(13)
<i>Z</i>	2	4	4	2
Radiation	0.71073	0.71073	0.71073	0.71073
T (K)	200(2)	200(2)	200(2)	200(2)
D_{calc} (gcm⁻³)	1.249	1.173	1.165	1.195
μ_{calc} (mm⁻¹)	0.652	0.501	0.603	0.361
<i>F</i>000	1396	1396	1282	670
<i>R</i>, <i>R</i>_w^{2a}	0.0467, 0.1308	0.0644, 0.2019	0.0459, 0.1374	0.0398, 0.1064
GoF	1.012	1.027	1.016	1.023

$$R = \frac{\sum |F_o| - |F_c|}{\sum |F|}. \quad R_w = \left[\frac{\sum (|F_o| - |F_c|)^2 / \sum w F_o^2}{\sum w F_o^2} \right]^{1/2}.$$

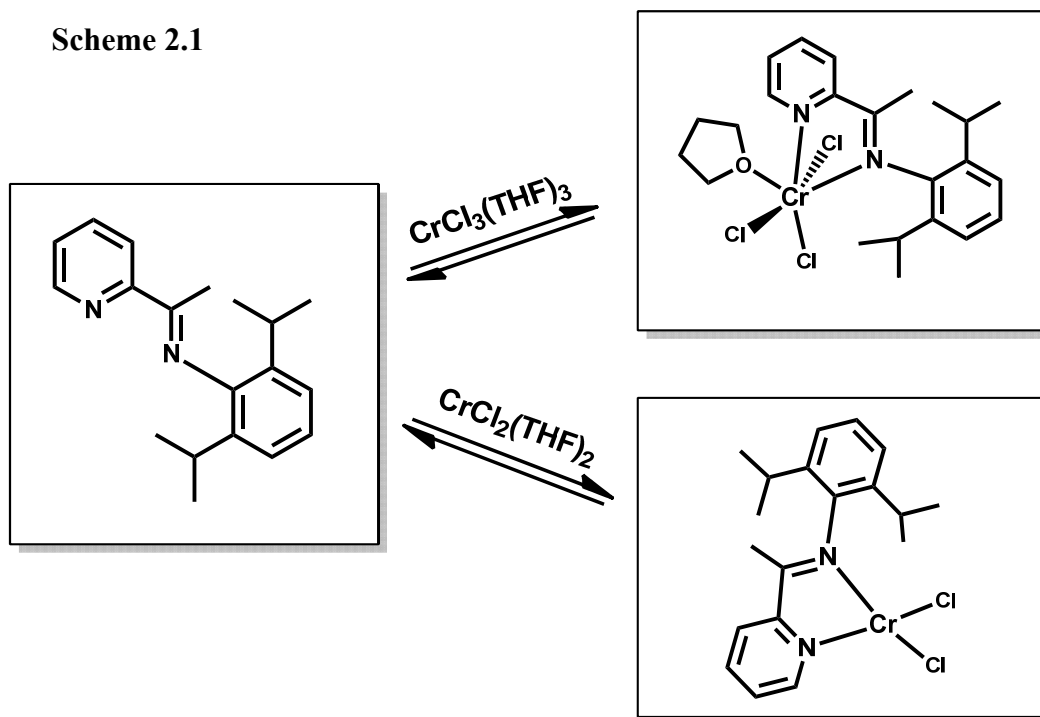
2.4 General Oligomerization and polymerization procedure

Catalytic runs were carried out in a 200 mL high pressure Buchi reactor containing a heating/cooling jacket. A measured amount of catalyst was dissolved in 100 mL of toluene or MeCy under N₂ prior to loading the reaction vessel. Solutions were heated using a thermostatic bath and charged with ethylene, maintaining the pressure throughout the run. The reaction mixtures were cooled to 0 °C before releasing the pressure and quenching with MeOH and HCl and the polymers obtained were isolated by filtration, rinsed and completely dried prior to measuring the mass.

2.5 Results and Discussion

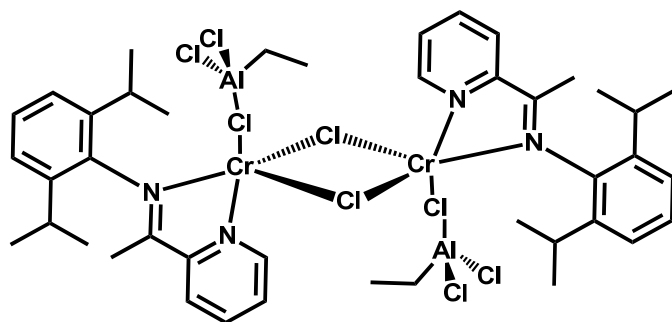
Treatment of 2-pyridyl-methyl-N-2,6-diisopropylphenylimine with either CrCl₃(THF)₃ or CrCl₂(THF)₂ respectively gave green or brown suspensions in toluene. Attempts to isolate products in crystalline form, in either toluene or THF were unsuccessful due to very poor solubility (Scheme 2.1).

Scheme 2.1

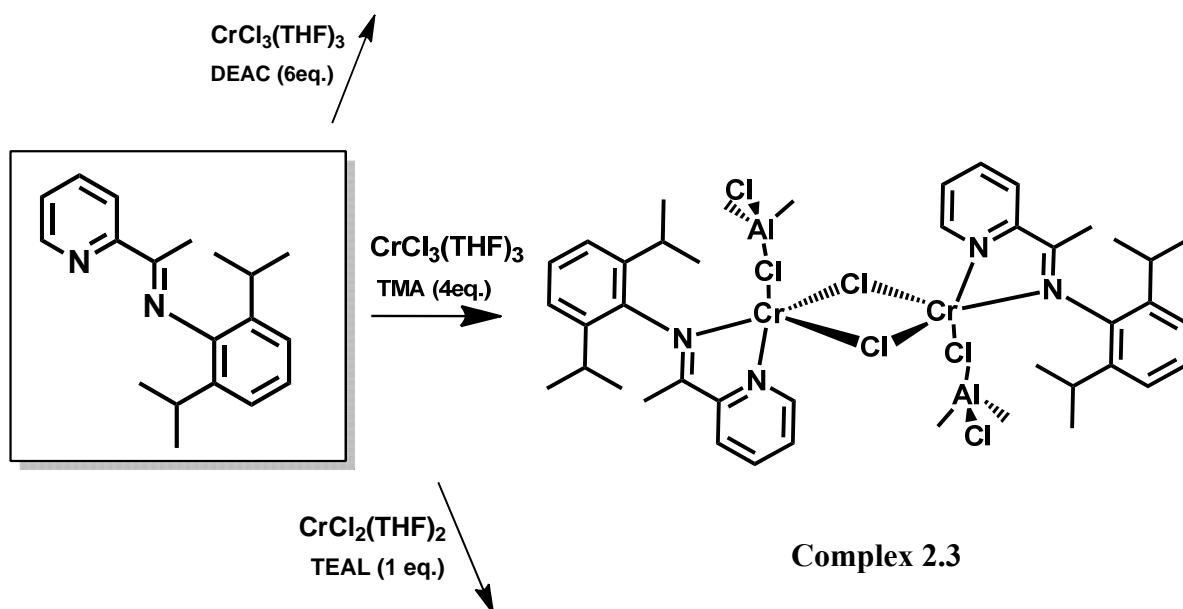


Aiming at forming complexes of higher solubility, we have treated these in situ generated materials with three different alkyl aluminum reagents (AlMe_3 , AlEt_2Cl , and AlEt_3) in various stoichiometric amounts. For this purpose, a suspension of $\text{CrCl}_3(\text{THF})_3$ in toluene and in the presence of the ligand 2-pyridyl-methyl-N-2,6-diisopropylphenylimine (**2a**) was treated with DEAC and TMA yielding ($\{[(2,6\text{-Me}_2\text{C}_6\text{H}_3)\text{N}-\text{C}(\text{C}_5\text{H}_4\text{N})(=\text{CH}_2)]\text{Cr}(\mu^2\text{-Cl})_2\}_2\{\text{AlCl}_3(\text{CH}_2\text{CH}_3)\}_2$) (**2.1**) and ($\{[(2,6\text{-Me}_2\text{C}_6\text{H}_3)\text{N}-\text{C}(\text{C}_5\text{H}_4\text{N})(=\text{CH}_2)]\text{Cr}(\mu^2\text{-Cl})_2\}_2\{\text{AlCl}_2(\text{CH}_3)_2\}_2$) (**2.3**) respectively. Attempts to use TEAL have also been carried out. The stronger reducing ability of TEAL with respect to TMA and DEAC advised us to use lower amount of alkyl aluminum (Scheme 2.3). All the complexes have been obtained in crystalline form and their structures clarified by X-ray analysis.

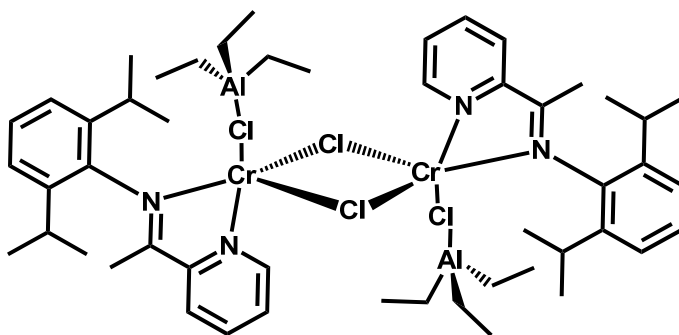
Scheme 2.3



Complex 2.1



Complex 2.3



Complex 2.2

The three complexes are symmetry-generated dimers possessing very similar geometries. Each nitrogen atom in each ligand acts as an electron donor to one metal centre and is bridged to an identical moiety by two chlorine atoms. The geometries of the two metal centres are distorted square-pyramidal. The basal plane is defined by two nitrogen [Cr-N(pyridyl) = 2.069(3); Cr-N(imino) = 2.073(3) Å] and two bridging chlorine atoms [Cr(1)-Cl(1,1a) = 2.3746(12); 2.3863(11) Å]. One Al unit is located on the axial position and connected to chromium via one bridging chloride (Figure 2.1, 2.2 and 2.3).

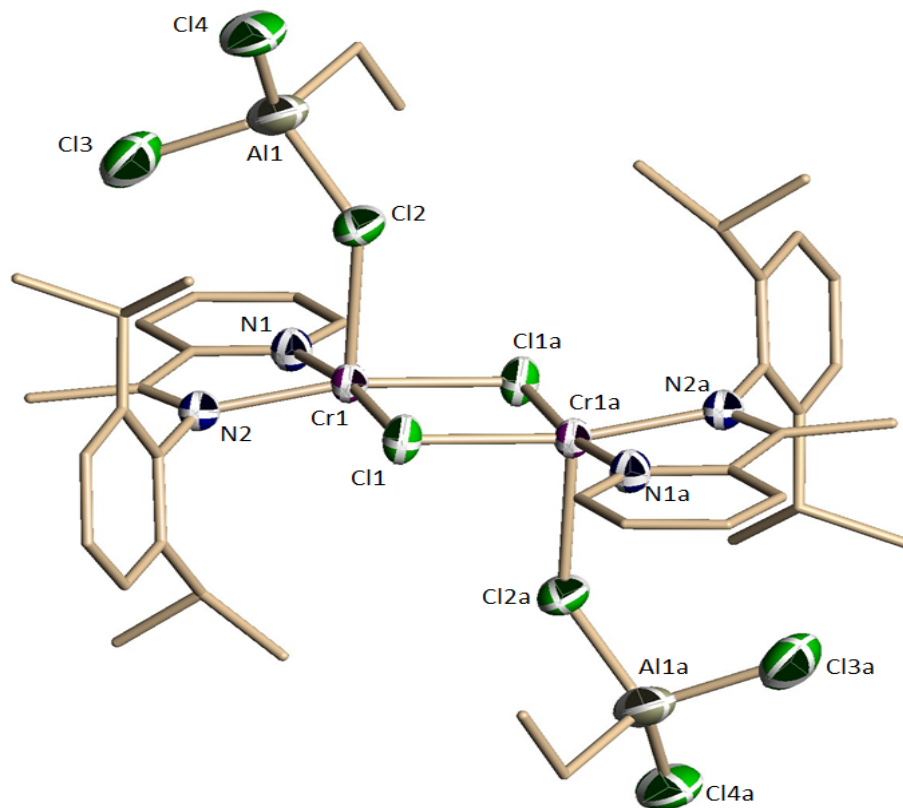


Figure 2.1. Partial thermal ellipsoid drawing for **2.1** at 50% probability level. Selected Bond lengths (Å) and angles (°) of **2.1**: Cr(1)-N(1) = 2.069(3), Cr(1)-N(2) = 2.073(3), Cr(1)-Cl(1) = 2.3746(12), Cr(1)-Cl(1)a = 2.3863(11), Cr(1)-Cl(2) = 2.6510(13), Al(1)-Cl(2) = 2.209(2),

Al(1)-Cl(3) = 2.150(2), Al(1)-Cl(4) = 2.076(5), N(1)-Cr(1)-N(2) = 78.16(13), N(1)-Cr(1)-Cl(1) = 171.61(10), N(2)-Cr(1)-Cl(1) = 96.24(10), N(1)-Cr(1)-Cl(1)a = 95.26(9), N(2)-Cr(1)-Cl(1)a = 164.23(10), Cl(1)-Cr(1)-Cl(1)a = 88.56(4), N(1)-Cr(1)-Cl(2) = 95.32(10), N(2)-Cr(1)-Cl(2) = 102.10(9), Cl(1)-Cr(1)-Cl(2) = 91.95(5), Cl(1)a-Cr(1)-Cl(2) = 92.70(4), Cr(1)-Cl(1)-Cr(1)a = 91.44(4), Al(1)-Cl(2)-Cr(1) = 127.09(8), Cl(4)-Al(1)-Cl(2) = 107.54(16), Cl(3)-Al(1)-Cl(2) = 105.79(8), Cl(4)-Al(1)-Cl(3) = 105.01(15).

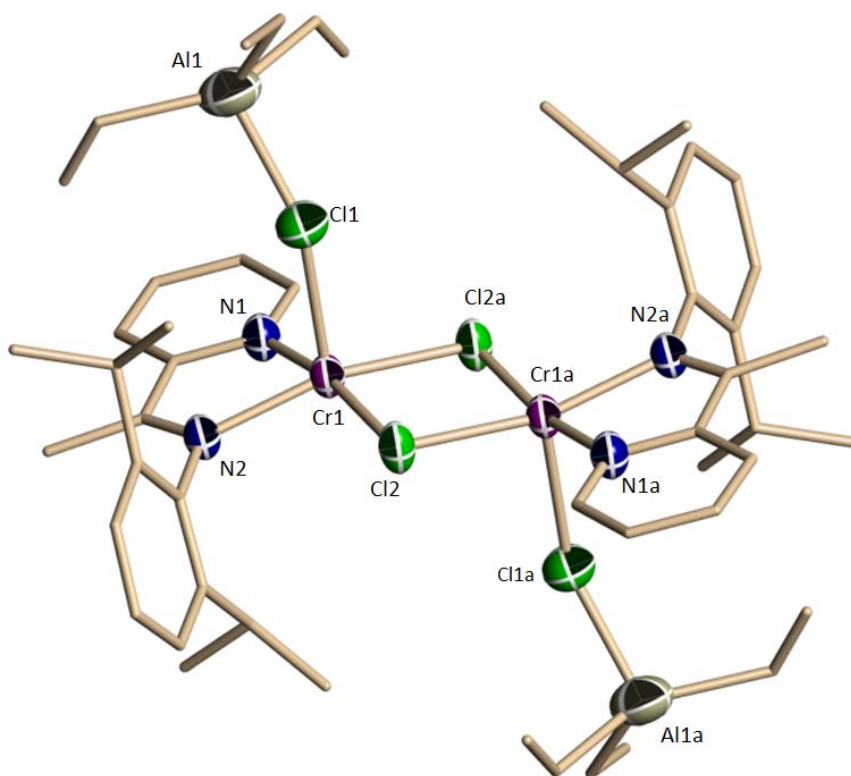


Figure 2.2. Partial thermal ellipsoid drawing for **2.2** at 50% probability level. Selected Bond lengths (Å) and angles (°) of **2.2**: Cr(1)-N(1)= 2.077(2), Cr(1)-N(2) = 2.090(2), Cr(1)-Cl(2)a = 2.3732(7), Cr(1)-Cl(2) = 2.3968(7), Cr(1)-Cl(1) = 2.5783(10), Al(1)-Cl(1) = 2.2935(15), N(1)-Cr(1)-N(2) = 78.10(9), N(1)-Cr(1)-Cl(2)a = 169.38(7), N(1)-Cr(1)-Cl(1) = 94.17(7), N(1)-Cr(1)-Cl(2) = 94.51(6), N(2)-Cr(1)-Cl(2)a = 96.16(7), N(2)-Cr(1)-Cl(2) = 160.14(7),

Cl(2)a-Cr(1)-Cl(2) = 87.99(3), N(2)-Cr(1)-Cl(1) = 101.57(7), Cl(2)a-Cr(1)-Cl(1) = 95.74(3),
 Cl(2)-Cr(1)-Cl(1) = 97.30(3), Cr(1)a-Cl(2)-Cr(1) = 92.01(3), Al(1)-Cl(1)-Cr(1) = 137.86(6).

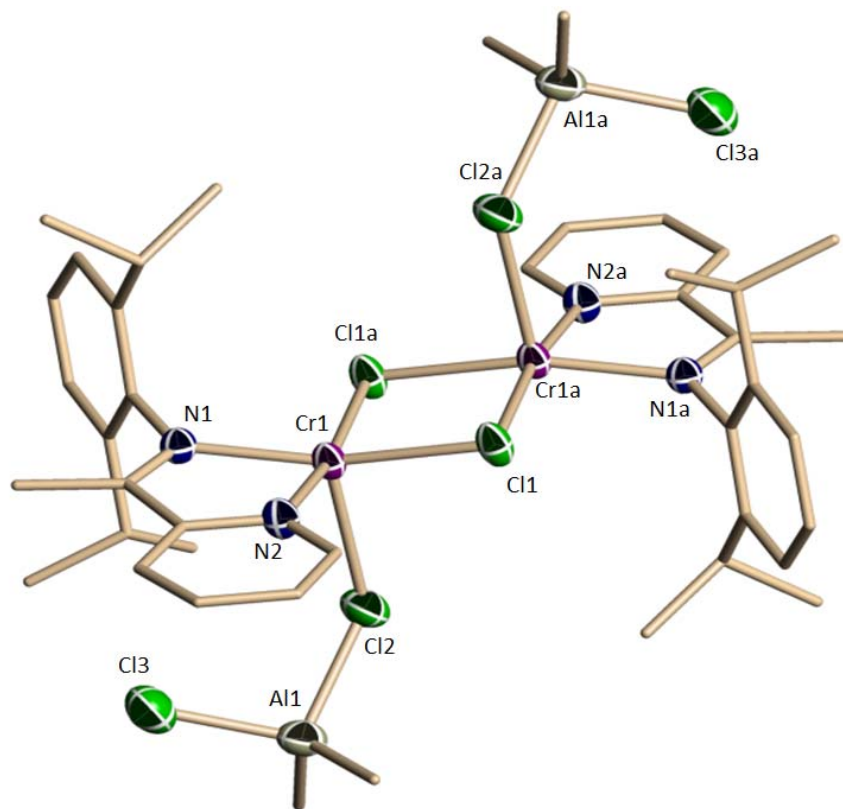
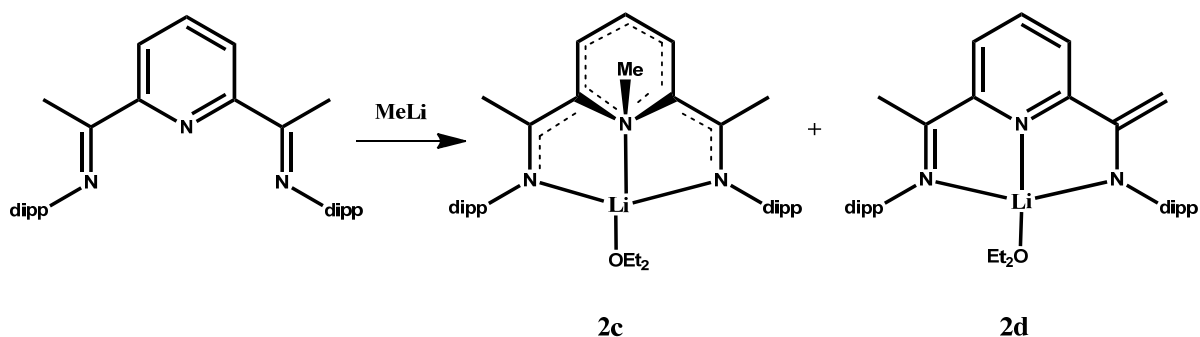


Figure 2.3. Partial thermal ellipsoid drawing for **2.3** at 50% probability level. Selected Bond lengths (Å) and angles (°) of **2.3**: Cr(1)-N(1) = 2.0733(18), Cr(1)-N(2) = 2.0723(18), Cr(1)-Cl(1) = 2.3751(6), Cr(1)-Cl(1)a = 2.3910(6), Cr(1)-Cl(2) = 2.5976(7), Al(1)-Cl(2) = 2.2428(10), Al(1)-Cl(3) = 2.1852(12), N(1)-Cr(1)-N(2) = 78.17(7), N(1)-Cr(1)-Cl(1) = 95.95(5), N(2)-Cr(1)-Cl(1) = 171.16(6), N(1)-Cr(1)-Cl(1)a = 161.30(5), N(2)-Cr(1)-Cl(1)a = 94.78(5), Cl(1)-Cr(1)-Cl(1)a = 88.80(2), N(1)-Cr(1)-Cl(2) = 104.53(5), N(2)-Cr(1)-Cl(2) = 95.34(6), Cl(1)-Cr(1)-Cl(2) = 92.52(2), Cl(1)a-Cr(1)-Cl(2) = 93.29(3), Cr(1)-Cl(1)-Cr(1)a = 91.20(2), Al(1)-Cl(2)-Cr(1) = 124.89(4), Cl(3)-Al(1)-Cl(2) = 104.54(4).

As mentioned in the Introduction, ligands containing a combination of pyridines and α -bonded imine functions have displayed non-innocent behaviour in the sense that they can be involved into both the redox and organometallic chemistry of the metal center.¹⁶⁻¹⁷ The ability of the bis-iminopyridine $\{\alpha,\alpha'-[2,6-(i\text{-Pr})_2\text{PhN}=\text{C}(\text{Me})]_2(\text{C}_5\text{H}_3\text{N})\}$ ligand to be alkylated at virtually any position and to engage in large spin-density transfers provides a particularly illustrative example. (Scheme 2.4).¹⁸⁻²⁰ In addition, this particular ligand has been proven versatile in the chemistry of chromium where it supported a full range of transformations spanning from dinitrogen reduction/hydrogenation to ethylene polymerization.²¹

Scheme 2.4



This behaviour prompted us to investigate the less sterically demanding 2,6-(*i*-Pr)₂PhN=C(Me)-(C₅H₃N) ligand. Among the features of this remarkable family of ligands there is also the possibility to undergo deprotonation, via carbanion attack, at the methyl groups bonded to the Me imine function.²² In turn, this reaction anionizes the imino nitrogen by generating a C-C double bond in a sort of ene-amido type of arrangement. While this transformation is widely documented for the bis-imino derivative, it has never been reported

for the mono iminopyridine derivatives. The anionization of the ligand not only would modify the electronic environment of the transition metal but it will increase its robustness, possibly preventing leaching and extraction by the aluminate activators. In turn this might increase catalyst life-time and performance. For the sake of simplicity, we have attempted one pot preparation by mixing, ligand, chromium precursor and MeLi (as a deprotonating agent) in the same reaction mixture. The reaction was carried out with two equivalents of ligand, one equivalent of $\text{CrCl}_3(\text{THF})_3$ and three equivalents of MeLi. The aim was to deprotonate the two methyl groups and also alkylates the last position of the trivalent chromium. The reaction proceeded smoothly and afforded the expected $\{[(2,6\text{-Me}_2\text{C}_6\text{H}_3)\text{N}-\text{C}(\text{C}_5\text{H}_4\text{N})(=\text{CH}_2)]\text{Cr}(\text{CH}_3)\}$ (**2.4**) in crystalline form and acceptable yield. The ligand underwent the expected deprotonation, thus becoming anionic, and the residual coordination site around the metal center was indeed filled by a Me function.

The crystal structure of complex **2.4** was entirely consistent with the proposed formulation. Examination of ligand bond lengths clearly showed deprotonation of the methyl groups attached to the imines with consequent loss of the imine functionality and formation of a C=C double bond [$\text{C}(1)\text{-C}(2) = 1.370(3) \text{ \AA}$; $\text{C}(20)\text{-C}(21) = 1.406(3) \text{ \AA}$; $\text{N}(1)\text{-C}(2) = 1.382(3) \text{ \AA}$, $\text{N}(3)\text{-C}(21) = 1.374(3) \text{ \AA}$]. The metal is surrounded by two anionic ligands in a distorted trigonal bipyramidal geometry where the Cr-Me group is located in one equatorial position [$\text{Cr}(1)\text{-N}(1) = 1.9892(18) \text{ \AA}$, $\text{Cr}(1)\text{-N}(2) = 2.0646(18) \text{ \AA}$, $\text{Cr}(1)\text{-N}(3) = 1.9894(18) \text{ \AA}$, $\text{Cr}(1)\text{-N}(4) = 2.0475(18) \text{ \AA}$, $\text{N}(4)\text{-Cr}(1)\text{-N}(2) = 174.13(7)^\circ$, $\text{N}(1)\text{-Cr}(1)\text{-C}(39) = 111.97(10)^\circ$, $\text{N}(3)\text{-Cr}(1)\text{-C}(39) = 105.97(10)^\circ$, $\text{N}(4)\text{-Cr}(1)\text{-C}(39) = 93.50(9)^\circ$, $\text{C}(39)\text{-Cr}(1)\text{-N}(2) = 92.36(9)^\circ$, $\text{N}(1)\text{-Cr}(1)\text{-C}(39) = 111.97(10)^\circ$, $\text{Cr}(1)\text{-C}(39) = 105.97(10)^\circ$].

The magnetic moment of **2.4** ($\mu_{\text{eff}} = 3.88 \mu_{\text{BM}}$) was as expected for the d^3 electronic configuration of trivalent chromium.

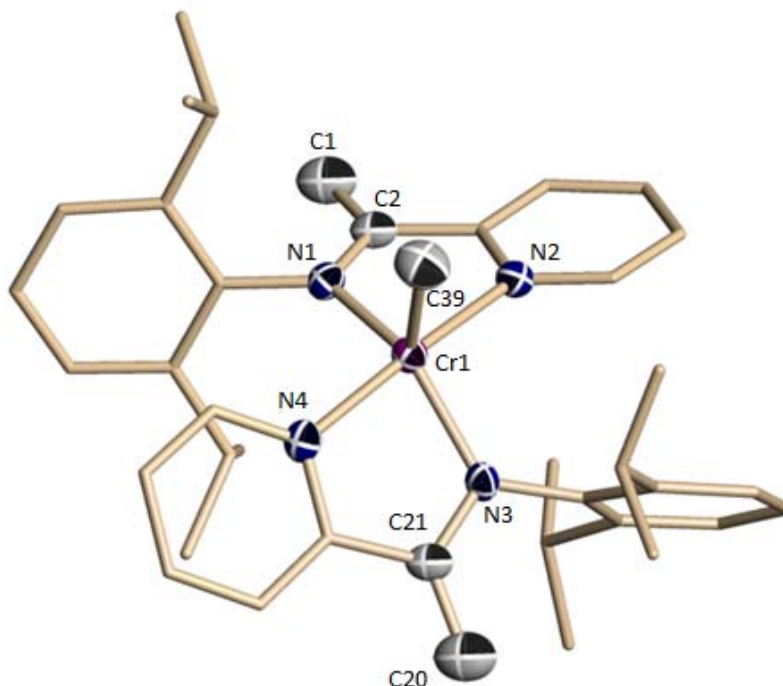


Figure 2.4. Partial thermal ellipsoid drawing for **2.4** at 50% probability level. Selected Bond lengths (\AA) and angles ($^\circ$) of **2.4**: Cr(1)-N(1) = 1.9892(18), Cr(1)-N(2) = 2.0646(18), Cr(1)-N(3) = 1.9894(18), Cr(1)-N(4) = 2.0475(18), Cr(1)-C(39) = 2.051(3), C(1)-C(2) = 1.370(3), C(20)-C(21) = 1.406(3), N(1)-Cr(1)-N(3) = 142.06(8), N(1)-Cr(1)-N(4) = 98.62(7), N(3)-Cr(1)-N(4) = 78.79(7), N(1)-Cr(1)-C(39) = 111.97(10), N(3)-Cr(1)-C(39) = 105.97(10), N(4)-Cr(1)-C(39) = 93.50(9), N(1)-Cr(1)-N(2) = 78.76(7), N(3)-Cr(1)-N(2) = 99.98(7), N(4)-Cr(1)-N(2) = 174.13(7), C(39)-Cr(1)-N(2) = 92.36(9).

The complexes above have been tested for ethylene catalytic oligomerization. Complexes **2.2** and **2.3** were not tested given that the only difference consisted of the presence of different alkyl substituents attached to aluminum.

When complex **2.1** (30 μmol) was exposed to ethylene under pressure (41 bars) and in the presence of 500 eq MAO a remarkably exothermic reaction took place. The initial temperature of 85 °C rose to 190 °C within 10 seconds and was followed by a steady drop to the initial temperature. This behaviour was clearly indicative of catalyst thermal decomposition. Therefore, lower loading (20 μmol) and a cooling system was used to maintain the temperature in a reasonable range. The other interesting feature of this catalyst was the absence of catalytic behavior below 85°C. We speculate that at such temperature the dimeric complex dissociates into the monomeric form, which in fact may be the active species of the catalytic cycle.^{23,24} Under optimized reaction conditions, complex ($\{[(2,6\text{-Me}_2\text{C}_6\text{H}_3)\text{N}-\text{C}(\text{C}_5\text{H}_4\text{N})(=\text{CH}_2)]\text{Cr}(\mu^2\text{-Cl})_2\{\text{AlCl}_3(\text{CH}_2\text{CH}_3)\}_2\}$) (**2.1**) produced a very large amount of polymer accompanied by a minor amount of light oligomers in a S-F distribution.

Complex **2.2** (entry 3^a in Table 2.2) displayed a catalytic behaviour identical to that of **2.1**. On the basis of this results and the close structural similarity, testing of **2.3** was considered as redundant.

As often observed in this chemistry,²⁵ when the solvent was changed to methylcyclohexane (MeCy) oligomer-free, waxy, low-molecular-weight polyethylene polymer (MW = 2996 g/mol, PDI = 1.754) was obtained (Table 2.2). The reaction was also considerably less exothermic but the low-molecular nature of the polymer did not change with respect to that obtained in toluene (MW = 4688 g/mol and PDI = 1.695). A series of experiments was carried out to study the catalytic behaviour of **2.4** in the presence of different activators. The employment of MAO as an activator gave higher activity comparing to combinations of MAO/TMA or MAO/TEAL.

The presence in complex **2.4** of an alkyl group bonded to chromium, along with aluminate residues, encouraged us testing for possible self-activating behaviour.

Unfortunately the catalyst displayed no such activity. On the other hand, our attempts to probe the activity of the complex **2.4** were necessarily carried out in MeCy where, regrettably, the complex has very low-solubility if any.

Table 2.2. Ethylene Oligomerization Results.

Entry	Cat (μmol)	Co-catalyst (equiv)	Temp ($^{\circ}\text{C}$)	Alkene (ml)	PE (g)	Activity (g/gCr.h)	MW	PDI
1 ^a	2.1 (10)	MAO(500)	85	10	30	142884	4688	1.695
2 ^b	2.1 (10)	DMAO(500)	85	-	23	88461	2996	1.754
3 ^a	2.2 (10)	MAO (500)	85	9	28	132442	4635	1.712
4 ^a	2.4 (20)	MAO(500)	60	24	-	33961	-	-
5 ^a	2.4 (20)	MAO/TMA(500/50)	60	10	traces	13750	-	-
6 ^a	2.4 (20)	MAO/TEAL(500/50)	60	5	traces	6875	-	-
7 ^a	2.4 (20)	-	80	-	-	-	-	-
8 ^b	2.4 (20)	DMAO	60	-	traces	-	-	-

Conditions: 40 bar (ethylene), 30 min reaction time. ^a100 mL of toluene. ^b100 mL of methylcyclohexane.

Table 2.3. Analysis of the α -olefin product distribution.

Entry	C6	C8	C10	C12	C14	C16	C18	α
1	25.50	16.60	14.30	12.70	11.20	10.40	9.20	0.71
3	18.39	17.49	14.35	14.48	14.27	13.39	12.43	0.78
4	22.69	25.54	17.31	13.11	9.74	7.06	5.04	0.65
5	22.67	21.13	15.77	13.29	11.86	12.52	8.82	0.72
6	26.16	23.59	18.73	14.04	10.21	7.27	5.07	0.63

2.6 Conclusion

In summary, in this chapter we have explored the utilization of the iminopyridine ligand as supporting ligand for chromium catalyzed ethylene oligo- and polymerization. Complexes containing both the chromium unit and the aluminate residue have been obtained and fully characterized. Unfortunately and in spite of the presence of both elements as part of the structure, no self-activating behaviour has been found and the catalysts produced large amount of polymer with a smaller amount of α -olefins.

Deprotonation of the ligand system has been carried out to improve ligand stability and resiliency. This simple modification switched the catalytic behaviour completely towards oligomerization, PE being produced only in traces. This remarkable difference may be attributed to the different abilities of the two forms of this ligand to stabilize different chromium oxidation states.

2.7 References

1. a) Reagan, W. K. (Phillips Petroleum Company) EP 0417477, **1991**; b) Tanaka, E.; Urata, H.; Oshiki, T.; Aoshima, T.; Kawashima, R.; Iwade, S.; Nakamura, H.; Katsuki, S.; Okanu, T. (Mitsubishi Chemical Corporation) EP 0611743, **1994**; c) Wu, F. J. (Amoco Corporation) US 5811618, **1998**; d) Grove, J. J. C.; Mahome, H. A.; Griesel, L. (Sasol Technology) WO 03/004158, **2002**; (e) Yoshida, T.; Yamamoto, T.; Okada, H.; Murakita, H. (Tosoh Corporation) US2002/0035029, **2002**; (f) Zhang, J.; Braunstein, P.; Hor, T. S. A. *Organometallics* **2008**, *27*, 4277. (g) Zhang, J.; Li, A.; Hor, T. S. A. *Organometallics* **2009**, *28*, 2935; (h) Nenu, C. N.; Weckhuysen, B. M. *Chem. Commun.* **2005**, 1865; (i) McGuinness, D. S.; Wasserscheid, P.; Keim, W.; Hu, C.; Englert, U.; Dixon, J. T.; Grove, C. *Chem. Commun.* **2003**, 334; (j) McGuinness, D. S.; Wasserscheid, P.; Keim, W.; Morgan, D. H.; Dixon, J. T.; Bollmann, A.; Maumela, H.; Hess, F. M.; Englert, U. *J. Am. Chem. Soc.* **2003**, *125*, 5272; (k) Carter, A.; Cohen, S. A.; Cooley, N. A.; Murphy, A.; Scutt, J.; Wass, D. F. *Chem. Commun.* **2002**, 858; (l) Vidyaratna, I.; Nikiforov, G. B.; Gorelsky, S. I.; Gambarotta, S.; Duchateau, R.; Korobkov, I. *Angew. Chem., Int. Ed.* **2009**, *48*, 6552; (m) Albahily, K.; Koc, E.; Al-Baldawi, D.; Savard, D.; Gambarotta, S.; Burchell, T. J.; Duchateau, R. *Angew. Chem., Int. Ed.* **2008**, *47*, 5816; (n) Kohn, R. D.; Haufe, M.; Kociok-Kohn, G.; Grimm, S.; Wasserscheid, P.; Keim, W. *Angew. Chem., Int. Ed.* **2000**, *39*, 4337; (o) Han, T.K.; Ok, M. A.; Chae, S. S.; Kang, S. O. (SK Energy Corporation) WO 2008/088178, **2008**; (p) Killian, E.; Blann, K.; Bollmann, A.; Dixon, J. T.; Kuhlmann, S.; Maumela, M. C.; Maumela, H.; Morgan, D. H.; Nongodlwana, P.; Overett, M. J.; Pretorius, M.; Hofener, K.; Wasserscheid, P. *J. Mol. Catal. A: Chem.* **2007**, *270*, 214; (q) McGuinness, D. S.; Overett, M.; Tooze, R. P.; Blann, K.; Dixon, J. T.; Slawin, A. M. Z.

Organometallics **2007**, *26*, 1108; (r) Bollmann, A.; Blann, K.; Dixon, J. T.; Hess, F. M.; Killian, E.; Maumela, H.; McGuinness, D. S.; Morgan, D. M.; Neveling, A.; Otto, S.; Overett, M.; Slawin, A. M. Z.; Wasserscheid, P.; Kuhlman, S. *J. Am. Chem. Soc.* **2004**, *126*, 14712; (s) Overett, M. J.; Blann, K.; Bollmann, A.; Dixon, J. T.; Haasbroek, D.; Killian, E.; Maumela, H.; McGuinness, D. S.; Morgan, D. H. *J. Am. Chem. Soc.* **2005**, *127*, 10723; (t) Blann, K.; Bollmann, A.; Dixon, J. T.; Hess, F. M.; Killian, E.; Maumela, H.; Morgan, D. H.; Neveling, A.; Otto, S.; Overett, M. J. *Chem. Commun.* **2005**, 622; (u) Klemps, C.; Payet, E.; Magna, L.; Saussine, L.; Le Goff, X. F.; Le Floch, P. *Chem. Eur. J.* **2009**, *15*, 8259.

2. (a) Greiner, E.; Gubler, R.; Inoguchi, Y. Linear Alpha Olefins, CEH Marketing Research Report, *Chemical Economics Handbook*; SRI International: Menlo Park, CA, May **2004**; (b) McGuinness, D. S.; Suttill, J. A.; Gardiner, M. G.; Davies, N. W. *Organometallics* **2008**, *27*, 4238; (c) Kirillov, E.; Roisnel, T.; Razavi, A.; Carpentier, J. F. *Organometallics* **2009**, *28*, 2401; (d) Tomov, A. K.; Chirinos, J. J.; Long, R. J.; Gibson, V. C. *J. Am. Chem. Soc.* **2005**, *127*, 10166; (e) Tomov, A. K.; Chirinos, J. J.; Long, R. J.; Gibson, V. C.; Elsegood, M. R. *J. Am. Chem. Soc.* **2006**, *128*, 7704.

3. (a) Karol, F. J.; Karapinka, G. L.; Wu, C.; Dow, A. W.; Johnson, R. N.; Carrick, W. L. *J. Polym. Sci., Part A: Polym. Chem.* **1972**, *10*, 2621; (b) Hogan, J. P.; Banks, R. L. (Phillips Petroleum Co.) U.S. Patent 2,825,721, **1958**; (c) Karapinka, G. L. (Union Carbide Corp.) Ger. Offen. DE 1,808,388, **1970**; (d) MacAdams, L. A.; Buffone, G. P.; Incarvito, C. D.; Rheingold, A. L.; Theopold, K. H. *J. Am. Chem. Soc.* **2005**, *127*, 1082; (e) Gibson, V. C.; Maddox, P. J.; Newton, C.; Redshaw, C.; Solan, G. A.; White, A. J. P.; Williams, D. J. *Chem. Commun.* **1998**, 1651; (f) Karapinka, G. L. (Union Carbide Corp.) U.S. Patent 3,709,853, **1973**; (g) Gibson, V. C.; Mastroianni, S.; Newton, C.; Redshaw, C.; Solan, G. A.; White, A. J. P.; Williams, D. J. *Dalton Trans.* **2000**, 1969; (h) Bhandari, G.; Kim, Y.;

- McFarland, J. M.; Rheingold, A. L.; Theopold, K. H. *Organometallics* **1995**, *14*, 738; (i) Esteruelas, M. A.; Lopez, A. M.; Mendez, L.; Olivan, M.; Onate, E. *Organometallics* **2003**, *22*, 395; (j) Enders, M.; Fernandez, P.; Ludwig, G.; Pritzkow, H. *Organometallics* **2001**, *20*, 5005; (k) Rogers, J. S.; Bu, X. H.; Bazan, G. C. *Chem. Commun.* **2000**, 1209.
4. Xiao, T.; Hao, P.; Kehr, G.; Hao, X.; Erker, G.; Sun, W. *Organometallics* **2011**, *30*, 4847.
5. Britovsek, G. J. P.; Gibson, V. C.; Kimberley, B. S.; Maddox, P. J.; Mctavish, S. J.; Solan, G. A.; White, J. P.; Williams, D. J. *Chem. Commun.* **1998**, 311, 849.
6. Reardon, D.; Conan, F.; Gambarotta, S.; Yap, G.; Wang, Q. *J. Am. Chem. Soc.* **1999**, *121*, 9318.
7. (b) Small, B. L.; Brookhart, M.; Bennett, A. M. A. *J. Am. Chem. Soc.* **1998**, *120*, 4049.
8. Small, B. L.; Carney, M. J.; Holman, D. M.; O'Rourke, C. E.; Halfen, J. A. *Macromolecules* **2004**, *37*, 4375.
9. Esteruelas, M. A.; Lo, A. M.; Me, L. *Organometallics* **2003**, *22*, 395.
10. Vidyaratne, I.; Scott, J.; Gambarotta, S.; Duchateau, R. *Organometallics* **2007**, *26*, 3201.
11. Benito, M.; Jesu, E. De.; Mata, F. J. De.; Flores, J. C.; Universitario, C. *Organometallics* **2006**, *25*, 3876.
12. Nienkemper, K.; Kotov, V. V.; Kehr, G.; Erker, G.; Fröhlich, R. *Eur. J. Inorg. Chem.* **2006**, *2006*, 366.

13. Gibson, V. C.; Reilly, R. K. O.; Wass, J. P.; White, J. P.; Williams, D. J. *Dalton Trans.* **2003**, *41*, 4.
14. Skupinska, J. *Chem. Rev.* **1991**, *91*, 613.
15. Giambastiani, G.; Luconi, L.; Kuhlman, R. L.; Hustad, P. D. *Olefin Upgrading Catalysis by Nitrogen-based Metal Complexes I*; Campora, J.; Giambastiani, G., Eds.; Springer Netherlands: Dordrecht, **2011**, Vol. 35.
16. Chandran, D.; Lee, K. M.; Chang, H. C.; Song, G. Y.; Lee, J. E.; Suh, H.; Kim, I. J. *Organomet. Chem.* **2012**, *718*, 8; (b) Barbaro, P.; Bianchini, C.; Giambastiani, G.; Guerrero, R. I.; Meli, A.; Oberhauser, W.; Segarra, A. M.; Sorace, L.; Toti, A. *Organometallics* **2007**, *26*, 4639; (c) Bianchini, C.; Giambastiani, G.; Guerrero, R. I.; Meli, A.; Oberhauser, W.; Sorace, L.; Toti, A. *Organometallics* **2007**, *26*, 5066.
17. (a) van Koten, G.; Jastrzebski, J. T. B. H.; Vrieze, K. *J Organomet Chem.* **1983**, *250*, 49; (b) Gibson V.C.; Redshaw C.; White, A.J.P, Williams, D. J. *J Organomet Chem.* **1998**, *550*, 453; (c) Gibson, V. C.; Halliwell, C. M.; Long, N. J.; Oxford, P. J.; Smith A. M.; White A. J. P, Williams, D. J. *Dalton Trans.* **2003**, 918.
18. Khorobkov, I.; Gambarotta, S.; Yap, G. P. A.; Budzelaar, P. H. M. *Organometallics* **2002**, *21*, 3088.
- 19 Clentsmith, G. K. B.; Gibson, V. C.; Hitchcock, P. B.; Kimberley, B. S.; Rees, C. W. *Chem. Commun.* **2002**, 1498.

20. Blackmore, I. J.; Gibson, V. C.; Hitchcock, P. B.; Rees, C. W.; Williams, D. J.; White, A. J. P. *J. Am. Chem. Soc.* **2005**, *127*, 6012.
21. Tondreau, A. M.; Stieber, S. C. E.; Milsman, C.; Lobkovsky, E.; Weyhermüller, T.; Semproni, S. P.; Chirik, P. J. *Inorg. Chem.* **2013**, *52*, 635.
22. Scott, J.; Gambarotta, S.; Korobkov, I.; Knijnenburg, Q.; Bruin, B. De; Budzelaar, P. H. M. *J. Am. Chem. Soc.* **2005**, *3*, 17204.
23. Crewdson, P.; Gambarotta, S.; Djoman, M. C.; Korobkov, I.; Duchateau, R. *Organometallics* **2005**, *24*, 5214.
24. Jabri, A.; Mason, C. B.; Sim, Y.; Gambarotta, S.; Burchell, T. J.; Duchateau, R. *Angew. Chem., Int. Ed.* **2008**, *47*, 9717.
25. (a) Shaikh, Y.; Albahily, K.; Sutcliffe, M.; Fomitcheva, V.; Gambarotta, S.; Korobkov, I.; Duchateau, R. *Angew. Chem., Int. Ed.* **2012**, *51*, 1366; (b) Thapa, I.; Gambarotta, S.; Duchateau, R.; Kulangara, S. V.; Chevalier, R. *Organometallics* **2010**, *29*, 4080; (c) Thapa, I.; Gambarotta, S.; Korobkov, I.; Murugesu, M.; Budzelaar, P. *Organometallics* **2012**, *31*, 486.

Chromium Complexes of a Pincer-type bis-Phosphinimide Ligand

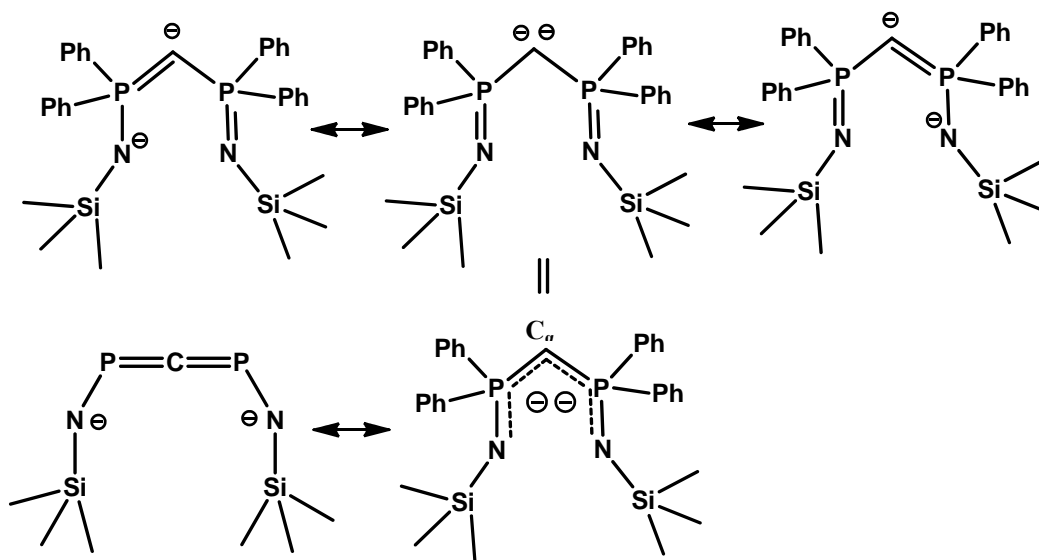
3.1 Introduction

Given the industrial relevance of catalysts for ethylene oligo- and polymerization, it comes with no surprise that a large amount of research effort has been invested for identifying the most versatile elements and designing appropriate supporting ligand. Among transition metals, chromium occupies a special place since it has provided commercially viable catalysts for ethylene polymerization, α -olefin statistical oligomerization and selective formation to 1-hexene and 1-octene. Therefore, there is no doubt that this element provides excellent substrates to study how ligand features may affect and determine the very type of catalytic behaviour. In particular, a large body of literature clearly indicates that ligands containing a combination of nitrogen and phosphorus donor atoms with a variety of chelating “bites” may generate a family of versatile catalysts for the above transformations, including useful switchable catalysts. The reasons for the unique versatility of these ligands remain unclear.

In the previous chapter, we have reviewed the ability of the bis-imino ligand to produce active catalysts with transition metals such as Fe, Co, Ni, Cr and Pd. We have also presented our modification of this ligand system and a study on the chemistry of its chromium derivative.¹⁻³

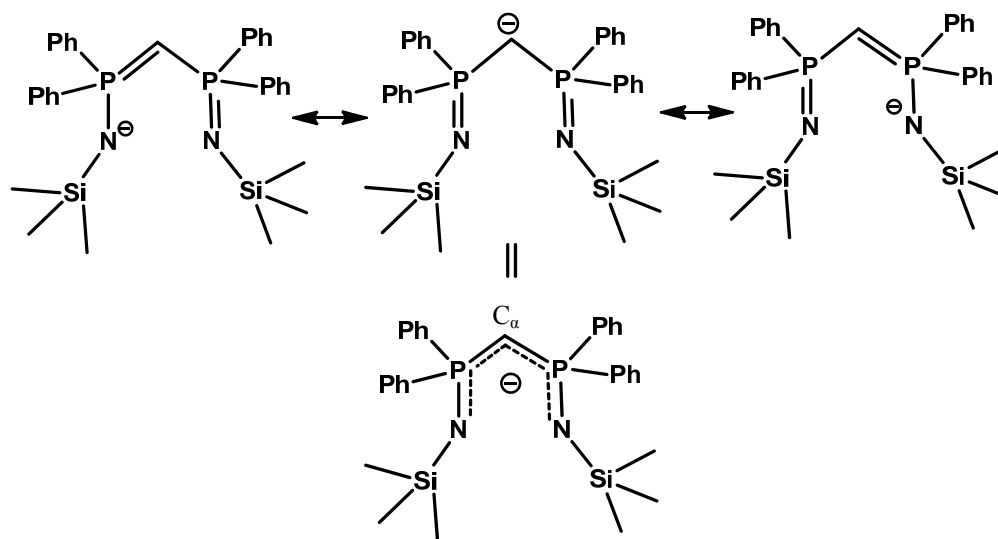
For the present study we have examined the well-known bis(iminophosphoranyl) methane, a ligand well established in coordination chemistry and which consists of two iminophosphorane units linked by a methylene bridge.⁴ This particular ligand shows a few interesting properties which are relevant to our research, hence encouraging further synthetic efforts. The neutral ligand may be readily deprotonated by organometallic derivatives at the carbon atom bridging the two phosphoric units and afford mono- and dianionic derivatives. The dianionic form has in fact attracted years ago the attention of inorganic chemists for the formal carbene-type of structures generated with a variety of metals. Cavell *et al.* have employed the dianionic system to prepare a long series of transition metals complexes, presented in the literature as carbene derivatives.⁹ In the end, the carbene structure is a mere deception of a short M..Cr distance observed in the crystal structures of a few complexes. As a matter of fact, resonance structures containing anionic nitrogens and an allenic P=C=P systems are most likely important contributors to the description of the electronic configuration (Scheme 3.1).^{5,6}

Scheme 3.1



The mono-deprotonated, anionic form of the ligand shows instead a rather symmetrical distribution of the single negative charge as a result of the resonance structures contributing to a pentadienyl-like type of arrangement (Scheme 3.2).^{7,8}

Scheme 3.2



Work from our group has shown that the monoanionic pincer-type ligand may stabilize the trivalent oxidation state of vanadium along with two rare mixed-valent V(II)/V(III) compounds.¹⁰ Furthermore, this ligand has been employed for the nickel catalyzed dimerization of ethylene with excellent activity (TOF = 324500 mol/mol (Ni).h).¹¹ A chromium complex chelated by this mono-anionic ligand was prepared by Stephan and co-workers in 2001 and reported to be a polymerization catalyst of moderate activity.¹²

We were attracted by the possibility of binding chromium complexes of this ligand to alkyl aluminum residues. The presence of four donor atoms in a semi-rigid chelating framework looks rather versatile for the purpose. Also the possibility of stabilizing

chromium's low oxidation states was of primary importance for our quest to Cr(I), an oxidation state which has been linked to the selectivity of the few existing selective oligomerization catalysts.¹³

3.2 Experimental

All reactions were carried out under a dry nitrogen atmosphere. Solvent were dried using an aluminum oxide solvent purification system. Elemental analyses were carried out with a Perkin-Elmer 2400 CHN analyzer. Samples for magnetic susceptibility were pre-weighed inside a dry box equipped with an analytical balance and sealed into calibrated tubes and measured with a Johnson Matthey Magnetic Susceptibility balance at room temperature. Data for X-ray crystal structure determination were obtained with a Bruker diffractometer equipped with a 1K Smart CCD area detector. Et₃Al was purchased from Strem and used as received. Methylaluminoxane (MAO, 20% in toluene) was purchased from Albemarle Corporation. *n*-butyllithium in hexane (2.5 M) was purchased from Aldrich Me₃Al depleted MAO (DMAO) was prepared by removing all volatiles with heating (50°C) and under reduced pressure for 6 hours. CrCl₃(THF)₃ and CrCl₂(THF)₂ were prepared according to standard procedures. The synthesis of CH₂(PPh₂NSiMe₃)₂ (**3a**) was carried out according to an established literature procedure.¹⁴

Preparation of [(CH(PPh₂NSiMe₃)₂)₂Cr(μ^2 -Cl)₂] (3.1)

Synthesis of the complex was performed according to a published method.¹² The reaction was carried out with 1 mmol of each starting material. Complex 3.1 was obtained as

a green crystalline mass (0.62 g, 0.48 mmol, 48 %), $\mu_{\text{eff}} = 4.21 \mu_{\text{B}}$. Elemental Analysis Calcd. (Found) for $\text{C}_{62}\text{H}_{78}\text{Cl}_2\text{Cr}_2\text{N}_4\text{P}_4\text{Si}_4$: C 57.71 (57.68), H 6.09 (6.16), N 4.30 (4.34). ESI-MS $m/z = 1288.24$ ($[\text{M}+\text{H}]^+$).

Preparation of $[(\text{CH}(\text{PPh}_2\text{NSiMe}_3)_2\text{Cl})_2\text{Cr}(\mu^2\text{-Cl})_2]$ (**3.2**)

A solution of *n*-butyllithium in hexane (2.5 M, 0.4 mL, 1 mmol) was added drop-wise to a cold solution of $\text{CH}_2(\text{PPh}_2\text{NSiMe}_3)_2$ (0.56 g, 1 mmol) in THF (5 mL). The resulting yellow solution was stirred overnight and then treated with $\text{CrCl}_3(\text{THF})_3$ (0.38 g, 1 mmol) also dissolved in THF (5 mL). A sudden reaction took place with color deepening. The solvent was replaced with toluene and the supernatant separated from the LiCl precipitate via centrifugation. The clear solution was concentrated and allowed to stand 2 days at -35°C upon which, green crystals of **3.2** separated. The crystalline mass was washed and dried *in vacuo* (0.54 g, 0.40 mmol, 40 %), $\mu_{\text{eff}} = 3.82 \mu_{\text{B}}$. Elemental Analysis Calcd. (Found) for $\text{C}_{62}\text{H}_{78}\text{Cl}_4\text{Cr}_2\text{N}_4\text{P}_4\text{Si}_4$: C 54.70 (54.74), H 5.78 (5.86), N 4.12 (4.14). ESI-MS $m/z = 1360.18$ ($[\text{M}+\text{H}]^+$).

Preparation of $\{[(\text{CH}_2(\text{PPh}_2\text{NSiMe}_3)_2\text{Cl})_2\text{Cr}(\mu^2\text{-Cl})_2]\} [\text{Et}_3\text{AlClAlEt}_2\text{Cl}]$ (**3.3**)

A mixture of $\text{CrCl}_3(\text{THF})_3$ (0.38 g, 1 mmol) and **3a** (0.56 g, 1 mmol) in toluene (10 mL) was cooled at -35°C and treated with neat TEAL (6 mmol, 0.68 g). The colour of the solution turned dark-green after 30 min. of stirring. The resultant suspension was centrifuged and the volume of the supernatant reduced *in vacuo* (5 mL). Light blue crystal of **3.3**

separated upon layering the solution with hexane (0.42 g, 0.27 mmol, 27 %), $\mu_{\text{eff}} = 1.82 \mu_{\text{B}}$. Elemental Analysis Calcd. (Found) for $\text{C}_{72}\text{H}_{105}\text{Al}_2\text{Cl}_4\text{Cr}_2\text{N}_4\text{P}_4\text{Si}_4$: C 55.34 (55.37), H 6.77 (6.83), N 3.59 (3.60). ESI-MS $m/z = 1561.35$ ($[\text{M}+\text{H}]^+$).

Preparation of $[(\text{CH}(\text{PPh}_2\text{NSiMe}_3)_2] \text{Cr}(\mu^2\text{-Cl})_2\text{Li}(\text{THF})_2$ (3.4)

A solution of ligand **3a** (0.56 g, 1 mmol) in THF (5 mL) was treated with *n*-butyllithium in hexane (2 M, 0.02 mL, 1 mmol) via drop-wise addition at low temperature. A solution of $\text{CrMeCl}_2 \cdot (\text{THF})_3$ (0.35 g, 1 mmol), in THF (10 mL), was subsequently added affording an instant color change to brown. The solution was stirred overnight and, after removing the solvent under reduced pressure, the residue was redissolved in THF (5 ml). The resulting suspension was centrifuged and X-ray quality, dark-yellow crystals were formed from the clear solution after standing for 3 days at -35°C . The crystals were filtered, washed with cold hexane and dried *in vacuo* (0.37 g, 0.45 mmol, 45 %), $\mu_{\text{eff}} = 2.84 \mu_{\text{B}}$. Elemental Analysis Calcd. (Found) for $\text{C}_{39}\text{H}_{55}\text{Cl}_2\text{CrLiN}_2\text{O}_2\text{P}_2\text{Si}_2$: C 56.31 (56.26), H 6.66 (6.72), N 3.37 (3.31). ESI-MS $m/z = 830.22$ ($[\text{M}+\text{H}]^+$).

3.3 X-Ray Diffraction

Suitable crystals were selected, mounted on a thin, glass fiber with paraffin oil, and cooled to the data. Data were collected on a Bruker AXS SMART 1 k CCD diffractometer. Data collection was performed with three batch runs at $\phi = 0.00$ deg (600 frames), at $\phi = 120.00$ deg (600 frames), and at $\phi = 240.00$ deg (600 frames). Initial unit-cell parameters

were determined from 60 data frames collected at different sections of the Ewald sphere. Semi-empirical absorption corrections based on equivalent reflections were applied. The systematic absences and unit-cell parameters were consistent for the reported space groups. The structures were solved by direct methods, completed with difference Fourier syntheses, and refined with full-matrix least-squares procedures based on F2. All non-hydrogen atoms were refined with anisotropic displacement parameters. When it was not possible to locate them, the hydrogen atoms were treated as idealized contributions. Relevant data on crystal structure solution and refinement are given Table 3.1.

Table 3.1. Crystal data and refinements for **3.1 – 3.4**.

	Complex 3.1	Complex 3.2	Complex 3.3	Complex 3.4
Formula	C _{37.50} H ₄₉ ClCr N ₂ P ₂ Si ₂	C _{70.22} H _{89.67} Cl _{2.78} Cr ₂ N ₄ P ₄ Si ₄	C ₈₂ H ₁₃₀ Al ₄ Cl ₆ Cr ₂ N ₄ P ₄ Si ₄	C ₃₉ H ₅₆ Cl ₂ CrLiN ₂ O ₂ P ₂ Si ₂
MW	733.36	1428.44	1832.76	832.82
Space group	Monoclinic, P2(1)/c	Triclinic, P-1	Monoclinic, C2/c	Monoclinic, P2(1)/n
<i>a</i> (Å)	11.6302(3)	13.7555(4)	30.9487(12)	11.3387(18)
<i>b</i> (Å)	18.4826(4)	14.9846(4)	18.1243(6)	11.6428(19)
<i>c</i> (Å)	18.6378(4)	20.5257(6)	23.0023(8)	33.433(5)
<i>α</i>, (deg)	90	105.083(2)	90	90
<i>β</i>, (deg)	101.4560(10)	98.735(2)	129.7350(10)	97.972(7)
<i>γ</i>, (deg)	90	108.201(2)	90	90
<i>V</i> (Å³)	3926.50(16)	3753.18(18)	9922.2(6)	4371.0(12)
<i>Z</i>	4	2	4	4
Radiation	0.71073	0.71073	0.71073	0.71073
T (K)	200(2)	200(2)	200(2)	200(2)
D_{calcd} (gcm⁻³)	1.241	1.264	1.227	1.266
<i>μ</i>_{calcd} (mm⁻¹)	0.530	0.579	0.569	0.546
<i>F</i>000	1548	1500	3872	1756
<i>R</i>, <i>R</i>_w^{2a}	0.0510, 0.1337	0.0627, 0.1315	0.0574, 0.1504	0.1143, 0.2674
GoF	1.045	1.015	1.007	1.077

$$R = \frac{\sum |F_o| - |F_c|}{\sum |F|}. \quad R_w = \left[\frac{\sum (|F_o| - |F_c|)^2}{\sum w F_o^2} \right]^{1/2}.$$

3.4 General Oligomerization and polymerization procedure

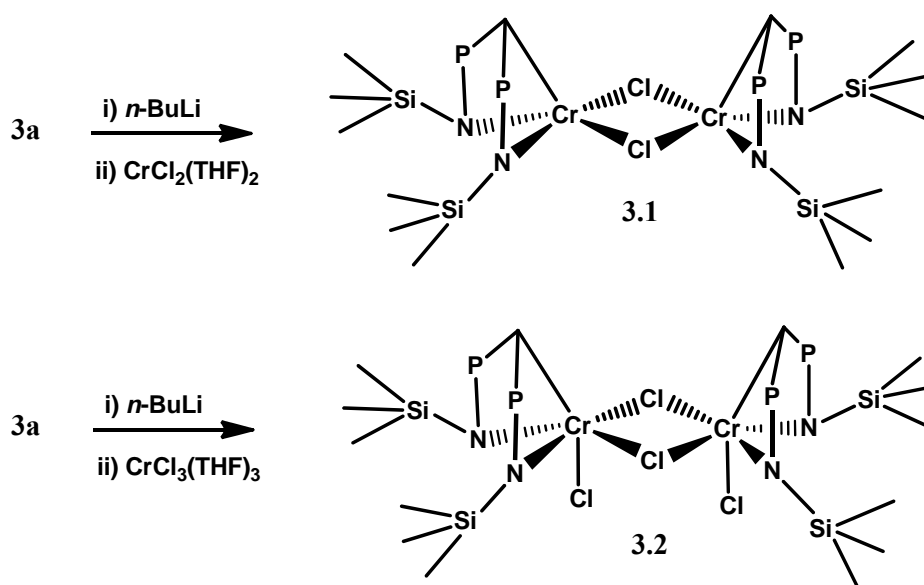
Oligomerization and polymerization reactions were carried out in 200 ml steel Buchi reactor equipped with mechanical stirrer and temperature probe. After catalyst injection into the reactor under a stream of N₂, the reactor was immediately pressurized with ethylene (600 psi). The reaction was allowed to run for 30 min. After the reaction time had expired, the reactor was cooled to 0 °C with an ice bath and depressurized. 50 mL of 10% MeOH and HCl was added to quench the reaction mixture. The organic phase was separated from the aqueous phase and analysis and yield of oligomers were obtained respectively by GC, by using calibrated standard solutions, and by ¹H-NMR.

3.5 Results and discussion

Mixing the non-deprotonated form of the ligand with both CrCl₃(THF)₃ and CrCl₂(THF)₂ gave no color change indicating that no reaction occurred at significant extent. In turn, this indicates that without the anionic drive of the ligand deprotonation, the two nitrogen donor atoms are not sufficiently coordinating. Henceforth, we have compared two possible routes. The first consisted of the deliberate ligand deprotonation followed by treatment with the appropriate chromium salt as described independently by both Cavell and Stephan.^{9,12} The other was instead the treatment of a mixture of non-deprotonated ligand and chromium with an alkyl aluminum. The idea behind this proposal was that possible cationization of the metal center would eventually provide sufficient acidity to compensate for the lack of ligand basicity and, in the end, permitting complexation.

The reaction of the ligand mono-deprotonated form with $\text{CrCl}_2(\text{THF})_2$ afforded $[(\text{CH}(\text{PPh}_2\text{NSiMe}_3)_2)_2\text{Cr}(\mu^2\text{-Cl})_2]$ (**3.1**) in complete agreement with Stephan's findings. This species was reported to give moderate catalytic activity for polymerization in presence of MAO (around $68 \times 10^3 \text{ g (PE) mol(Al)}^{-1} \text{ bar}^{-1} \text{ h}^{-1}$).¹² Given the fundamental role of the chromium oxidation states in determining a specific catalytic behaviour,¹⁵ we have also attempted the preparation of the trivalent analogue. The in situ deprotonation of **3a** with *n*-BuLi, followed by addition of $\text{CrCl}_3(\text{THF})_3$ afforded the trivalent analogue $[(\text{CH}(\text{PPh}_2\text{NSiMe}_3)_2\text{Cl})_2\text{Cr}(\mu^2\text{-Cl})_2]$ (**3.2**).

Scheme 3.3



The structure of **3.2** was elucidated by X-ray crystallographic analysis. The molecule possesses the same dimeric structure as observed in **3.1** with two bridging chlorine linking two identical metallic unit. Each chromium atom is in a distorted octahedral environment [N(2)-Cr(1)-N(1) = 96.40(13) Å, N(2)-Cr(1)-C(2) = 73.39(15) Å, N(1)-Cr(1)-C(2) = 72.13(14) Å, N(1)-Cr(1)-Cl(2) = 97.0(3) Å, N(2)-Cr(1)-Cl(2) = 99.4(3) Å, N(2)-Cr(1)-Cl(1)

= 89.44(10) Å, N(1)-Cr(1)-Cl(1) = 167.13(11) Å, Cl(2)-Cr(1)-Cl(1) = 93.3(3) Å, Cl(1)a-Cr(1)-Cl(1) = 81.31(5) Å] with the equatorial plane defined by two bridging chlorine [Cr(1)-Cl(1)a = 2.4064(13) Å, Cr(1)-Cl(1) = 2.4234(13) Å] and the two nitrogen atom [Cr(1)-N(2) = 2.099(4) Å, Cr(1)-N(1) = 2.112(3) Å] of the ligand. The two axial positions are occupied by the terminally bonded chlorine atom and the ligand deprotonated carbon atom [Cr(1)-Cl(2) = 2.276(12) Å, Cr(1)-C(2) = 2.315(5) Å, Cl(2)-Cr(1)-C(2) = 165.7(3)°] (Figure 3.1).

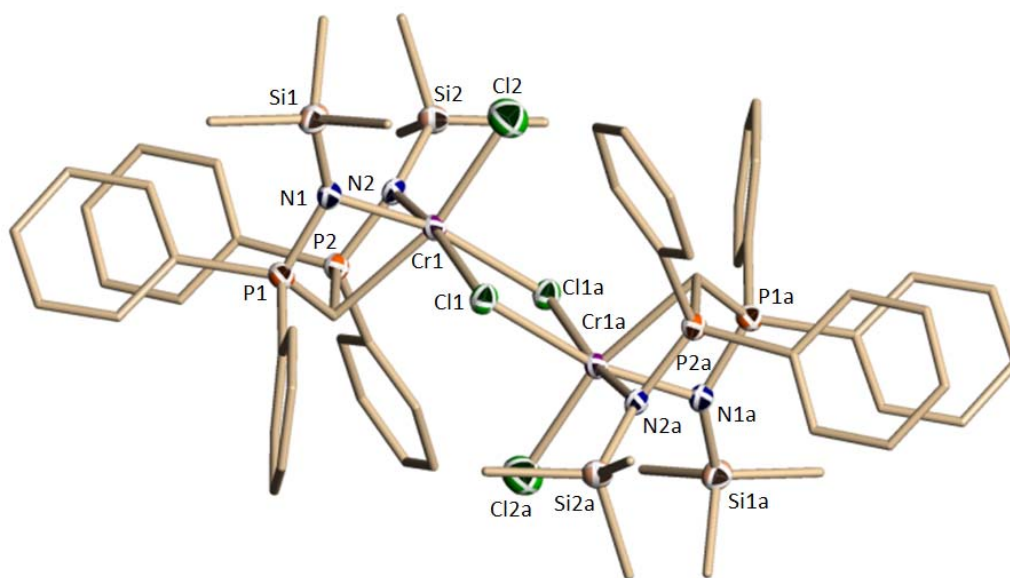


Figure 3.1. Partial thermal ellipsoid drawing for **3.1** at 50% probability level. Selected Bond lengths (Å) and angles (°) of **3.1**: Cr(1)-N(2) = 2.099(4), Cr(1)-N(1) = 2.112(3), P(1)-C(2) = 1.735(4), P(2)-C(2) = 1.751(5), Cr(1)-Cl(2) = 2.276(12), Cr(1)-C(2) = 2.315(5), Cr(1)-Cl(1)a = 2.4064(13), Cr(1)-Cl(1) = 2.4234(13), Cr(1)-P(1) = 2.7718(14), Cr(1)-P(2) = 2.7777(14), N(1)-Si(1) = 1.737(4), N(2)-Si(2) = 1.736(4), N(1)-P(1) = 1.594(4), N(2)-Cr(1)-N(1) = 96.40(13), N(2)-Cr(1)-C(2) = 73.39(15), N(1)-Cr(1)-C(2) = 72.13(14), N(1)-Cr(1)-Cl(2) = 97.0(3), N(2)-Cr(1)-Cl(2) = 99.4(3), N(2)-Cr(1)-Cl(1) = 89.44(10), N(1)-Cr(1)-Cl(1) = 167.13(11), Cl(2)-Cr(1)-Cl(1) = 93.3(3), Cl(1)a-Cr(1)-Cl(1) = 81.31(5), Cl(2)-Cr(1)-C(2) =

165.7(3), N(2)-Cr(1)-Cl(1) = 166.45(11), C(2)-Cr(1)-Cl(1)a = 98.13(12), C(2)-Cr(1)-Cl(1) = 98.80(11), Cl(2)-Cr(1)-Cl(1) = 91.1(3), N(1)-Cr(1)-Cl(1)a = 90.81(10), P(1)-N(1)-Cr(1) = 95.83(17), P(2)-N(2)-Cr(1) = 96.43(17), P(1)-Cr(1)-P(2) = 66.20(4), Cr(1)a-Cl(1)-Cr(1) = 98.69(4), N(1)-P(1)-C(2) = 103.2(2).

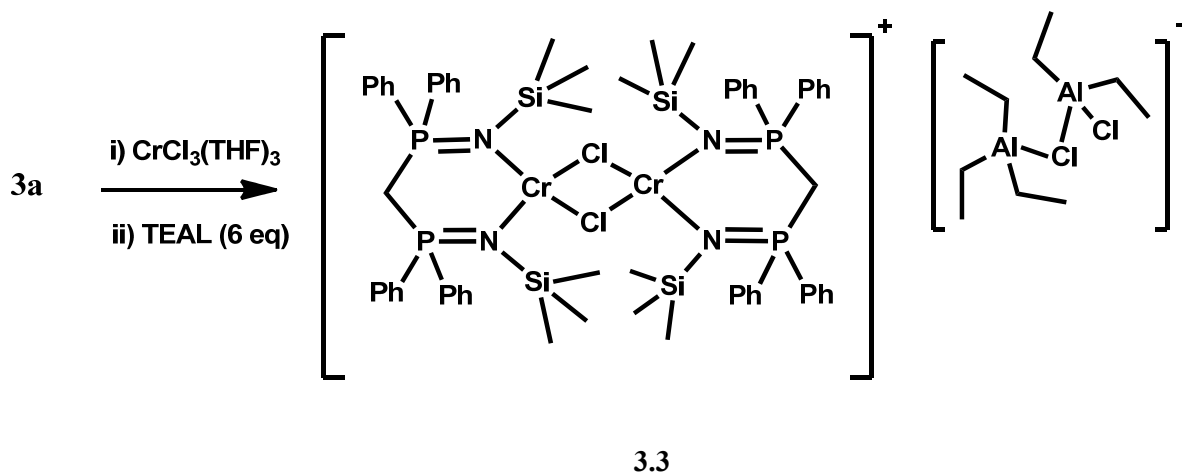
The C_α-Cr distance is consistent [Cr(1)-C(2) = 2.315(5) Å] with the formation of a C-Cr bond and examination of the C-P and P-N bond distances [P(1)-C(2) = 1.735(4) Å, N(1)-P(1) = 1.594(4) Å, N(1)-P(1)-C(2) = 103.2(2)^o], indicate the presence of electronic delocalization along the ligand backbone.

The Cr...Cr distance [Cr(1)-Cr(1a) = 3.65 Å] is in the non-bonding range as expected for a trivalent dimer with bridging chlorine.¹⁶ The magnetic moment [$\mu_{\text{eff}} = 3.82 \mu_{\text{B}}$] was entirely consistent with the presence of two magnetically uncoupled trivalent chromium centers.

As mentioned above, we have also attempted the complexation of the ligand with chromium salts in the presence of alkyl aluminum as a cationizing agent. The idea behind this attempt was to prevent deprotonation at the C_α atom of the ligand (Scheme 3.4).^{17,18}

The reaction of CrCl₃(THF)₃ with the ligand and TEAL was carried out in toluene. The utilization of six equivalents of TEAL was deemed necessary to extract the molecules of THF from the coordination sphere of the metal thus enhancing its Lewis acidity. A new complex $\{[(\text{CH}_2(\text{PPh}_2\text{NSiMe}_3)_2\text{Cl})_2\text{Cr}(\mu^2\text{-Cl})_2]\}[\text{Et}_3\text{AlClAlEt}_2\text{Cl}]$ (**3.3**), containing mixed-valent chromium, was obtained from the reaction (Scheme 3.4).

Scheme 3.4



The formulation and connectivity was yielded by an X-ray crystal structure. The structure is dimeric with two identical metallic units bridged by two chlorine atoms and with each unit composed by one chromium connected to the intact ligand (Figure 3.2).

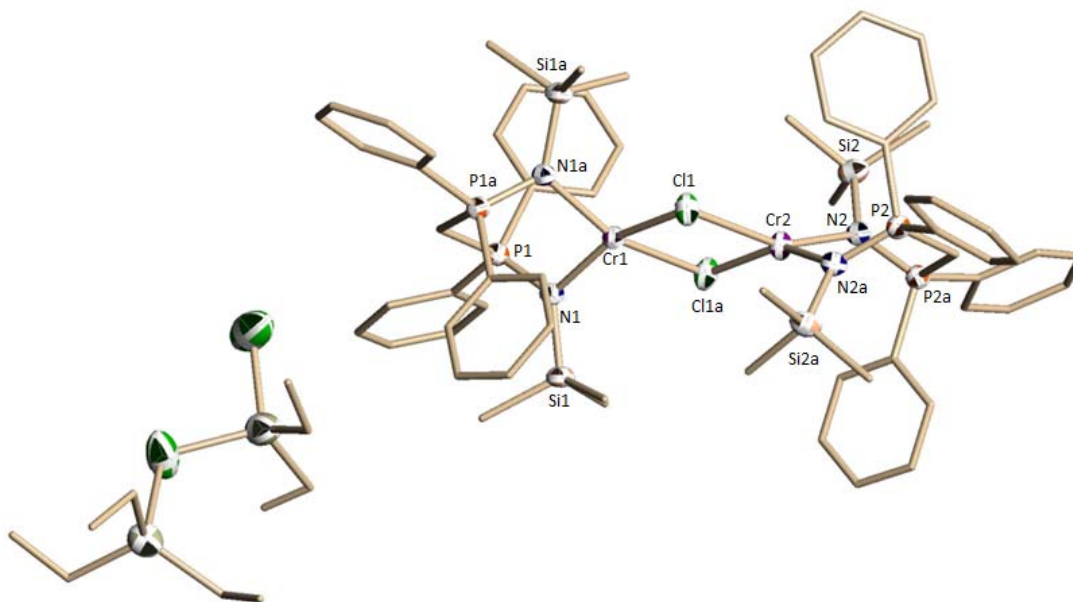
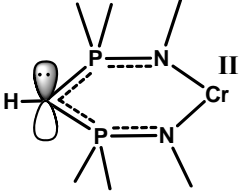
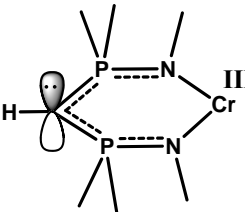
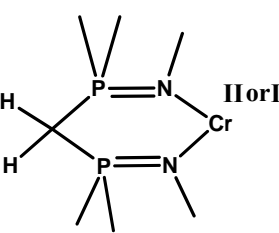


Figure 3.2. Partial thermal ellipsoid drawing for **3.3** at 50% probability level. Selected Bond lengths (Å) and angles (°) of **3.3**: Cr(1)-N(1) = Cr(1)-N(1)a = 2.104(3), Cr(1)-Cl(1) = Cr(1)-Cl(1)a = 2.3953(12), Cr(2)-N(2) = Cr(2)-N(2)a = 2.088(3), Cr(2)-Cl(1) = Cr(2)-Cl(1)a = 2.4129(12), P(1)-C(1) = 1.818(3), P(2)-C(17) = 1.818(3), N(1)a-Cr(1)-N(1) = 95.29(17), N(1)a-Cr(1)-Cl(1)a = N(1)-Cr(1)-Cl(1) = 159.09(9), N(1)-Cr(1)-Cl(1)a = N(1)a-Cr(1)-Cl(1) = 94.02(9), Cl(1)a-Cr(1)-Cl(1) = 83.63(5), N(2)a-Cr(2)-N(2) = 95.06(17), N(2)a-Cr(2)-Cl(1) = N(2)-Cr(2)-Cl(1)a = 153.43(9), N(2)-Cr(2)-Cl(1) = N(2)a-Cr(2)-Cl(1)a = 96.77(9), Cl(1)-Cr(2)-Cl(1)a = 82.89(5), P(2)-N(2)-Cr(2) = 116.02(17), P(1)a-C(1)-P(1) = 111.2(3), Cr(1)-Cl(1)-Cr(2) = 96.74(4), P(2)a-C(17)-P(2) = 111.2(3).

Each chromium is surrounded by two nitrogen atoms and two chlorine bridging atoms in an overall distorted square planar geometry, [N(1a-Cr(1)-N(1)= 95.29(17)°, N(1)-Cr(1)-Cl(1)a = 94.02(9)°, N(1)a-Cr(1)-Cl(1)= 94.02(9)°, Cl(1)a-Cr(1)-Cl(1)= 83.63(5)°] (Figure 3.2). The ligand system is non-deprotonated showing very long non-bonding distance of the C_α with the metal center [3.74 Å]. Also the P-C distances are in the range expected for single bonds, therefore reiterating that the ligand has not been anionized. Comparative bond distances and angles of the ligand backbone as a function of the presence of H atoms on the C_α are given in Table 3.2.

Table 3.2. Selected bond lengths (Å) and bond angles (°) for compounds **3.1- 3.3**.

		Cr-C (Å)	C-P (Å)	N-P (Å)	PCP(°)
3.1		2.28	1.75	1.60	121.35
3.2		2.32	1.73	1.62	123.47
3.3		3.74	1.82	1.58	111.25

One dimeric aluminate counteranion is present in the lattice, therefore assigning a single positive charge to the dichromium unit. In turn, this attributes a mixed valence Cr(I)Cr(II) state to the dimeric unit. The room temperature magnetic moment of **3.3** [$\mu_{\text{eff}} = 1.82 \mu_{\text{B}}$] is as expected for a $S = 1/2$ species and confirmed the mixed-valent state. The extensive reduction of the initial trivalent state to a mixed valence Cr(I)/Cr(II) is impressive but not entirely unexpected and fits with that of some selective oligomerization catalysts where TEAL also acts as both reducing and cationizing agent.

The reduction of the metal center observed during the formation of **3.4** possibly suggests an intrinsic instability of the organochromium derivatives of this ligand system. To probe this point, we have attempted a synthesis identical to that of **3.1** but using $\text{MeCrCl}_2(\text{THF})_3$ instead of $\text{CrCl}_3(\text{THF})_3$ as a starting material. The reaction proceeded in a very similar manner affording a new *divalent* complex formulated as $[(\text{CH}(\text{PPh}_2\text{NSiMe}_3)_2)\text{Cr}(\mu^2\text{-Cl})_2\text{Li}(\text{THF})_2]$ (**3.4**) on the basis of its crystal structure.

The complex is monomeric and consists of a chromium atom in a distorted square pyramidal environment (Figure 3.3). The ligand is present in its normal monoanionic form showing geometrical parameters in agreement with those of $[(\text{CH}(\text{PPh}_2\text{NSiMe}_3)_2)_2\text{Cr}(\mu^2\text{-Cl})_2]$ (**3.1**) The three ligand donor atoms occupy two equatorial positions and one axial with one of the two nitrogen donor atoms. As usual the axial bond $[\text{Cr}(1)\text{-N}(2) = 2.291(7) \text{ \AA}]$ is more elongated with respect to the equatorial $[\text{Cr}(1)\text{-N}(1) = 2.170(7) \text{ \AA}]$. The last two equatorial positions are occupied by two chlorine atoms in turn bridging one $\text{Li}(\text{THF})_2$ residue.

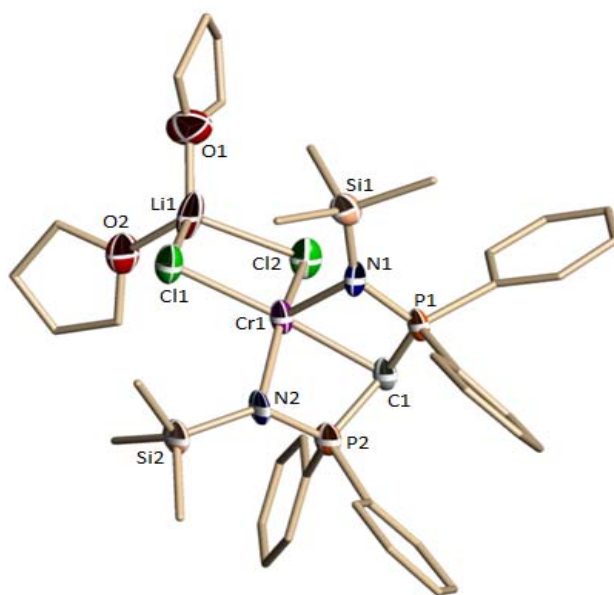


Figure 3.3. Partial thermal ellipsoid drawing for **3.4** at 50% probability level. Selected Bond lengths (\AA) and angles ($^\circ$) of **3.4**: $\text{Cr}(1)\text{-N}(1) = 2.170(7)$, $\text{Cr}(1)\text{-N}(2) = 2.291(7)$, $\text{Cr}(1)\text{-C}(1) =$

2.259(8), Cr(1)-Cl(1) = 2.382(3), Cr(1)-Cl(2) = 2.432(2), Cl(1)-Li(1) = 2.336(18), Cl(2)-Li(1) = 2.343(16), N(1)-P(1) = 1.581(7), N(2)-P(2) = 1.588(7), P(1)-C(1) = 1.762(9), P(2)-C(1) = 1.735(9), Li(1)-O(2) = 1.88(2), Li(1)-O(1) = 1.95(2), N(1)-Cr(1)-C(1) = 72.7(3), N(1)-Cr(1)-N(2) = 95.6(3), C(1)-Cr(1)-N(2) = 72.2(3), N(1)-Cr(1)-Cl(1) = 101.30(19), C(1)-Cr(1)-Cl(1) = 173.4(2), N(2)-Cr(1)-Cl(1) = 106.11(19), N(1)-Cr(1)-Cl(2) = 148.3(2), C(1)-Cr(1)-Cl(2) = 95.6(2), N(2)-Cr(1)-Cl(2) = 109.0(2), Cl(1)-Cr(1)-Cl(2) = 91.00(9), N(1)-Cr(1)-Li(1) = 135.9(4), C(1)-Cr(1)-Li(1) = 141.0(4), N(2)-Cr(1)-Li(1) = 118.8(4), Cl(1)-Cr(1)-Li(1) = 45.5(3), Cl(2)-Cr(1)-Li(1) = 45.6(3), Li(1)-Cl(1)-Cr(1) = 87.8(4), Li(1)-Cl(2)-Cr(1) = 86.5(4), O(2)-Li(1)-O(1) = 106.0(8), Cl(2)-Li(1)-Cl(1) = 94.4(6).

Complex **3.4** is clearly divalent as suggested by the square-pyramidal coordination geometry and indicated by the room temperature magnetic moment [$\mu_{\text{eff}} = 4.71 \mu_{\text{B}}$] as expected for the high-spin configuration of pentacoordinated Cr(II). The divalent state of **3.4** indicates that reduction occurred during the chlorine replacement in turn indicating that the organometallic function did not survive the ligand complexation. This, again, reiterates the intrinsic instability of the organo-chromium derivatives supported by this ligand system thus explaining the catalytic behaviour of all these complexes.

Complex **3.2** in presence of DMAO in toluene produces a significant amount of Schulz-Flory distribution of α -olefins along with a small amount of waxy polymer. The unselective behaviour of this catalyst can be simply explained with the irreversible reduction of Cr(III) to Cr(II) and consequent stabilization of this oxidation state.¹⁹ The reaction carried out in toluene in the presence of the MAO activator caused a decline in activity, concomitantly increasing the yield of waxy polymer.⁶ Other co-catalyst modifications, such

as addition of TEAL (10%) to DMAO caused faster catalyst deactivation. This behaviour was in part anticipated since more reducing aluminum alkyl co-catalysts probably have a poisoning effect on the reactivity of this catalyst as suggested by the reduction to both **3.3** and **3.4**.

Complex **3.3** in the presence of different co-catalyst, also produces a S-F distribution of oligomers but with lower amount of polymer. We were also able to increase its activity by decreasing the co-catalyst loading. This may be understood if we bear in mind that this species is a mixed valence Cr(II)/Cr(I) and possibly more resilient against further reduction. This complex was also tested for self-activating behaviour without success. We speculate that the neutral form of the ligand may cause in this case lability and which in turn may lead to leaching with consequent rapid deactivation.

Not surprisingly then, the testing of complex **3.4**, carried out under conditions identical to those employed for **3.1**, exhibited the same behaviour.¹²

Table 3.3. Ethylene Oligomerization results.

Entry	Catalyst	Cocatalyst (equiv)	Temp (°C)	Alkene (mL)	PE (g)	Activity (g/gCr.h)
1 ^a	3.2	MAO(500)	60	15	3.2	26778
2 ^a	3.2	DMAO(500)	60	64	0.9	89730
3 ^a	3.2	DMAO/TEAL(500/50)	60	40	2.5	59807
4 ^b	3.2	MAO(500)	60	-	-	-
5 ^b	3.2	MAO/TEAL(500/50)	60	-	-	-
6 ^a	3.3 ^c	MAO	60	5	0.8	5608
7 ^a	3.3 ^c	DMAO	60	11	2.6	13416
8 ^a	3.3	-	60	-	-	-
9 ^b	3.3	-	60	-	-	-
10 ^a	3.4	MAO	60	Trace	1.2	2308
11 ^a	3.1	MAO	60	Trace	1.4	2692

Conditions: Loading 20 μmol of complex, 40 bar (ethylene), 30 min reaction time. ^a100 mL of toluene. ^b100 mL of methylcyclohexane. ^cCatalyst loading 30 μmol .

Table 3.4. Analysis of the α -olefin product distribution.

Entry	C6 (%)	C8 (%)	C10 (%)	C12 (%)	C14 (%)	C16 (%)	C18 (%)	α
1	21.84	20.93	16.95	13.87	11.03	8.64	6.82	0.69
2	18.64	24.31	18.74	14.40	10.62	7.70	5.61	0.69
3	21.97	21.68	17.63	13.98	10.7	7.99	6.06	0.67
6	20.22	21.99	16.11	15.24	9.28	5.25	4.55	0.66
7	27.84	24.99	18.86	15.00	11.13	8.58	6.22	0.65

3.6 Conclusion

In this chapter we have isolated a series of chromium complexes with various oxidation states supported by the established phosphoranimine ligand in both anionic and neutral forms. The ability of this ligand system to stabilize mixed-valent chromium Cr(II)/Cr(I) was a pleasant surprise. Also the catalytic behaviour of **3.2**, containing trivalent chromium, has been optimized by using the appropriate co-catalyst and temperature. This system provided statistical mixtures of oligomers with high activity and only insignificant amounts of undesirable polymer. Both features make this catalytic system desirable from the commercial point of view.

3.7 References

1. Britovsek, G. J. P.; Gibson, V. C.; Kimberley, B. S.; Maddox, P. J.; Mctavish, S. J.; Solan, G. A.; White, J. P.; Williams, D. J. *Chem. Commun.* **1998**, 311, 849.
2. Gibson, V. C.; Redshaw, C.; Solan, G. A. *Chem. Rev.* **2007**, 107, 1745.
3. (a) Bianchini, C.; Mantovani, G.; Meli, A.; Migliacci, F.; Laschi, F. *Organometallics* **2003**, 22, 2545; (b) Esteruelas, M. A.; Lopez, A. M.; Mendez, L.; Olivan, M.; Onate, E.; *Organometallics* **2003**, 22, 395; (c) H. Sugiyama.; G. Aharonian.; S. Gambarotta.; G. P. A. Yap.; P. H. M. Budzelaar. *J. Am. Chem. Soc.* **2002**, 124, 12268; (d) Ittel, S. D.; Johnson, L. K.; Brookhart, M. *Chem. Rev.* **2000**, 100, 1169.
4. Steiner, A.; Zacchini, S.; Richards, P. I. *Coord. Chem. Rev* **2002**, 227, 193.
5. Demange, M.; Boubekeur, L.; Auffrant, A.; M'zailles, N.; Ricard, L.; Le Goff, X.; Le Floch, P. *New J. Chem.* **2006**, 30, 1745.
6. Klemps, C.; Buchard, A.; Houdard, R.; Auffrant, A.; Mézailles, N.; Le Goff, X. F.; Ricard, L.; Saussine, L.; Magna, L.; Le Floch, P. *New J. Chem.* **2009**, 33, 1748.
7. Kocher, N.; Leusser, D.; Murso, A.; Stalke, D. *Chemistry (Weinheim an der Bergstrasse, Germany)* **2004**, 10, 3622.
8. (a) Al-Benna, S.; Sarsfield, M. J.; Thornton-Pett, M.; Ormsby, D. L.; Maddox, P. J.; Brès, P.; Bochmann, M. *J. Chem. Soc., Dalton Trans.* **2000**, 4247; (b) K. Kreischer.; J. Kipke.; M. Bauerfeind.; J. Sundermeyer.; *Z. Anorg. Allg. Chem.* **2001**, 627, 1023.

9. Kasani, A.; Babu, R. P. K.; McDonald, R.; Cavell, R. G. *Angew. Chem., Int. Ed.* **1999**, *2*, 1483.
- (10) Aharonian, G.; Feghali, K.; Gambarotta, S.; Yap, G. P. *Organometallics* **2001**, *20*, 2616.
- (11) Buchard, A.; Auffrant, A.; Klemps, C.; Vu-Do, L.; Boubekeur, L.; Goff, X. F. Le; Floch, P. Le. *Chem. Commun.* **2007**, 1502.
- (12) Wei, P.; Stephan, D. W. *Organometallics* **2002**, *21*, 1308.
- (13) Vidyaratne, I.; Nikiforov, G. B.; Gorelsky, S. I.; Gambarotta, S.; Duchateau, R.; Korobkov, I. *Angew. Chem. Int. Ed.* **2009**, *48*, 6552.
- (14) Appel, R.; Ruppert, I. *Z. Anorg. Allg. Chem.* **1974**, *406*, 131.
- (15) (a) Albahily, K.; Koç, E.; Al-Baldawi, D.; Savard, D.; Gambarotta, S.; Burchell, T. J.; Duchateau, R. *Angew. Chem. Int. Ed.* **2008**, *47*, 5816; (b) Temple, C. N.; Jabri, A.; Crewdson, P.; Gambarotta, S.; Korobkov, I. *Angew. Chem. Int. Ed.* **2006**, *45*, 7050; (c) Temple, C. N.; Gambarotta, S.; Korobkov, I.; Duchateau, D. *Organometallics* **2007**, *26*, 4598.
- (16) Horvath, S.; Gorelsky, S. I.; Gambarotta, S.; Korobkov, I. *Angew. Chem., Int. Ed.* **2008**, *47*, 9937.
- (17) Albahily, K.; Al-Baldawi, D.; Gambarotta, S.; Duchateau, R.; Koç, E.; Burchell, T. J. *Organometallics* **2008**, *27*, 5708.

(18) Albahily, K.; Koç, E.; Al-Baldawi, D.; Savard, D.; Gambarotta, S.; Burchell, T. J.; Duchateau, R. *Angew. Chem., Int. Ed.* **2008**, *47*, 5816.

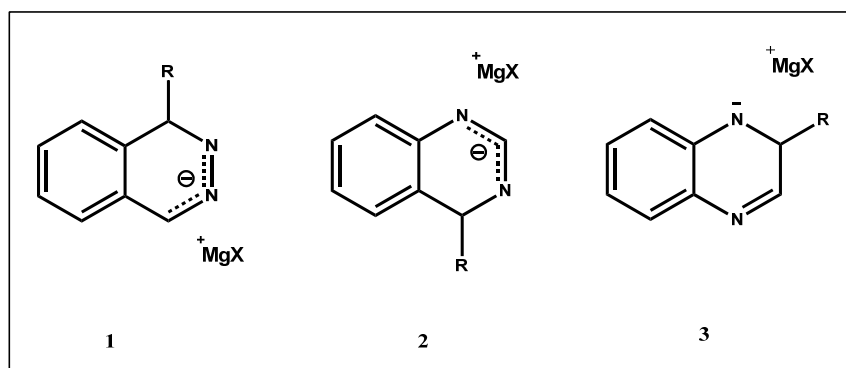
(19) Jabri, A.; Mason, C. B.; Sim, Y.; Gambarotta, S.; Burchell, T. J.; Duchateau, R. *Angew. Chem., Int. Ed.* **2008**, *47*, 9717.

Radical Chemistry of Alkyl Aluminum

4.1 Introduction

Poly-condensed aromatic molecules based on pyridine, such as polyazine, display an impressive collection of attractive features spanning tendency to stabilize and promote formation of organic radicals,¹ light-harvesting properties,² formation of robust coordination compound,³ photoconductive properties,⁴ etc. In this family of compounds, 2,3-bis(2-pyridyl) quinoxaline (DPQ) seems to be especially versatile, having displayed excellent characteristics as chromophore for biological applications such as in the field of anticancer agents.⁵ Quinoxaline derivatives are also frequently encountered as pharmacologically active substances. Last but not least, substituted quinoxaline find applications as dyes,⁶ electroluminescent materials,⁷ semiconducting materials⁸ and DNA binding agents.⁹

With such a diversified range of reactivity, the interaction of these molecules with organometallic residues is also of interest.¹⁰ Nucleophilic addition at the C=N bond of the quinoxalines gives with Grignard reagents only mono-addition products, presumably due to deactivation of the second C=N bond in the intermediate metal complexes.^{10b,c}



Scheme 4.1

In the case of quinoxalines instead (e.g. number 3 in Scheme 4.1) the charge delocalization is less and double alkylation becomes permissible (Scheme 4.1).^{10d}

Polyazine compounds give an unusual reactivity with alkyl aluminum in the sense that they produce paramagnetic species by promoting the homolytic cleavage of one Al-C bond.¹¹ These species are often anionic, organic-centered radicals where spin-density has been localized in some of the ring positions with consequent partial loss of aromaticity. Even further, these unusual complexes belong to the category of the so-called “low-valent synthons”, this name being derived by the deceiving appearance of the aluminate residues as low-valent aluminum.^{11a} Given this behaviour, there is no surprise that radical anions of quinoxaline derivatives can be readily obtained by the usage of an alkali metal (potassium) and 18-crown-6.¹² On the opposite, radical cationic species are rare and, yet, have been observed by reaction at a mercury electrode. Thus, there is no doubt that these species have a unique versatility in terms of electron transfer since they may be involved in either reduction or oxidation.

As a continuation of our studies on electron transfer reactions promoted by this family of derivatives¹³ herein, we describe the reaction of 2,3-bis(2-pyridyl)quinoxaline (DPQ) with different AlR_3 ($R=Me, Et$) surprisingly affording a stable radical cationic species in addition to double alkylation of one of the quinoxaline rings.

4.2 Experimental

All reactions were carried out under a nitrogen atmosphere using drybox or Schlenk techniques since all complexes (or operation) reported in this work were extremely oxygen

and water sensitive. Solvents were dried using columns containing activated aluminum oxide to remove water and purged by vacuum and nitrogen for deoxygenation. $\text{CrCl}_2(\text{THF})_2$ and $\text{CrCl}_3(\text{THF})_3$ were prepared according to established procedures. Methylaluminoxane (MAO, 30% in toluene) was purchased from Albemarle Corporation, $\text{Al}(\text{Et})_3$ and $\text{Al}(\text{Me})_3$ from Strem and used as received. Elemental analysis was accomplished with a Perkin-Elmer 2400 CHN analyzer. Magnetic measurements were performed with a Johnson Matthey Magnetic Susceptibility balance at room temperature. The NMR spectra were recorded with a Bruker Avance 300 MHz spectrometer at 300 K. Data for X-ray crystal structure determination were obtained with a Bruker diffractometer equipped with a 1K Smart CCD area detector. Mass spectra were obtained on a Micromass Quattro-LC Electrospray-Triple Quadrupole Mass Spectrometer. A 300 mL Parr reactor equipped with a temperature control instrument and stirrer was used for testing the catalytic activities. EPR spectra were recorded at both room temperature and 100 K with a Bruker Elexsys E580 (X band = 9.8 GHz) machine with samples sealed in a 0.03 mm quartz cell under inert atmosphere. The synthesis of 2,3-bis(2-pyridyl)quinoxaline (DPQ) ($\text{C}_{18}\text{H}_{12}\text{N}_4$) (**4a**) was carried out according to a reported procedure exactly.¹⁴

4.2.1 Synthesis of complexes

Preparation of $[\text{AlMe}_3]\{[\text{AlMe}_2]_2(\mu-\kappa^2:\kappa^2-\text{C}_{20}\text{H}_{18}\text{N}_4)\}$ (**4.1**)

A solution of 2,3-bis(2-pyridyl)quinoxaline (**4a**) (0.28 g, 1 mmol) in toluene (6 mL) was cooled at $-35\text{ }^\circ\text{C}$ for 30 min and then treated with neat TMA (0.22 g, 3 mmol). After

stirring for one hour, the resulting green suspension was centrifuged. Light yellow crystal of **4.1** separated upon layering the solution with hexane (0.23 g, 0.47 mmol, 47%). Elemental Analysis Calcd. (Found) for $C_{27}H_{39}Al_3N_4$: C 64.78 (65.01), H 7.85 (7.98), N 11.19 (11.31). ESI-MS $m/z = 500.26$ ($[M+H]^+$). 1H NMR (C_6D_6): δ 7.6 (m, 4H, Ar H), 7.35 (m, 4H, Ar H), 6.55 (m, 4H, Ar H), 1.6 (s, 6H, CH_3), 0.83 (s, 12H, CH_3), -0.13 (s, 9H, CH_3).

Preparation of $\{[AlMe_2]_2(\mu-\kappa^2:\kappa^2-C_{18}H_{12}N_4)\}(AlCl_2Me_2)$ (**4.2**)

A mixture of $CrCl_3(THF)_3$ (0.38 g, 1 mmol) and 2,3-bis(2-pyridyl)quinoxaline (**4a**) (0.28 g, 1 mmol) in toluene (10 mL) was cooled at $-35^\circ C$ and treated with neat TMA (0.72 g, 10 mmol). The colour of the solution turned dark-brown after 30 min. of stirring. The resulting suspension was centrifuged and the volume of the supernatant reduced *in vacuo* (4 mL). Brown crystal of **4.2** separated after 3 days upon layering the solution with hexane. (0.44 g, 0.62 mmol, 62%), $\mu_{eff} = 1.69 \mu_B$. Elemental Analysis Calcd. (Found) for $C_{24}H_{31}Al_3Cl_2N_4$: C 54.66 (54.71), H 5.92 (6.00), N 10.62 (10.68). ESI-MS $m/z = 526.14$ ($[M+H]^+$).

Preparation of $[AlEt_2]_2(\mu-\kappa^2:\kappa^2-C_{18}H_{12}N_4)$ (**4.3**)

A mixture of $CrCl_2(THF)_2$ (0.27 g, 1 mmol) and 2,3-bis(2-pyridyl)quinoxaline (**4a**) (0.28 g, 1 mmol) in toluene (10 mL) was cooled at $-35^\circ C$ and treated with neat TEAL (1.14 g, 10 mmol). The colour of the solution turned dark-green after one hour of stirring. The

resulting suspension was centrifuged. Dark-blue crystal of **4.3** separated after 5 days upon layering the solution with hexane. (0.44 g, 0.62 mmol, 62%), $\mu_{\text{eff}} = 2.51 \mu_{\text{B}}$. Elemental Analysis Calcd. (Found) for $\text{C}_{26}\text{H}_{32}\text{Al}_2\text{N}_4$: C 68.70 (68.75), H 7.10 (7.15), N 12.33 (12.37). ESI-MS $m/z = 454.23$ ($[\text{M}+\text{H}]^+$).

Preparation of $(\text{C}_{18}\text{H}_{12}\text{N}_4)\text{CrCl}_2\text{Me}(\text{THF})_3$ (4.4**)**

A mixture of $\text{CrMeCl}_2(\text{THF})_3$ (0.35 g, 1 mmol) and 2,3-bis(2-pyridyl)quinoxaline (**4a**) (0.28 g, 1 mmol) in toluene (7 mL) was stirred overnight. The resulting green solution was centrifuged and stored at $-35\text{ }^\circ\text{C}$ for 2 days. Green crystals of **4.4** separated which were washed with cold hexanes and dried *in vacuo*. (0.32 g, 0.65 mmol, 65%), $\mu_{\text{eff}} = 3.91 \mu_{\text{B}}$. Elemental Analysis Calcd. (Found) for $\text{C}_{23}\text{H}_{22}\text{Cl}_2\text{CrN}_4\text{O}$: C 55.99 (56.03), H 4.49 (4.51), N 11.36 (11.40). ESI-MS $m/z = 492.06$ ($[\text{M}+\text{H}]^+$).

4.3 Computational Methods

Quantum-mechanical calculations were performed using the Gaussian 03 (Revision B.03) program package.¹⁵ Geometry optimization of all compounds was performed at the B3LYP hybrid density functional¹⁶⁻¹⁸ level with a 6-311++G (d,p) basis set.¹⁹⁻²¹ An ultra-fine grid was selected for relevant numerical integrations (for details see Gaussian's manual). The harmonic vibrational frequencies were evaluated to verify the nature of stationary points and indeed all studied structures are minima according to their force constant Hessian eigenvalues. The obtained geometry of the compounds (for complete structural information,

see Table S1 in the Supporting Information) are consistent with the observed solid state structures.

Magnetic shieldings were computed at the same level with the most-widely used gauge-including atomic orbitals (GIAO) method.^{22,23} (GIAO-B3LYP/6-311++G(d,p). The bulk solvent effects of benzene (the solvent used in the experimental part) were taken into account by the conductor-like polarizable Continuum model (CPCM) method.^{24,25} Also all computed NMR chemical shifts were reported on scale in ppm with respect to TMS, calculated at the same above level.

For the computation of contact hyperfine coupling constants (hfcc) using the B3LYP functional, two effective basis sets EPR-III^{26,27} and N07Ddiff^{28,29} were chosen, since they have been introduced as the best choices for the calculation of hfcc.²⁶⁻³⁰ It should be added that due to the lack of the EPR-III basis set for third-row atoms, TZVP³¹ basis set was used for Al and EPR-III basis sets on all other atoms. These basis sets have been augmented by polarization and diffuse functions with core σ -type Gaussians non-contracted and a number of tight σ -type functions added. Furthermore, contraction coefficients and functions were specifically optimized to reproduce experimental isotropic hyperfine couplings in a standard set of molecules.³² Next, toluene solvent effects on hfcc of radicals at room temperature were modeled by CPCM approach. The SOMO and spin density images have been obtained by the Gauss View program.³³

4.4 X-Ray Diffraction

Suitable crystals were selected, mounted on a thin, glass fiber with paraffin oil, and cooled to the data collection temperature. Data were collected on a Bruker AXS SMART 1 k CCD diffractometer. Data collection was carried out with three batch runs at $\varphi = 0.00^\circ$ (600 frames), $\varphi = 120.00^\circ$ (600 frames), and $\varphi = 240.00^\circ$ (600 frames). Initial unit-cell parameters were determined from 60 data frames collected at different sections of the Ewald sphere. Semiempirical absorption corrections based on equivalent reflections were applied. The systematic absences and unit-cell parameters were consistent with the reported space groups. The structures were solved by direct methods, completed with difference Fourier syntheses, and refined with full-matrix least-squares procedures based on F2. All the non-hydrogen atoms in all the structures were refined with anisotropic displacement parameters. All hydrogen atoms were processed as idealized contributions. All scattering factors are contained in several versions of the SHELXTL program library, with the latest version used being v.6.12. Relevant data on crystal structure solution and refinement are given Table 4.1.

Table 4.1. Crystal data and refinements for **4.1 – 4.4**.

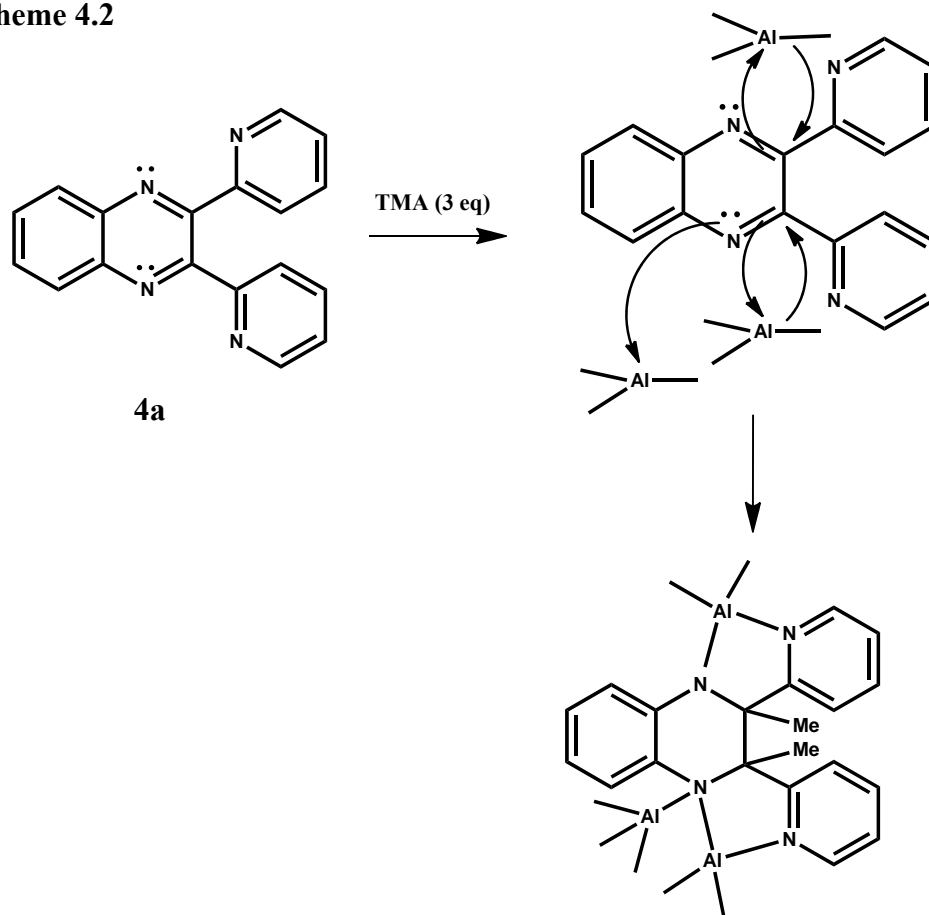
	Complex 4.1	Complex 4.2	Complex 4.3	Complex 4.4
Formula	C _{64.50} H ₉₀ Al ₆ N ₈	C _{27.50} H ₃₄ Al ₃ Cl ₂ N ₄	C ₂₆ H ₃₂ Al ₂ N ₄	C ₂₅ H ₂₇ Cl ₂ CrN ₄ O _{1.50}
MW	1139.32	572.43	454.23	530.41
Space group	Triclinic,P-1	Triclinic,P-1	Monoclinic, P2(1)/c	Triclinic,P-1
<i>a</i> (Å)	13.5752(5)	9.0703	18.2176(7)	8.8818(4)
<i>b</i> (Å)	16.5644(7)	11.6896(3)	19.7794(7)	8.9581(4)
<i>c</i> (Å)	19.7550(8)	16.0930(3)	14.1903(6)	16.2858(7)
<i>α</i>, (deg)	72.131(2)	100.6550(10)	90	104.871(3)
<i>β</i>, (deg)	71.871(2)	105.6700(10)	102.819(2)	97.750(3)
<i>γ</i>, (deg)	67.825(2)	106.5470(10)	90	93.564(3)
<i>V</i> (Å³)	3817.8(3)	1510.16(6)	4985.8(3)	1234.57(9)
<i>Z</i>	2	2	4	2
Radiation	0.71073	0.71073	0.71073	0.71073
T (K)	200(2)	200(2)	200(2)	200(2)
D_{calcd} (gcm⁻³)	0.991	1.259	1.211	1.427
<i>μ</i>_{calcd} (mm⁻¹)	0.122	0.326	0.137	0.708
<i>F</i>000	1222	600	1936	550
<i>R</i>, <i>Rw</i>^{2a}	0.0895, 0.2733	0.0361, 0.1136	0.0584, 0.1799	0.0430, 0.1128
GoF	1.030	1.013	1.017	1.014

$$R = \frac{\sum |F_o| - |F_c|}{\sum |F|}. \quad R_w = \left[\frac{\sum (|F_o| - |F_c|)^2}{\sum w F_o^2} \right]^{1/2}.$$

4.5 Result and discussion

When 2,3-bis(2-pyridyl)quinoxaline was treated with three equivalents of TMA, a new diamagnetic compound $[\text{AlMe}_3]\{[\text{AlMe}_2]_2(\mu\text{-}\kappa^2\text{:}\kappa^2\text{-C}_{20}\text{H}_{18}\text{N}_4)\}$ (**4.1**) was obtained as a yellow crystalline mass (Scheme 4.2).

Scheme 4.2



The connectivity was conclusively demonstrated by an X-ray crystal structure showing the coordination of two Me_2Al units bonded to four nitrogen of 2,3-bis(2-pyridyl)quinoxaline ligand [$\text{Al}(1)\text{-N}(3) = 1.980(4) \text{ \AA}$, $\text{Al}(1)\text{-N}(1) = 2.021(4) \text{ \AA}$, $\text{Al}(2)\text{-C}(24) = 1.959(6) \text{ \AA}$, $\text{Al}(2)\text{-C}(23) = 1.958(5) \text{ \AA}$, $\text{N}(3)\text{-Al}(1)\text{-N}(1) = 82.41(15)^\circ$], and with each aluminum in a distorted tetrahedral environment [$\text{N}(3)\text{-Al}(1)\text{-N}(1) = 82.41(15)$, $\text{N}(2)\text{-Al}(2)\text{-N}(4) = 83.16(18)^\circ$]. A

third aluminate group (Me_3Al) was found attached to one N(pyridyl) atom of the ligand [$\text{Al}(3)\text{-N}(1) = 2.084(4) \text{ \AA}$]. The Al-N bond distance [$\text{Al}(3)\text{-N}(1) = 2.084(4) \text{ \AA}$] is longer while comparing to those formed by the two R_2Al moieties. Two methyl groups were found bonded to the carbon atoms of the pyrazine ring in a *trans* arrangement.

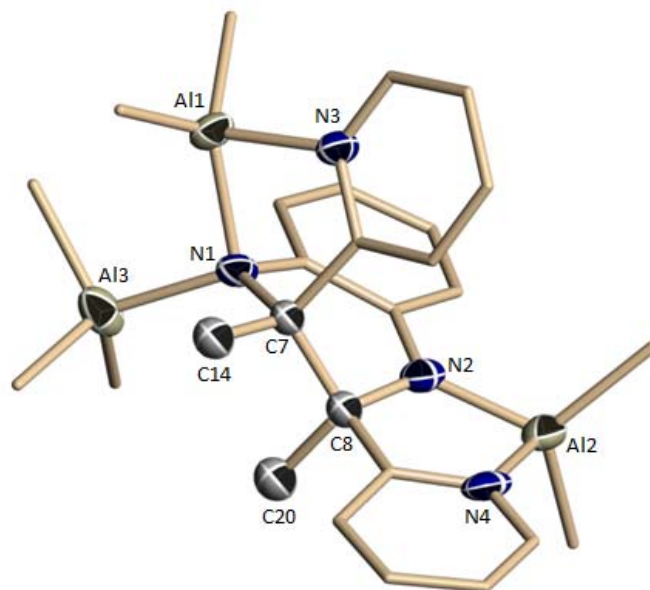


Figure 4.1. Partial thermal ellipsoid drawing for **4.1** at 50% probability level. Selected Bond lengths (\AA) and angles ($^\circ$) of **4.1**: $\text{Al}(1)\text{-N}(3) = 1.980(4)$, $\text{Al}(1)\text{-N}(1) = 2.021(4)$, $\text{Al}(1)\text{-C}(21) = 1.952(7)$, $\text{Al}(1)\text{-C}(22) = 1.966(5)$, $\text{Al}(2)\text{-N}(2) = 1.861(4)$, $\text{Al}(2)\text{-N}(4) = 1.968(5)$, $\text{Al}(2)\text{-C}(24) = 1.959(6)$, $\text{Al}(2)\text{-C}(23) = 1.958(5)$, $\text{Al}(3)\text{-N}(1) = 2.084(4)$, $\text{Al}(3)\text{-C}(25) = 1.977(6)$, $\text{Al}(3)\text{-C}(27) = 1.979(7)$, $\text{Al}(3)\text{-C}(26) = 1.998(7)$, $\text{Al}(3)\text{-N}(1) = 2.084(4)$, $\text{C}(7)\text{-C}(8) = 1.568(6)$, $\text{N}(2)\text{-C}(8) = 1.452(6)$, $\text{N}(2)\text{-C}(6) = 1.392(6)$, $\text{N}(1)\text{-C}(7) = 1.523(5)$, $\text{N}(1)\text{-C}(1) = 1.468(6)$, $\text{N}(3)\text{-Al}(1)\text{-N}(1) = 82.41(15)$, $\text{N}(2)\text{-Al}(2)\text{-N}(4) = 83.16(18)$, $\text{Al}(1)\text{-N}(1)\text{-Al}(3) = 101.30(17)$, $\text{C}(25)\text{-Al}(3)\text{-N}(1) = 116.1(2)$, $\text{C}(25)\text{-Al}(3)\text{-C}(27) = 110.7(3)$, $\text{C}(25)\text{-Al}(3)\text{-C}(26) = 105.7(3)$, $\text{C}(7)\text{-N}(1)\text{-Al}(3) = 124.3(3)$, $\text{C}(7)\text{-N}(1)\text{-Al}(1) = 105.4(3)$, $\text{C}(8)\text{-N}(2)\text{-Al}(2) =$

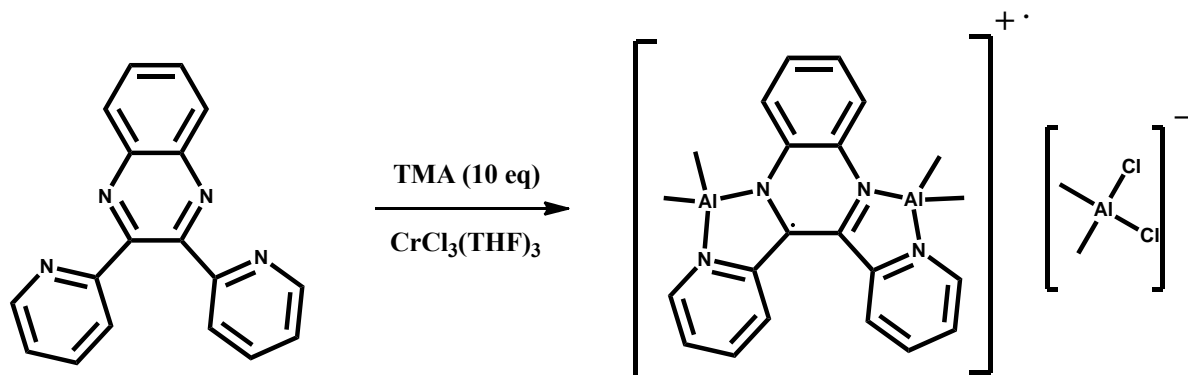
118.1(3), C(20)-C(8)-C(7) = 110.4(4), C(14)-C(7)-C(8) = 114.9(4), C(14)-C(7)-N(1) = 109.8(4), N(2)-C(8)-C(20) = 110.9(4), C(6)-N(2)-C(8) = 114.6(4), C(1)-N(1)-C(7) = 110.5(3), N(1)-C(7)-C(8) = 108.4(4), N(2)-C(8)-C(7) = 107.9(3), C(6)-C(1)-N(1) = 122.5(4), N(2)-C(6)-C(1) = 122.5(4).

The $^1\text{H-NMR}$ spectrum showed, in addition to the expected resonances, the peaks of the methyl group of the $[\text{AlMe}_2]$ units notably shifted to 0.83 ppm. This is possibly an effect of the negative charge at the nitrogen atom of the ligand, as suggested by the difference of chemical shift of an AlMe_3 unit coordinated to a neutral phenazine ligand (-0.31 ppm).³⁴ In the present case, the chemical shift of the methyl resonance of the AlMe_3 connected to the pyridyl group can be observed at 0.13 ppm. Finally, two methyl groups, attached to the ring system, show one singlet at 1.58 ppm therefore indicating that double alkylation has occurred.

The formation of **4.1** is a straightforward process and is visualized in Scheme 4.2. The reaction involves the addition of one methyl group from each of the two TMA to the pyrazine ring. Each of the two pyridyl moieties also coordinates one of the two $\text{Al}(\text{CH}_3)_2$ units.

When the reaction of 2,3-bis(2-pyridyl)quinoxaline (DPQ) with excess of TMA (10 equivalents) was carried out in the presence of $\text{CrCl}_3(\text{THF})_3$ (1 eq) a different species formulated as $\{[\text{AlMe}_2]_2(\mu-\kappa^2:\kappa^2-\text{C}_{18}\text{H}_{12}\text{N}_4)\}(\text{AlCl}_2\text{Me}_2)$ (**4.2**) was isolated in crystalline form (Scheme 4.3). The larger excess of TMA was necessary for ensuring the complete THF abstraction from the chromium salt. Interestingly, this complex *per se* does not contain chromium but, different from **4.1**, is paramagnetic. The $^1\text{H-NMR}$ spectrum of **4.2** only

showed broad and overlapping features. Therefore, the connectivity was inferred by an X-ray crystal structure.



Scheme 4.3

The structure of **4.2** consists of the ligand, apparently intact, coordinated to two AlMe₂ residues in an overall cationic $\{[AlMe_2]_2(\mu-\kappa^2:\kappa^2-C_{18}H_{12}N_4)\}$ structure counterbalanced by one non-coordinated aluminate anion [AlCl₂Me₂]⁻. The coordination geometry of each aluminum center is distorted tetrahedral with narrow N-Al-N angles [N(2)-Al(1)-N(1) = 82.24(5)^o, N(4)-Al(2)-N(3) = 82.18(5)^o] and is defined by one nitrogen of a pyridyl moiety and one nitrogen of quinoxaline [Al(1)-N(2) = 1.9377(11) Å, Al(1)-N(1) = 1.9601(12) Å, Al(2)-N(4) = 1.9303(11) Å, Al(2)-N(3) = 1.9557(12) Å]. All the other bond distances and angles are in the normal range.

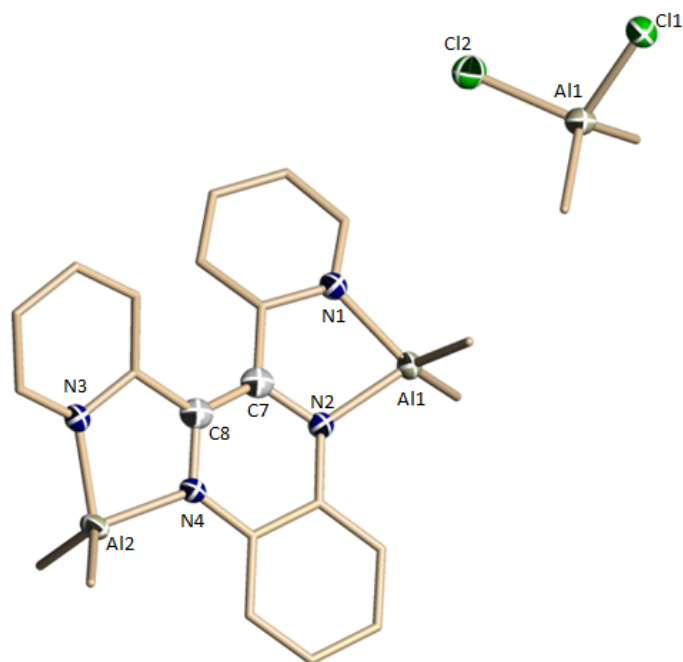


Figure 4.2. Partial thermal ellipsoid drawing for **4.2** at 50% probability level. Selected Bond lengths (Å) and angles (°) of **4.2**: Al(1)-N(2) = 1.9377(11), Al(1)-C(19) = 1.9491(16), Al(1)-C(20) = 1.9523(17), Al(1)-N(1) = 1.9601(12), Al(2)-N(4) = 1.9303(11), Al(2)-C(21) = 1.9448(18), Al(2)-C(22) = 1.9518(17), Al(2)-N(3) = 1.9557(12), Al(3)-Cl(1) = 2.2069(5), Al(3)-Cl(2) = 2.2037(6), N(4)-C(8) = 1.3700(15), N(2)-C(7) = 1.3730(16), C(7)-C(8) = 1.3931(16), N(2)-Al(1)-N(1) = 82.24(5), C(19)-Al(1)-N(1) = 111.43(7), C(20)-Al(1)-N(1) = 109.66(7), N(2)-Al(1)-C(19) = 113.62(6), N(2)-Al(1)-C(20) = 110.92(6), C(19)-Al(1)-C(20) = 121.97(8), N(4)-Al(2)-N(3) = 82.18(5), C(22)-Al(2)-N(3) = 112.76(7), C(21)-Al(2)-N(3) = 110.60(7), N(4)-Al(2)-C(21) = 116.82(8), N(4)-Al(2)-C(22) = 108.66(6), C(21)-Al(2)-C(22) = 119.81(8), Cl(2)-Al(3)-Cl(1) = 105.88(2).

The measurement of the magnetic susceptibility confirmed the paramagnetism as caused by the presence of one unpaired electron ($\mu_{\text{eff}} = 1.69 \mu_{\text{B}}$). This reveals that this species is in fact a radical cation as already hinted by the crystal structure.

The EPR spectrum of **4.2** consists of a single wave plot indicative of the presence of one unpaired electron. The g value (2.0054 G) suggests that spin density is mainly localized on the quinoxaline ring. However, in sharp contrast with the anionic radical species of phenazine which showed a very complex hyperfine structure,^{11b} the EPR spectrum recorded in toluene at 100 K did not exhibit hyperfine coupling. Spectral simulation spectrum was attempted via DFT obtaining a g value (2.0032 G) in reasonable agreement with the experimental one.

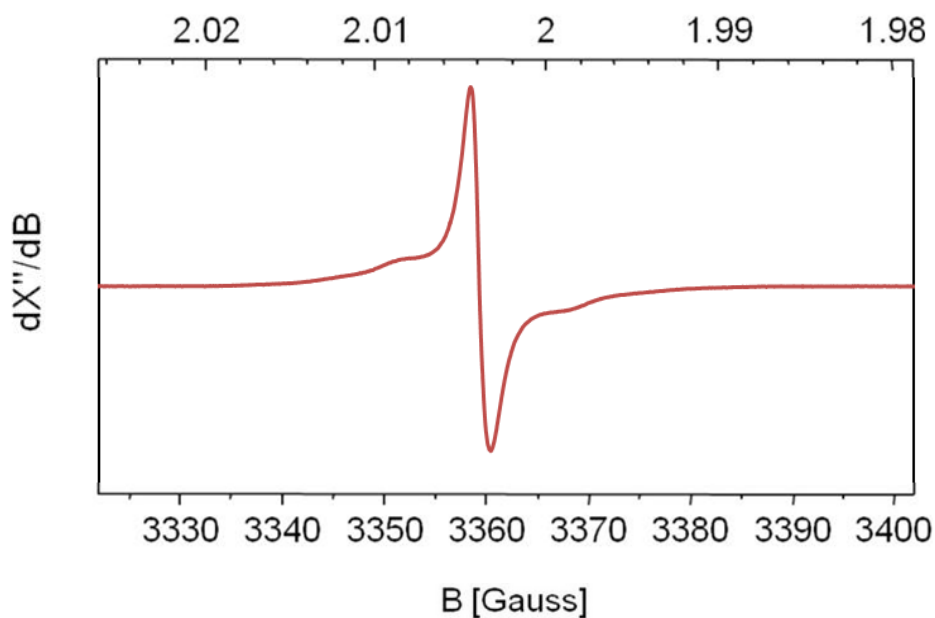


Figure 4.3 EPR spectrum of $\{[\text{AlMe}_2]_2(\mu\text{-}\kappa^2\text{:}\kappa^2\text{-C}_{18}\text{H}_{12}\text{N}_4)\}(\text{AlCl}_2\text{Me}_2)$ (**4.2**) recorded in toluene glass at 100 K.

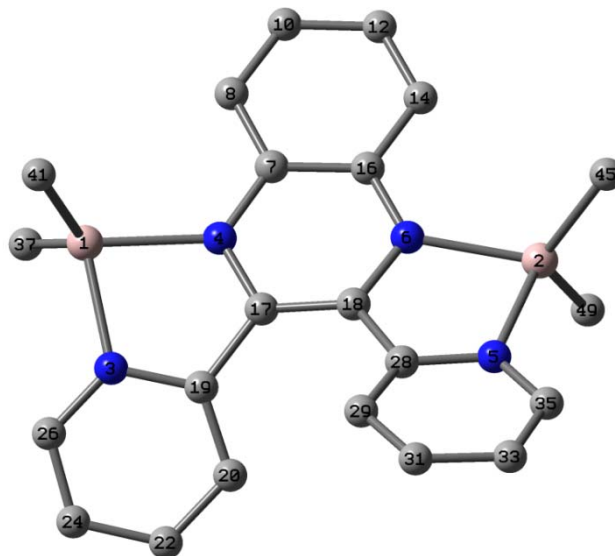
DFT calculation of **4.2** was carried out on the crystallographic atomic coordinates. Excellent agreement of the calculated geometrical parameters with the experimental lend credibility to the computational output (Table 4.2).

Table 4.2. Selected bond distances and angles (calculated versus experimental)

Bond distance (Å) and angles (°)	Experimental	Calculated
Al(1)-N(2)	1.938	1.984
Al(1)-C(19)	1.984	1.963
Al(1)-N(1)	1.960	2.012
N(4)-C(8)	1.370	1.384
N(2)-C(1)	1.384	1.385
C(7)-C(8)	1.393	1.401
N(2)-Al(1)-N(1)	82.24	80.98
C(20)-Al(1)-N(1)	109.66	110.5
C(19)-Al(1)-C(20)	121.97	124.39

The values in Table 4.3 show the spin density on each corresponding atom of the complex with the largest being on the nitrogen atoms of the pyrazine rings.

Table 4.3. DFT calculated Spin densities value on each atom of the $\{[AlMe_2]_2(\mu-\kappa^2:\kappa^2-C_{18}H_{12}N_4)\}^+$.



Atom	a.u.	Atom	a.u.
1 Al(27)	-0.00811	19 C(13)	-0.00298
2 Al(27)	-0.00811	20 C(13)	0.00139
3 N(14)	0.00502	22 C(13)	0.00101
4 N(14)	0.05931	24 C(13)	0.00099
5 N(14)	0.00503	26 C(13)	-0.00057
6 N(14)	0.05932	28 C(13)	-0.00298
7 C(13)	-0.00500	29 C(13)	0.00139
8 C(13)	0.00018	31 C(13)	0.00101
10 C(13)	0.00315	33 C(13)	0.00099
12 C(13)	0.00315	35 C(13)	-0.00057
14 C(13)	0.00018	37 C(13)	0.00368
16 C(13)	-0.00501	41 C(13)	0.00544
17 C(13)	-0.00236	45 C(13)	0.00368
18 C(13)	-0.00236	49 C(13)	0.00545

Figure 4.4 highlights an excellent agreement between the SOMO and spin density distribution ($S = 1/2$). Both show π character with the unpaired electron extensively delocalized onto the quinoxaline moiety of the molecule.

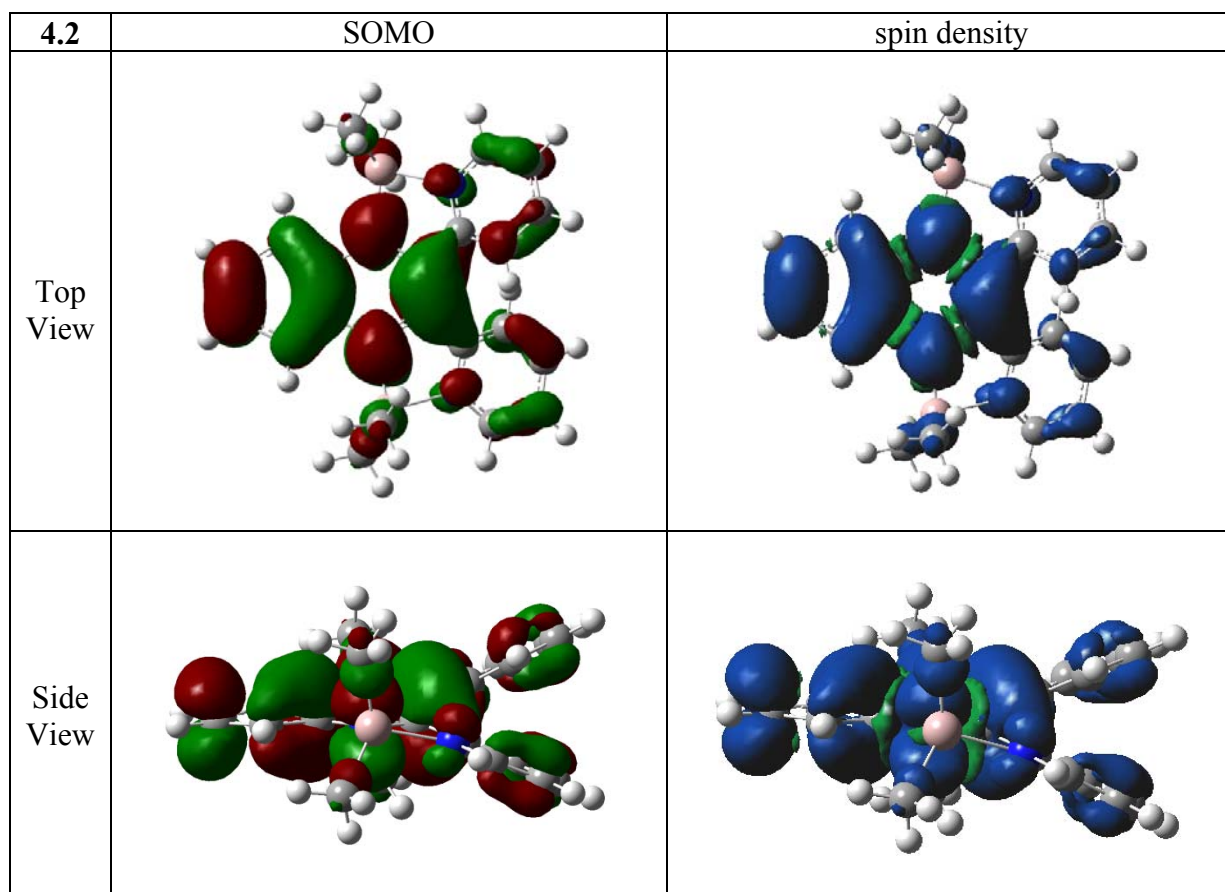
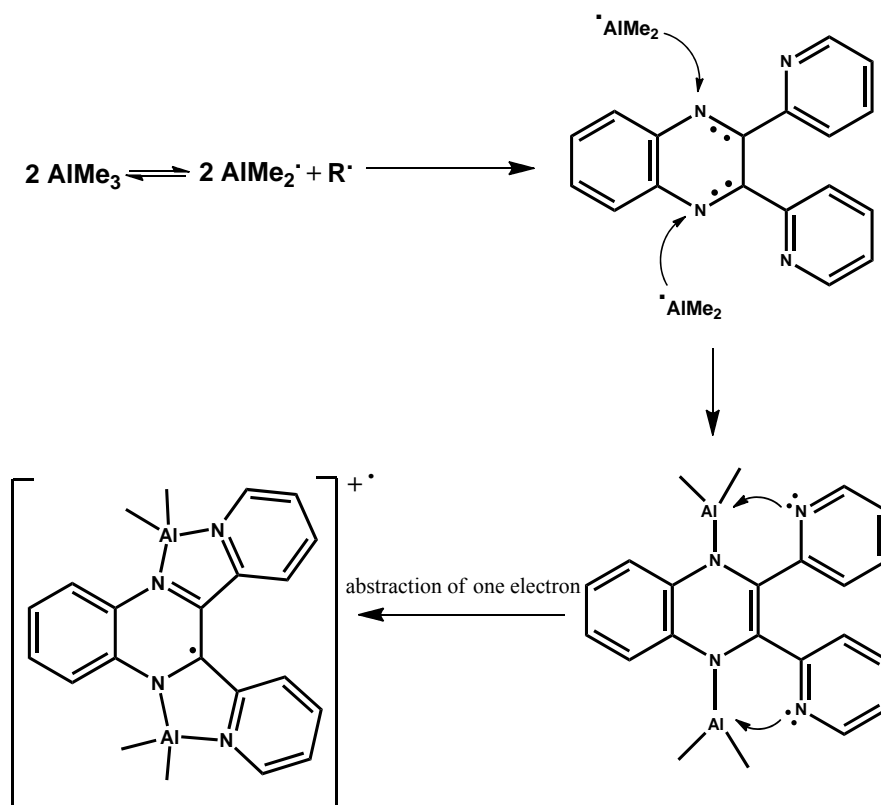


Figure 4.4. The SOMO and spin density plots for **4.2** (blue = positive spin density, green = negative spin density).

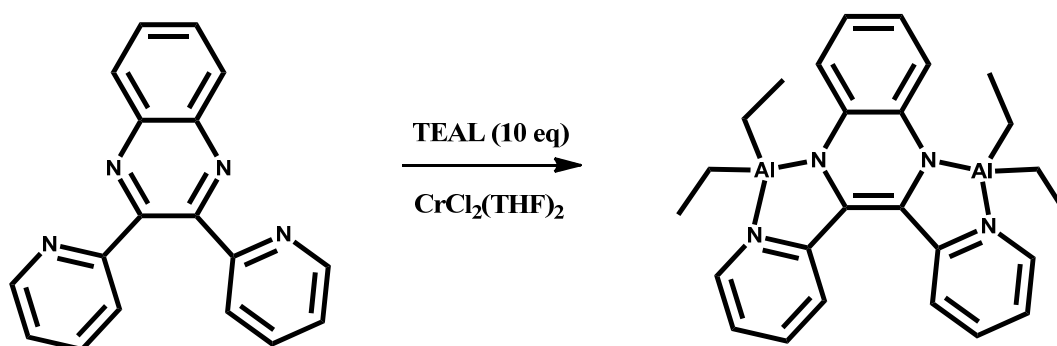
The formation of $\{[\text{AlMe}_2]_2(\mu\text{-}\kappa^2\text{:}\kappa^2\text{-C}_{18}\text{H}_{12}\text{N}_4)\}(\text{AlCl}_2\text{Me}_2)$ (**4.2**) does not have a straightforward explanation. The formation of two AlR_2 residues implies that two initial AlR_3 units have undergone radical cleavage (Scheme 4.4). The two *formally* divalent AlR_2

units can of course “di-anionize” the pyrazine ring by localizing a double bond between the two carbons contiguous to the two nitrogens. What remains unclear is the subsequent one-electron extraction from the C-C double bond to generate the radical cation. The drive for this reaction, which implies a further radical attack, is especially hard to understand since it involves a formal oxidation as carried out by either alkyl aluminum or organic radicals. In fact, these species normally behave as reducing agents and not as oxidants. The role of chromium in this reaction remains even more mysterious since its presence is a necessity for the reaction to afford **4.2**. It is tempting to speculate that intermediate Cr-alkyl may produce the radicals necessary to attack the olefinic bond. It should be reiterated that only the chromium starting material may be the source of the chlorine atom present in the aluminate counter-cation.

Scheme 4.4. Rationalization for formation of complex **4.2**



When the reaction leading to **4.3** was carried out by adding the more reducing TEAL (10 eq) to the cold mixture of 2,3-bis(2-pyridyl)quinoxaline (DPQ) and $\text{CrCl}_2(\text{THF})_2$ [also more reducing than $\text{CrCl}_3(\text{THF})_3$], the new paramagnetic compound $[\text{AlEt}_2]_2(\mu\text{-}\kappa^2\text{:}\kappa^2\text{-C}_{18}\text{H}_{12}\text{N}_4)$ (**4.3**) was obtained (Scheme 4.5).



Scheme 4.5

The connectivity was yielded by an X-ray crystal structure. The structure consists of the ligand apparently unmodified and connected to two Et_2Al residues. The ligand bond distances and angles are basically identical to those of **4.1** $[\text{AlMe}_3]\{[\text{AlMe}_2]_2(\mu\text{-}\kappa^2\text{:}\kappa^2\text{-C}_{20}\text{H}_{18}\text{N}_4)\}$ and **4.2** $\{[\text{AlMe}_2]_2(\mu\text{-}\kappa^2\text{:}\kappa^2\text{-C}_{18}\text{H}_{12}\text{N}_4)\}(\text{AlCl}_2\text{Me}_2)$ thus indicating that no anomalies are present in the ligand. Even in this case, the role of chromium remains obscure.

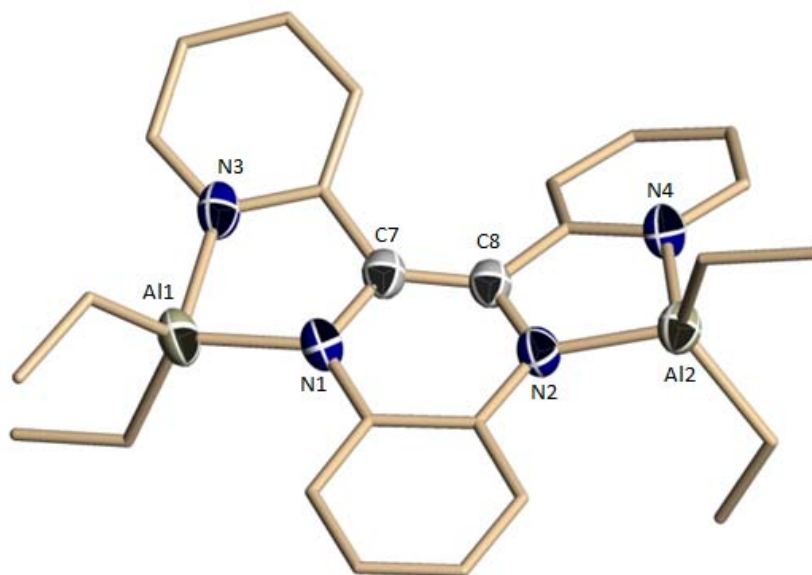


Figure 4.5. Partial thermal ellipsoid drawing for **4.3** at 50% probability level. Selected Bond lengths (Å) and angles (°) of **4.3**: Al(1)-N(1) = 1.881(2), Al(1)-N(3) = 1.956(3), Al(1)-C(21) = 1.971(3), Al(1)-C(19) = 1.972(3), Al(1)-C(21) = 1.971(3), Al(2)-N(2) = 1.875(2), Al(2)-N(4) = 1.951(2), Al(2)-C(23) = 1.971(3), Al(2)-C(25) = 1.970(3), C(7)-C(8) = 1.377(3), N(2)-C(8) = 1.395(3), N(1)-C(7) = 1.407(3), N(1)-Al(1)-N(3) = 82.69(9), N(1)-Al(1)-C(21) = 116.73(11), N(3)-Al(1)-C(21) = 107.63(12), N(1)-Al(1)-C(19) = 114.35(12), N(3)-Al(1)-C(19) = 110.37(14), C(21)-Al(1)-C(19) = 118.66(13), N(2)-Al(2)-N(4) = 82.88(9), N(2)-Al(2)-C(23) = 114.60(12), N(4)-Al(2)-C(23) = 108.76(12), N(2)-Al(2)-C(25) = 112.34(10), N(4)-Al(2)-C(25) = 113.18(12), C(23)-Al(2)-C(25) = 119.33(12), C(8)-C(7)-N(1) = 120.0(2), C(7)-C(8)-N(2) = 121.2(2).

According to the connectivity as yielded by the crystal structure, the complex is expected to be diamagnetic. However, the $^1\text{H-NMR}$ spectra gave a clear indication of

paramagnetism due to broad overlapping features. In addition, the magnetic moment measured at room temperature with a guy balance gave a value [$\mu_{\text{eff}} = 2.51 \mu_{\text{B}}$] in agreement with the presence of two unpaired electrons. Furthermore, solutions of **4.3** at both 100 K and room temperature gave identical EPR spectra. The spectra consist of a broad single line signal very weak in intensity and with shoulder wings corresponding to canonical peaks due to the fine-structure D tensor. In turn, this suggests the existence of triplet state as the dominant form with a small population of singlet (Scheme 4.6). One has only to assume that the triplet form, by having integer S , is EPR-silent.

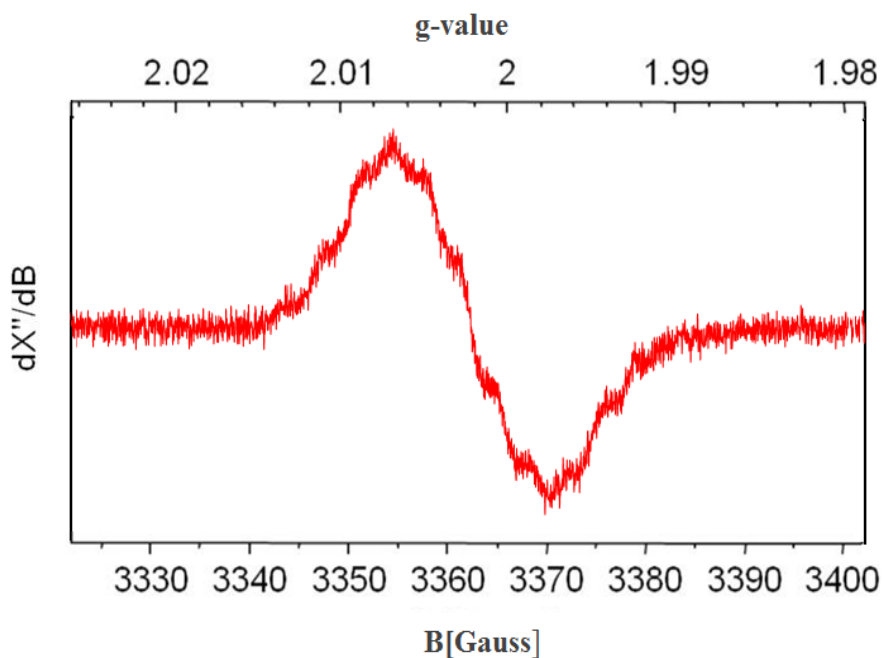
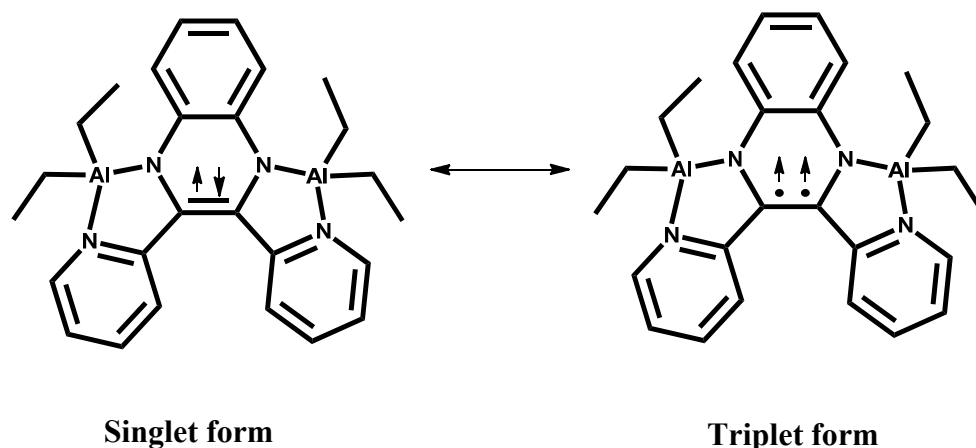


Figure 4.6. EPR spectrum of $[\text{AlEt}_2]_2(\mu\text{-}\kappa^2\text{:}\kappa^2\text{-C}_{18}\text{H}_{12}\text{N}_4)$ (**4.3**) recorded at room temperature.



Scheme 4.6

To substantiate this theory we have carried out DFT calculation. The molecular orbital pictures and energy diagrams of HOMO and LUMO for **4.1** and **4.3** are illustrated in Figure 4.7. The most striking feature is that the HOMO-LUMO energy gap of **4.3** is smaller than for **4.1**. The triplet–singlet energy difference can be approximated by difference of the energies of the singly occupied HOMO-LUMO orbitals. This led us to suppose that the **4.3** singlet–triplet energy gap (ΔE_{S-T}) should be small. To compute ΔE_{S-T} , unconstrained geometry optimizations and harmonic frequency calculations have been carried out at the B3LYP/6-311++G(d,p) level for the excited states (triplet) of **4.3** in toluene. The **4.3** triplet was optimized as a local minimum. It is important to observe that the geometry of **4.3** in singlet and triplet states are very similar.

On the basis of DFT calculations, the singlet state of **4.3** is the ground state and lies only 3.1 kcal/mol below its triplet. From a theoretical point of view, what causes the relative stability of the **4.3** triplet is that, the two SOMOs of the **4.3** diradical are close in energy ($\Delta E_{SOMOs}=0.02$ eV). Accordingly, Hund’s rule suggests a triplet ground state for such a system. Secondly, the two SOMOs are nearly disjoint, meaning that one SOMO has density

on one set of atoms (mostly delocalized on quinoxaline) and the second SOMO has density only on atoms not in the first set (mainly delocalized on pyridine rings). The plots of the SOMOs are given in Figure 4.8.

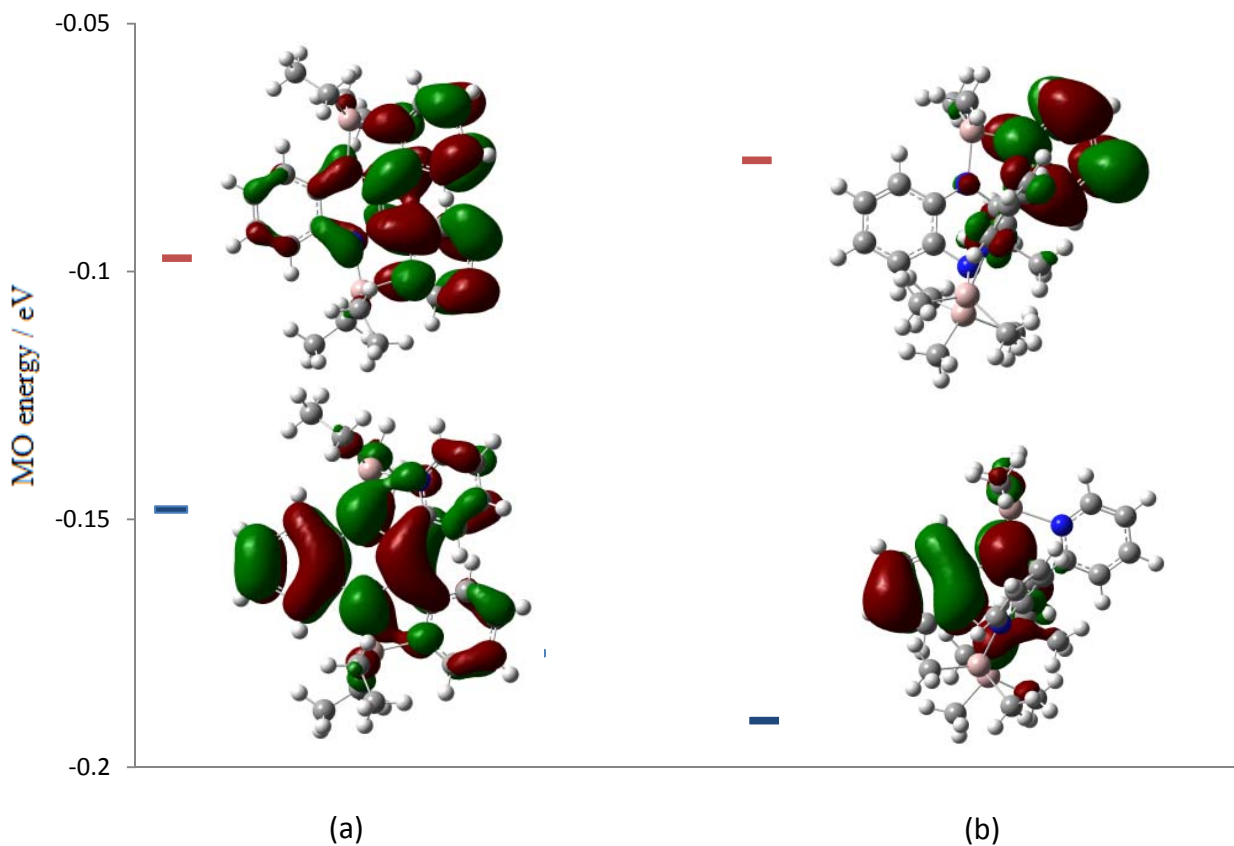


Figure 4.7. Molecular orbital pictures and energy diagrams of HOMO (blue line) and LUMO (red line) for (a) **4.3** and (b) **4.1**. Calculations carried out at the BLYP/6-311++G(d,p) level of theory.

In such a situation and on the basis of Borden-Davidson rule,^{35,36} the electrons in the two SOMOs of **4.3** are more or less isolated and therefore have reduced electrostatic

repulsion. Therefore, the singlet state will not violate the Pauli exclusion principle and will be energy competitive with the triplet state. In fact, this rule suggests that electron correlation lowers the singlet state below the triplet. This lends credibility to the assumption of the simultaneous existence of both states in toluene solvent at room temperature and explains the low intensity of the EPR spectra. This feature can indeed be attributed to the low population of compound in singlet state.

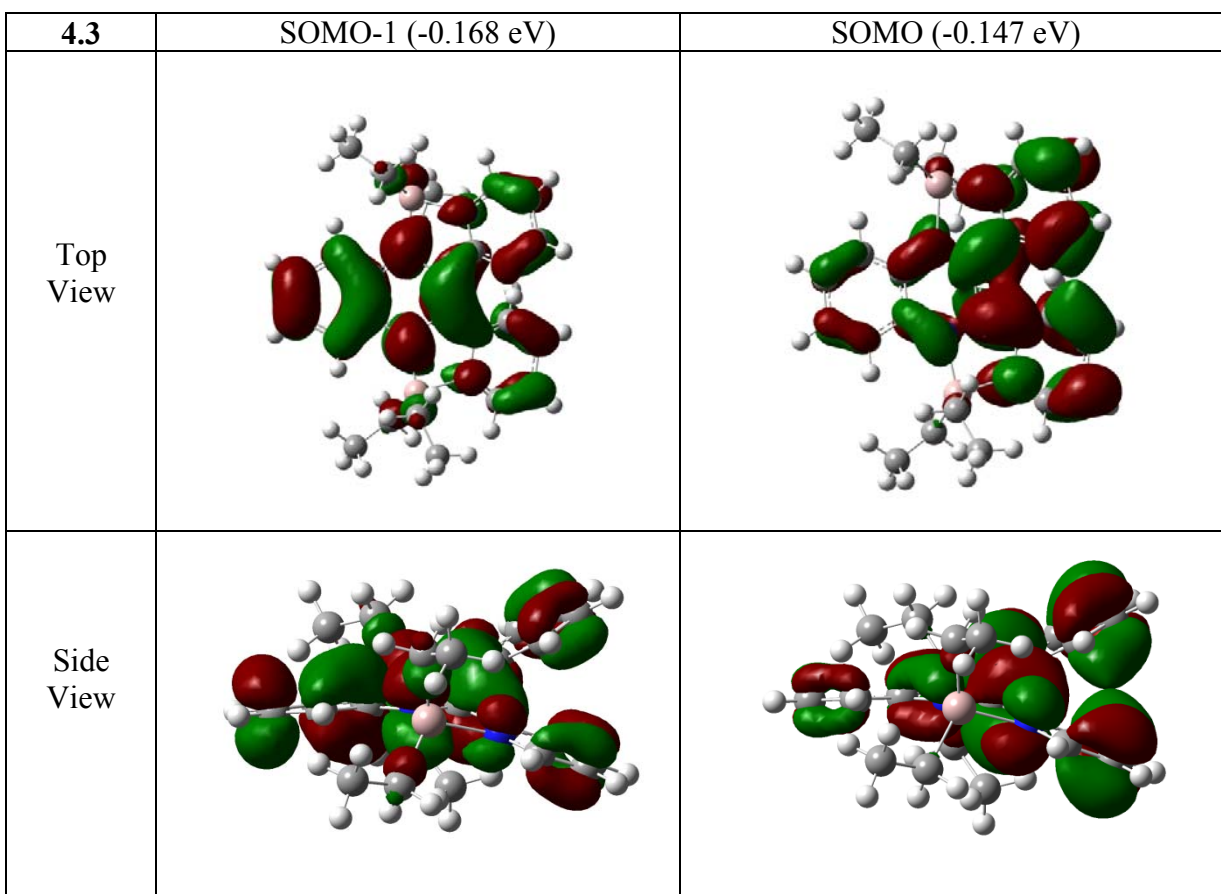
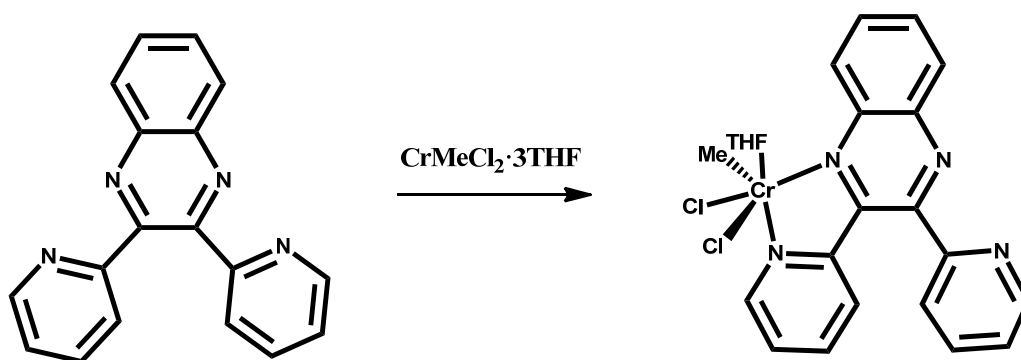


Figure 4.8. The shape of singly occupied molecular orbitals (SOMOs) of the triplet of 4.3.

The formation of the complex aluminates as described above may be only achieved with the intervention of chromium, although this metal is not present in the final structure. In an attempt to clarify the role of the transition metal in the above transformations we have also attempted the direct reaction of 2,3-bis(2-pyridyl)quinoxaline with two equivalent of $\text{CrCl}_2\text{Me}(\text{THF})_3$. Different from the above cases where there was no indication for a direct ligand to chromium interaction, in this case a new species formulated as $(\text{C}_{18}\text{H}_{12}\text{N}_4)\text{CrCl}_2\text{Me}\cdot(\text{THF})_3$ (**4.4**) was obtained (Scheme 4.7). Chromium showed just σ -coordination to the pyridine and pyrazine nitrogen donor atoms from one side of the ligand.



Scheme 4.7

The structure of 4.4 was elucidated by an X-ray crystal structure. The complex consists of a chromium center surrounded by the two nitrogen of the DPQ ligand, a methyl group, two chlorine atoms and a molecule of THF in an overall distorted octahedral environment [Cr(1)-N(3) = 2.0795(18) Å, Cr(1)-N(1) = 2.1638(18) Å, Cr(1)-C(19) = 2.057(2) Å, Cr(1)-O(1) = 2.2223(16) Å, Cr(1)-Cl(2) = 2.3115(7), Cr(1)-Cl(1) = 2.3244(7) Å].

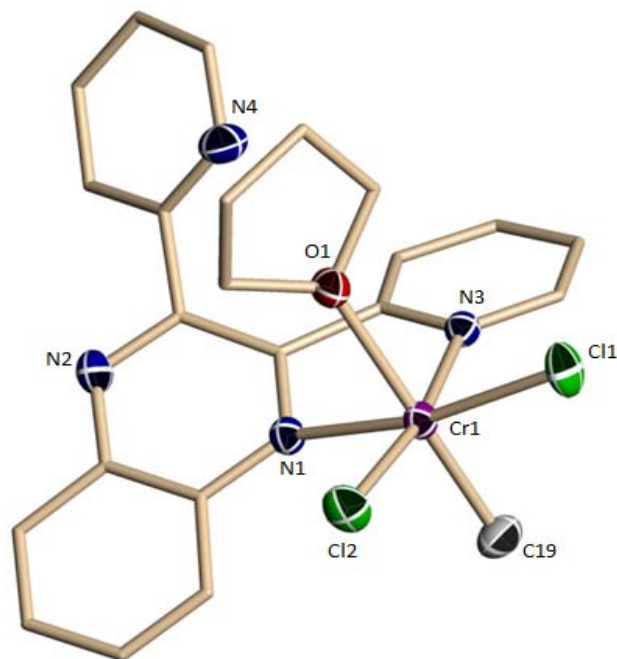


Figure 4.9. Partial thermal ellipsoid drawing for **4.4** at 50% probability level. Selected Bond lengths (Å) and angles (°) of **4.4**: Cr(1)-N(3) = 2.0795(18), Cr(1)-N(1) = 2.1638(18), Cr(1)-C(19) = 2.057(2), Cr(1)-O(1) = 2.2223(16), Cr(1)-Cl(2) = 2.3115(7), Cr(1)-Cl(1) = 2.3244(7), C(19)-Cr(1)-N(3) = 89.84(9), C(19)-Cr(1)-N(1) = 92.65(9), N(3)-Cr(1)-N(1) = 77.60(7), C(19)-Cr(1)-O(1) = 172.30(9), N(3)-Cr(1)-O(1) = 83.65(6), N(1)-Cr(1)-O(1) = 81.95(6), C(19)-Cr(1)-Cl(2) = 97.44(8), N(3)-Cr(1)-Cl(2) = 170.31(5), N(1)-Cr(1)-Cl(2) = 95.61(5), O(1)-Cr(1)-Cl(2) = 88.59(5), C(19)-Cr(1)-Cl(1) = 94.13(8), N(3)-Cr(1)-Cl(1) = 92.47(5), N(1)-Cr(1)-Cl(1) = 167.96(5), O(1)-Cr(1)-Cl(1) = 90.28(5), Cl(2)-Cr(1)-Cl(1) = 93.37(3).

The fact that the complex has retained the alkyl function and the original trivalent state, indicates that reduction of the metal center, radical cleavage of the aluminum-C bonds and the several transformations, where the 2,3-bis(2-pyridyl) quinoxaline (DPQ) ligand acted

as an electron buffer, are not triggered by one element only. A combination of both elements is required to provide both the Lewis acidity and the reducing power which both are important components of these complex transformations.

4.6 Conclusion

In conclusion we have herein reported that 2,3-bis(2-pyridyl) quinoxaline (DPQ) ligand readily reacts with different alkyl aluminum (TMA and TEAL) in the presence or absence of chromium to form a set of unique compounds.

In this work, a stable cation radical was successfully isolated and characterized. Its EPR spectrum confirms that in $\{[\text{AlMe}_2]_2(\mu\text{-}\kappa^2\text{:}\kappa^2\text{-C}_{18}\text{H}_{12}\text{N}_4)\}(\text{AlCl}_2\text{Me}_2)$ (**4.2**) the unpaired electron is ligand localized. Also DFT calculation further confirmed the localization of charge at the pyrazine ring. Regrettably the role of chromium remains speculative.

Furthermore, we have successfully prepared and characterized a unique diradical species containing aluminum and ligand. This species exists in equilibrium between the triplet and singlet species. Moreover, computational efforts were successfully employed to rationalize this behaviour in terms of small HOMO-LUMO gap as reflecting on a very small singlet-triplet energy difference. Finally, we have obtained an unprecedented dimethylation of the quinoxaline ring utilizing alkyl aluminum. The reaction consists of a transfer of two alkyl groups to the carbon-carbon double bond of the DPQ ligand linking the two nitrogen atoms.

4.7 References

1. (a) Deuchert, K.; Hunig, S. *Angew. Chem. Int. Ed.* **1975**, *17*, 875; (b) Kaim, W. *J. Organomet. Chem.* **1981**, *215*, 325; (c) Kaim, W. *Angew. Chem. Int. Ed.* **1980**, *19*, 911; (d) Kosower, E. M.; Cotter J. L. *J. Am. Chem. Soc.* **1964**, *86*, 5524; (e) Stone, E. W.; Maxi, A. *J. Chem. Phys.* **1963**, *39*, 1635; (f) R. L. Ward, *J. Am. Chem. Soc.* **1962**, *84*, 332.
2. (a) Kalyanasundaram, K. In *Photochemistry of Polypyridine and Porphyrin Complexes*. Academic Press: London, **1992**; (b) Zigler, D. F.; Wang, J.; Brewer, K. J. *Inorg. Chem.* **2008**, *47*, 11342; (c) Balzani, V.; Juris, A.; Venturi, M.; Campagna, S.; Serroni, S. *Chem. Rev.* **1996**, *96*, 759; (d) Campagna, S.; Puntoriero, F.; Nastasi, F.; Bergamini, G.; Balzani, V. *Top. Curr. Chem.* **2007**, *280*, 117; (e) Kumaresan, D.; Shankar, K.; Vaidya, S.; Schmechl, R. H. *Top. Curr. Chem.* **2007**, *281*, 101; (f) Indelli, M. T.; Chiorboli, C.; Scandola, F. *Top. Curr. Chem.* **2007**, *280*, 215.
3. Sadimenko, A. P. *Adv. Heterocycl. Chem.* **2007**, *95*, 221.
4. (a) Abe, H.; Nomura, R.; Seo, S.; Shitagaki, S.; Tokuda, A. US20120286257. (b) Kawakami, S.; Nomura, R.; Nomura, H.; Ohsawa, N.; Seo, S. US20090072718.
5. (a) Lindsley, C. W.; Zhao, Z.; Leister, W. H.; Robinson, R. G.; Barnett, S. F.; Defeo-Jones, D.; Jones, R. E.; Hartman, G. D.; Huff, J. R.; Huber, H. E.; Duggan, M. E. *Bioorg. Med. Chem. Lett.* **2005**, *15*, 761; (b) Carta, A.; Sanna, P.; Usai, D.; Zanetti, S. *II, Farmaco.* **2001**, *56*, 933; (c) Sanna, P.; Carta, A.; Loriga, M.; Zanetti, S.; Sechi, L. *II, Farmaco.* **1999**, *54*, 161; (d) Monge, A.; Martinez-Crespo, F. J.; Cerain, A. L.; Palop, J. A.; Narro, S.; Senador, V.; Marin, A.; Sainz, Y.; Gonzalez, M.; Hamilton, E.; Barker, A. J. *Med. Chem.*

1995, 38, 4488; (e) Staszewska, A.; Stefanowicz, P.; Szewczuk, Z. *Tetrahedron. Lett.*, **2005**, 46, 5525.

6. (a) Arun, V.; Robinson, P. P.; Manju, S.; Leeju, P.; Varsha, G.; Digna, V.; Yusuf, K. K. *M. Dyes and Pigments*, **2009**, 82, 268; (b) Chang, D. W.; Lee, H. J.; Kim, J. H.; Park, S. Y.; Park, S.; Dai, L.; Baek, J. *Organic. Lett.* **2011**, 13, 3880; (c) Jaung, J. *Dyes and Pigments* **2006**, 71, 245; (d) Kumar, A.; Kumar, S.; Saxena, A.; De, A.; Mozumdar, S. *Catal. Commun.* **2008**, 778; (e) Sherif, S.; Ekladios, L.; Elmal, G. *J. Prakt. Chem.* **1970**, 312.

7. Thomas, K. R. J.; Velusamy, M.; Lin, J. T.; Chuen, C. H.; Tao, Y. T. *Chem. Mater.* **2005**, 17, 1860.

8. Dailey, S.; Feast, W. J.; Peace, R. J.; Sage, I. C.; Till, S.; Wood, E. L.; *J. Mater. Chem.* **2001**, 11, 2238.

9. (a) Hegedus, L. S.; Greenberg, M. M.; Wendling, J. J.; Bullock, P. J. *J. Org. Chem.* **2003**, 68, 4179; (b) Carlson, D. L.; Huchital, D. H.; Mantilla, E. J.; Sheardy, R. D.; Murphy, W. R. *J. Am. Chem. Soc.* **1993**, 115, 6424.

10. (a) Kaim, W. *J. Organomet. Chem.* **1980**, 201, 5C-8C; (b) Cheeseman, G.W.H.; Gxstink, E. S. *Adv. Heterocycl. Chem.* **1978**, 22, 367; (c) Porter, A. E. A. *Comprehensive Organic Chemistry*. Pergamon Press: Oxford, **1979**, Vol. 4, 136; (d) Epifani, E.; Florio, S.; Ingrosso, G.; Sgarra, R.; Stasi, F. *Tetrahedron* **1987**, 43, 2767; (e) Kauffmann, T.; Hopp, G.; Laarmann, B.; Stegemann, D.; Wingbermihle, D. *Tetrahedron Lett.* **1990**, 31, 511.

11. (a) Scott, J.; Gambarotta, S.; Korobkov, I.; Knijnenburg, Q.; de Bruin, B.; Budzelaar, P. H. M. *J. Am. Chem. Soc.* **2005**, 127, 17204; (b) Shuster, V.; Gambarotta, S.; Nikiforov, G.

B.; Korobkov, I.; Budzelaar P. H. M. *Organometallics* **2012**, *31*, 7011; (d) Koster, R.; Benedikt, G.; Schrotter, H. W. *Angew. Chem. Int. Ed.* **1964**, *76*, 649; (d) Koster, R.; Benedikt, G.; Schrotter, H. W. *Angew. Chem. Int. Ed.* **1964**, *3*, 514; (e) Ziegler, E.; Fuchs, G.; Lehmkuhi, H. *Z. Anorg. Allg. Chem.* **1967**, *355*, 145; (f) Hoberg, H.; Ziegler, E. *Angew. Chem. Int. Ed.* **1967**, *79*, 411; (g) Hoberg, H.; Ziegler, E. *Angew. Chem. Int. Ed.* **1967**, *6*, 452.

12. Kaim, W. *J. Chem. Soc., Perkin Trans. I.* **1984**, 1767.

13. (a) Schoonover, J. R.; Bates, W. D.; Meyer, T. J. *Inorg. Chem.* **1995**, *34*, 6421; (b) Sugiyama, H.; Korobkov, I.; Gambarotta, S.; Moeller, A.; Budzelaar, P. H. M. *Inorg. Chem.* **2004**, *43*, 57; (c) Maruyama, M.; Murukami, K. *J. Electroanal. Chem.* **1979**, *102*, 221; (d) Minsky, A.; Cohen, Y.; Rabinovitz, M. *J. Am. Chem. Soc.* **1985**, *107*, 1501; (e) Cohen, Y.; Meyer, A. Y.; Rabinovitz, M. *J. Am. Chem. Soc.* **1986**, *108*, 7039.

14. Kumbhar, A.; Kamble, S.; Barge, M.; Rashinkar, G.; Salunkhe, R. *Tetrahedron Lett.* **2012**, *53*, 2756.

15. Gaussian 03, Revision B.03, Frisch, M. J.; Trucks, G. W.; Schlegel, H. B.; Scuseria, G. E.; Robb, M. A.; Cheeseman, J. A.; Montgomery, J.; Vreven, T.; Kudin, K. N.; Burant, J. C.; Millam, J. M.; Iyengar, S. S.; Tomasi, J.; Barone, V.; Mennucci, B.; Cossi, M.; Scalmani, G.; Rega, N.; Petersson, G. A.; Nakatsuji, H.; Hada, M.; Ehara, M.; Toyota, K.; Fukuda, R.; Hasegawa, J.; Ishida, M.; Nakajima, T.; Honda, Y.; Kitao, O.; Nakai, H.; Klene, M.; Li, X.; Knox, J. E.; Hratchian, H. P.; Cross, J. B.; Adamo, C.; Jaramillo, J.; Gomperts, R.; Stratmann, R. E.; Yazyev, O.; Austin, A. J.; Cammi, R.; Pomelli, C.; Ochterski, J. W.; Ayala, P. Y.; Morokuma, K.; Voth, G. A.; Salvador, P.; Dannenberg, J. J.; Zakrzewski, V.

G.; Dapprich, S.; Daniels, A. D.; Strain, M. C.; Farkas, O.; Malick, D. K.; Rabuck, A. D.; Raghavachari, K.; Foresman, J. B.; Ortiz, J. V.; Cui, Q.; Baboul, A. G.; Clifford, S.; Cioslowski, J.; Stefanov, B. B.; Liu, G.; Liashenko, A.; Piskorz, P.; Komaromi, I.; Martin, R. L.; Fox, D. J.; Keith, T.; Al-Laham, M. A.; Peng, C. Y.; Nanayakkara, A.; Challacombe, M.; Gill, P. M. W.; Johnson, B.; Chen, W.; Wong, M. W.; Gonzalez, C.; Pople, J. A. Gaussian, Inc., Pittsburgh PA, **2003**.

16. Lee, C.; Yang, W.; Parr, R. G. *Phys. Rev. B*. **1988**, *37*, 785.

17. Becke, A. D. *J. Chem. Phys.* **1993**, *98*, 5648.

18. Stephens, P. J.; Devlin, F. J.; Chabalowski, C. F.; Frisch, M. J. *J. Phys. Chem.* **1994**, *98*, 11623.

19. Krishnan, R.; Binkley, J. S.; Seeger, R.; Pople, J. A. *J. Chem. Phys.* **1980**, *72*, 650.

20. Hariharan, P. C.; Pople, J. A. *Theor. Chem. Acc.* **1973**, *28*, 213.

21. Hehre, W. J.; Ditchfie, R.; Pople, J. A. *J. Chem. Phys.* **1972**, *56* 2257.

22. Ditchfield, R. *Mol. Phys.* **1974**, *27*, 789.

23. Wolinski, K.; Hinton, J. F.; Pulay, P. *J. Am. Chem. Soc.* **1990**, *112*, 8251.

24. Barone, V.; Cossi, M. *J. Phys. Chem. A*, **1998**, *102*, 1995.

25. Cossi, M.; Scalmani, G.; Rega, N.; Barone, V. *J. Comp. Chem.* **2003**, *24*, 669.

26. Barone, V. In *Recent Advances in Density Functional Methods*, edited by Chong, D. P. World Scientific, Singapore, **1995**, p. 287.

27. Rega, N.; Cossi, M.; Barone, V. *J. Chem. Phys.* **1996**, *105*, 11060.

28. Barone, V.; Cimino, P. *Chem. Phys. Lett.* **2008**, *454*, 139.

29. Barone, V.; Cimino, P.; Stendardo, E. *J. Chem. Theory Comput.* **2008**, *4*, 751.

30. Barone, V.; Cimino, P. *J. Chem. Theory Comput.*, **2009**, *5*, 192.

31. Godbout, N.; Salahub, D. R.; Andzelm, J.; Wimmer, E. *Can. J. Chem.* **1992**, *70*, 560.

32. Munzarová, M. L. In *Calculation of NMR and EPR Parameters, Theory and Applications*, Kaupp, M.; Bühl, M.; Malkin, V. G. Wiley-VCH, Weinheim, Germany, **2004**, ch. 29, P 463.
33. GaussView, Version 3.07, Dennington, R.; Keith, T.; Millam, J.; Eppinnett, K.; Hovell, W. L.; Gilliland, R. Semichem, Inc., Shawnee Mission, KS, **2003**.
34. Sakurada, Y.; Huggins, M. L.; Anderson, W. R., Jr. *J. Phys. Chem.* **1964**, *65*, 1934.
35. Borden, W. T.; Davidson, E. R. *J. Am. Chem. Soc.* **1977**, *99*, 4587.
36. Borden, W. T.; Davidson, E. R. *Diradicals*, John Wiley & Sons, New York, **1982**, 1.

Conclusion

In this thesis I have described the results of efforts to isolate and characterise intermediates as generated by the interaction of chromium catalyst precursors and aluminates activators. The ultimate goal was to address the issue of the chromium oxidation state and to gain a good grasp on the mechanism of selective oligomerization. For this purpose, I have also synthesized various chromium-based catalysts and used different activators as reducing agents.

Firstly, di- and trivalent chromium complexes supported by iminopyridine, in both neutral and monoanionic form, were fully characterised and tested. Divalent complexes afforded mainly polyethylene along with a statistical mixture of oligomers. The trivalent analogues, containing two monoanionic ligands, afforded a Schulz-Flory distribution of linear α -olefins and trace amounts of polymer.

In a separate aspect of this work, we have used the phosphoranimine ligand for the preparation and characterization of a series of chromium complexes with the ligand in both anionic and neutral forms. In turn, this has enabled to establish a convincing link between catalytic activity and chromium oxidation state. Testing of the catalytic behaviour and attempts to isolate catalytically active species enabled the isolation of a rare mixed-valence Cr(I)/Cr(II) species. The activity of the trivalent chromium precursor, which produced non-selective ethylene oligomerization with high activity, was optimized by using the appropriate co-catalyst and its outcome meets the expectations of a commercial catalyst.

In an attempt to maximize the charge transfer ability of the ligand vis-à-vis the stabilization of low-valent chromium, we have investigated the behaviour of Cr/Aluminate systems with 2,3-bis(2-pyridyl)quinoxaline (DPQ), a well-known polyazine ligand capable of performing interesting radical transformations. Surprisingly and in spite of proving the presence of chromium as essential for the reactivity, we managed to isolate only organic radicals coupled to aluminate species. The role of chromium remains therefore mysterious. The electronic structure of the organic radicals has been fully elucidated by a combination of DFT calculation and EPR studies. Remarkably, experimental and computational work has demonstrated the existence of co-existence (or equilibria) of both singlet and triplet forms of the same species. In addition, we have discovered an unprecedented dimethylation on the quinoxaline ring which is a rare example of carbon carbon bond formation with loss of aromaticity of the pyrazine ring.

In this thesis, the undoubted roles of oxidation states of the chromium in the catalytic activity, which can be modified by applying various ancillary ligands and alkyl aluminums as the important activator in the oligomerization and polymerization processes, were brought to the light. This idea can guide the researcher to find effective strategies to design catalysts for specific purposes or make efforts to rationalize the catalytic activity by isolation of active species. The realization of this challenge led to the radical chemistry and the resultant chromium complexes and alkyl aluminum species are worthwhile for future study.

Appendix

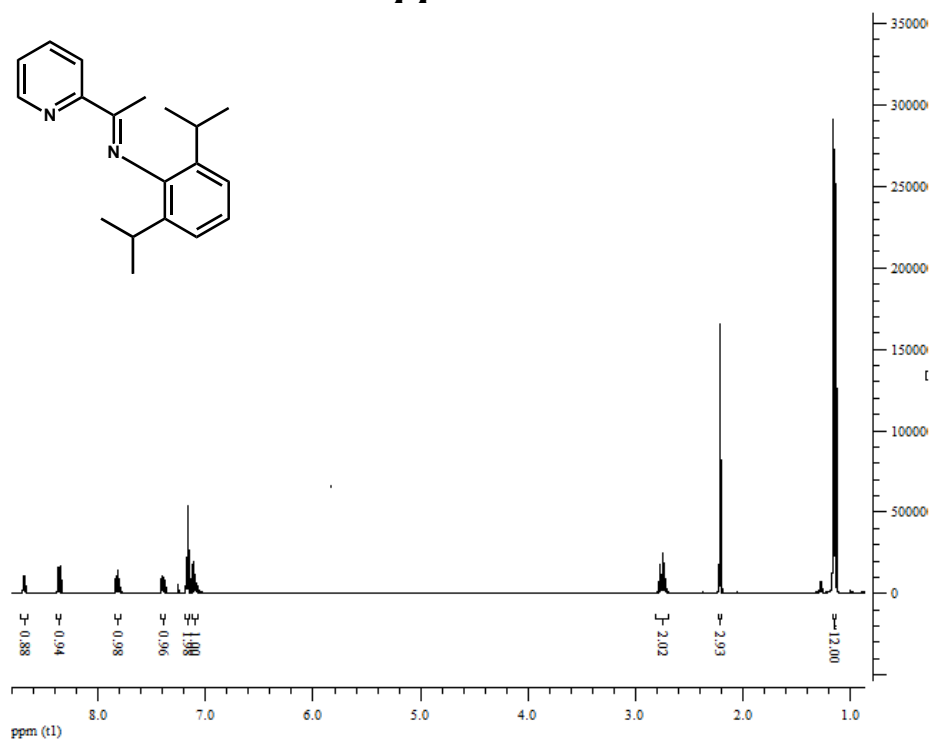


Figure 5.1. ¹H NMR of 2a

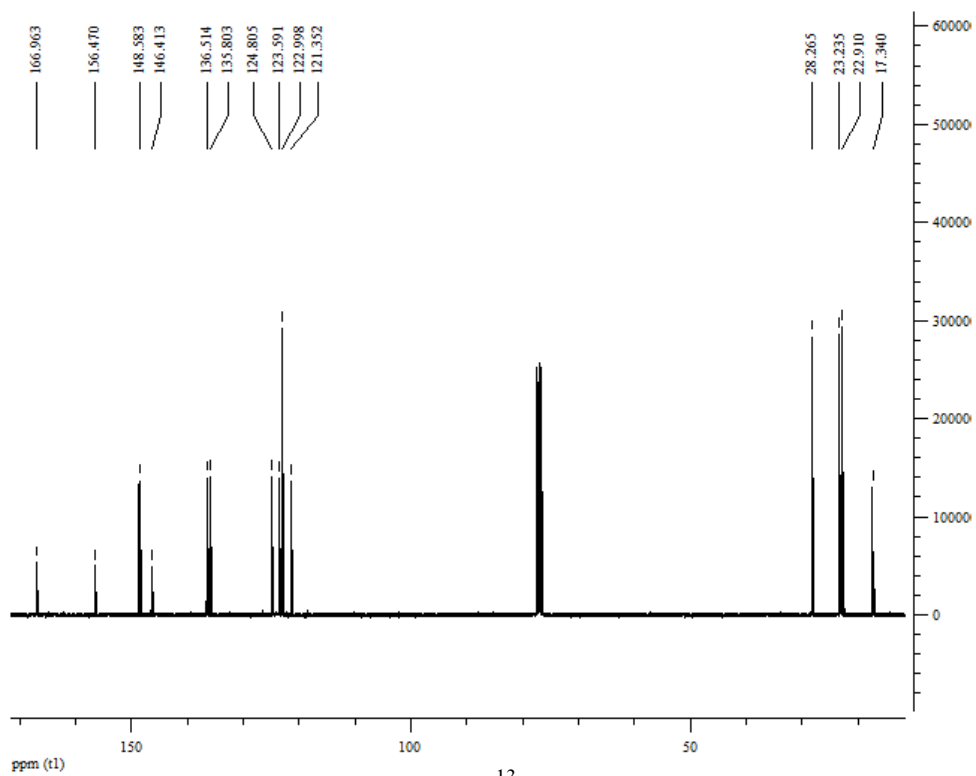


Figure 5.2. ¹³C NMR of 2a